United States
Department of
Agriculture

Forest Service

Technology &
Development
Program

5200–Forest Pest
Management
9052-2822-MTDC

Selection and Verification of Spray Droplet Evaporation Model

Briefing Paper & Progress Report

Objective

To develop an improved model that can be incorporated into the FSCBG, AGDISP, or any other spray model to predict changes in droplet size and concentration due to evaporation.

Background

A critical factor in the aerial spray predictions models is the evaporation rate associated with the spray droplets. Evaporation affects the droplet size and hence the terminal velocity of the drop. Consequently, evaporation has significant impact on the time and space distribution of the spray. A study by Dr. Banaugh, in 1979, revealed that most of the theoretical research was done for pure liquid drops. In order to have information for the spray models, a study was sponsored at Colorado State University to measure evaporation rate of droplets from 13 pesticide mixtures under simulate free fall conditions. No further use was made of the windtunnel and it was removed and dismantled. Both the AGDISP and FSCBG are configured to accept data from the simulated tests or to calculate evaporation rate for pure liquids when certain physical properties are known.

This year a new study was sponsored to review and update the status of droplet evaporation research and development. Eight organizations have been identified that have done recent testing of droplet evaporation. The U.S. Army, CRDEC, at Aberdeen Proving Ground has developed the most complete and thorough evaporation model for multi-component mixtures, including emulsions and suspensions. NUSSE4 (the CRDEC model) can simulate up to five components. The five components can include two volatile and three non-volatile components. Only limited validation of the model predictions have been made to date.

Since the pesticide tank mixes have changed, we no longer have valid experimental results for the spray model, nor do we have multi-component models operational.
Methods

We plan to obtain the NUSSE3 and NUSSE4 models and make them operational on a Forest Service computer. We will determine the physical constants needed to exercise the model and obtain those constants from the pesticide manufacturers if possible. We plan to obtain experimental measurements of new tank mixes and compare those results to the model predictions. Comparisons of previous experimental results will be made to existing models. Revisions to the model will be proposed based on comparisons to experimental measurements.

Revision

Early examination of the NUSSE models revealed that their current use is limited to certain specialized compounds of interest to the Army. Further investigation of the single component evaporation model, already a part of the FSCBG code required measurements of physical properties that are difficult to measure even in a laboratory.

We are therefore recommending that we pursue an alternative approach. This is, contract for measurement of evaporation of single droplets. This is the method that was developed under contract by Colorado State University in the early 1980's. (Appendix A). The direct measurement of a matrix of droplet diameters, temperatures, relative humidities, and tank mixes can be input directly into either AGDISP or FSCBG.

The system developed by Colorado State University is documented, but has been dismantled. We have not been successful in identifying another laboratory that has an operational system to measure droplet evaporation directly.

Most of the funding for this project is intact and can be applied to a contract to develop a system and conduct measurements of evaporation rates of single droplets.

Workplan Revised July 1, 1990

Selection and Verification of Spray Droplet Evaporation Model

	Assignment	1990				1991			
		1	2	3	4	1	2	3	4
Compare AGDISP and FSCBG Predictions to 1984 Laboratory Measurements	***Thompson*** ***Teske***			x	x				
Measure Evaporation Rates of Single Droplets	***Contractor*** ***Ekblad*** ***Barry***			x	x	x	x		
Write request for proposals									
Evaluate proposals									
Award contract									
Monitor contract									
Prepare Quadratic Coefficients for AGDISP and FSCBG inputs	***Contractor***							x	

Appendix–*Determination of Evaportion Rates of Pesticide Droplets*

Determination of Evaporation Rates of Pesticide Droplets

FINAL REPORT

Prepared by
Rick S. Dennison
Civil Engineering Department
Colorado State University

James B. Wedding, Ph.D.
Director, Aerosol Science Laboratory
Affiliated with the
Research Institute of Colorado

Prepared for
U. S. Department of Agriculture
Forest Service
Equipment Development Center
Missoula, MT 59801

Robert B. Ekblad
Project Leader

Contract No. 53-0343-8-105
(Work under this contract was completed in July 1982)

Pesticide Precautionary Statement

This publication reports research involving pesticides. It does not contain recommendations for their use, nor does it imply that the uses discussed here have been registered. All uses of pesticides must be registered by appropriate State and/or Federal agencies before they can be recommended.

CAUTION: Pesticides can be injurious to humans, domestic animals, desirable plants, and fish or other wildlife—if they are not handled or applied properly. Use all pesticides selectively and carefully. Follow recommended practices for the disposal of surplus pesticides and pesticide containers.

3400—Forest Pest Management
8434 2801

FOREWORD

This report is published as a part of a USDA Forest Service program to improve aerial application of pesticides, specifically by using pesticides and delivery systems tailored to the forest environment. The program is conducted jointly by the Equipment Development Center, Missoula, Mont., and Forest Pest Management Staff, Washington Office at Davis, Calif., under the sponsorship of State and Private Forestry.

Details of the aerial application improvement program are explained in two Forest Service reports, A Problem Analysis: Forest and Range Aerial Pesticide Application Technology (Equipment Development Center Rpt. 7934 2804, July 1979, Missoula, Mont.) and Recommended Development Plan for An Aerial Spray Planning and Analysis System (Forest Pest Management Rpt. FPM 82-2, February 1982, Davis, Calif.).

The system of computer models developed to optimize spray program design and operation and evaluate assessment of environmental risk posed by aerial spray operations must include predictions of evaporation rates of spray droplets. The classic theoretical evaporation equations are suitable for pure liquids, such as water, but have not been extended to more complex mixtures, emulsions, and suspensions ordinarily used in spraying. The alternate to the use of theoretical equations is experimental measurement under controlled conditions.

This report contains the results of an extensive series of experimental measurements of droplet evaporation rates. Fourteen tank mixes representing a variety of pesticides, a commonly used antidrift additive, and water were examined.

Four sizes of droplets were examined under simulated free fall conditions for a wide variety of temperature and relative humidity conditions. Enough data were taken to insure that a reasonably accurate estimate of other droplets and conditions could be made by interpolation. Some examples of evaporation rates are included in the report but the majority of the data are stored on magnetic tape at the USDA Fort Collins Computer Center. Complete instructions for retrieving the data are included in the report.

The study and measurements were conducted by the Aerosol Science Laboratory of the Engineering Research Center at Colorado State University under contract to the USDA Forest Service.

The droplet evaporation facility has been retained at the Aerosol Science Laboratory and is available for analysis of other tank mixes on a contract basis.

A report on Equipment Development and Test Project 2664, Optimum-Size Spray Droplets, funded by the Forest Pest Management Staff.

Final Report

DETERMINATION OF EVAPORATION RATES OF PESTICIDE DROPLETS

An experimental study was conducted to measure the rates of mass transfer from 13 pesticide mixtures plus water under simulated free fall conditions. Droplets were captured on a wire and air that was conditioned at various temperatures and relative humidities was passed by the pendant droplet in a closed loop wind tunnel facility. Droplets having nominal diameters of 50, 100, 250, and 400 microns generated using a vibrating reed aerosol generator were sized at each time step and the wind tunnel velocity adjusted to the corresponding terminal velocity. The droplet diameter was determined using a Reticon solid state camera and an on-line Texas Instruments microcomputer.

The data for water were used to obtain an equation of the Sherwood number (Sh) as a function of the Reynolds (Re) and Schmidt (Sc) numbers. The resulting correlation equation, $Sh = 1.755 + 0.535 (Re^{1/2} Sc^{1/3})$, agreed well with previous authors. The data obtained for the other test solutions were reduced to plots of percent of mass loss versus time. These curves allowed direct application of the results obtained in this study.

The measurement and control of the air humidity presented a possible source of error. However, the data reported generally represent the mass transfer of freely falling spray droplets. An overall error of approximately 9% resulted from this experimental procedure and facility.

Rick S. Dennison
Civil Engineering Department
Colorado State University
Fort Collins, Colorado 80523
Spring, 1982

TABLE OF CONTENTS

Chapter

Page

LIST OF TABLES

LIST OF FIGURES

LIST OF SYMBOLS

Symbol	Description	Dimensions
A	Area	L^2
a	Droplet radius	L
C	Function of Re, Sc; $C = Re^{1/2}Sc^{1/3}$	none
C_D	Drag Coefficient	none
Count	Pixel count due to droplet and wire	none
c	Vapor concentration	ML^{-3}
D	Diffusion coefficient	L^2T^{-1}
Delta	Error in third order equations	L
Diam	Droplet diameter	L
F	Ventilation factor	none
g	Acceleration due to gravity	LT^{-2}
k	Thermal conductivity	$MLT^{-3}deg^{-1}$
L	Half of the length of the supporting wire	L
M_a	Molecular weight of air	$Mole^{-1}$
M_ℓ	Molecular weight of liquid	$Mole^{-1}$
m	Mass of droplet	M
NCAL	Averaged pixel calibration count	none
Nu	Nusselt number	none
NWIRE	Averaged pixel count due to wire	none
0	Initial conditions at the surface	none
Pr	Prandtl number	none
P	Partial vapor pressure	$ML^{-1}T^{-2}$
R	Universal gas constant	$L^2T^{-2}Mole^{-1}deg^{-1}$

Symbol	Description	Dimensions
Re	Reynolds number	none
r	radial distance	L
S	droplet surface area	L^2
Sc	Schmidt number	none
Sh	Sherwood number	none
T	Temperature	degrees
t	Time	T
t_v	Kinzer and Gunn time interval	T
V	Velocity	LT^{-1}
V_T	Terminal velocity	LT^{-1}
w	Width of wire	L
X	Vapor density ratio	none
∞	Free stream conditions in surrounding fluid	none
α	Linear regression coefficient, intercept	none
β	Mass transfer coefficient	none
$\ell\frac{dm}{dt}$	Rate of heat transfer	ML^2T^{-3}
ρ_a	Density of air	ML^{-3}
ρ_p	Density of droplet	ML^{-3}
μ	Viscosity	$ML^{-1}T^{-1}$

Chapter 1

INTRODUCTION

The control and management of various forest insects has been accomplished recently with the aid of aerially disseminated pesticides. In order to optimize this use of the pesticide spray, several parameters must be determined. These parameters include initial droplet size distribution, volatility of the material, height and width of the spray release, and the cloud behavior affected by the aircraft and atmospheric fluid dynamics. Complete knowledge of the above could allow the efficient application of pesticides from aircraft. The purpose of the present study was to examine several spray solutions and determine their corresponding time rate evaporation histories. Droplets were to be examined under simulated free fall conditions for a variety of temperature and relative humidity combinations of the passing airstream.

Chapter 2

THEORETICAL CONSIDERATIONS

2.1 Evaporation from Stationary Droplets

Early work with mass transfer was performed by Maxwell (8) for the evaporation of a spherical droplet. In this study, Maxwell developed an expression for the rate of mass loss of a droplet:

$$\left(\frac{dm}{dt}\right)_0 = -4\pi Dr^2 \frac{dc}{dr} \tag{2.1}$$

Equation 2.1 assumes the radii of the droplets are large compared to the mean free path of the surrounding fluid. This expression defines the droplet evaporation for the simplest case, that of a quiescent, homogeneous medium. Langmuir (7) also derived equation 2.1 in an independent study performed years later. Integration of equation 2.1 and the substitution of boundary conditions yields:

$$\left(\frac{dm}{dt}\right)_0 = -4\pi aD(C_0 - C_\infty) \tag{2.2}$$

where a is the droplet radius, C_0 is the concentration of vapor at the surface, and C_∞ is the free stream concentration. Assuming the vapor of the evaporating liquid obeys the ideal gas laws, the concentration of the vapor can be expressed as a partial vapor pressure, P, such that:

$$C = \frac{PM_\ell}{RT} \tag{2.3}$$

Substitution of equation 2.3 into equation 2.2 reduces the integrated Maxwell equation:

$$\left(\frac{dm}{dt}\right)_0 = - \frac{4\pi a D M_\ell}{R} \left(\frac{P_0}{T_0} - \frac{P_\infty}{T_\infty}\right) \tag{2.4}$$

where P_0 and T_0 describe the conditions at the droplet surface and P_∞ and T_∞ correspond to the surrounding medium.

2.2 Effects of Forced Convection

The mass transfer process of a droplet in a motionless, uniform medium is completely defined by equation 2.4. When a relative motion between the droplet and the medium is introduced, the effects of forced convection are described by the Sherwood number, Sh. This dimensionless chemical engineering parameter is defined as:

$$Sh = \frac{2a\left(\frac{dm}{dt}\right)_c}{DS\ (C_0 - C_\infty)} \tag{2.5}$$

where $\left(\frac{dm}{dt}\right)_c$ is the convective mass rate and S is the droplet surface area. Equation 2.5 can be rearranged to include the integrated form of Maxwell's equation (2.2) for motionless evaporation:

$$Sh = \frac{2a\left(\frac{dm}{dt}\right)_c}{\left[-4\pi a^2 D(C_0 - C_\infty)\right]} = 2\,\frac{\left(\frac{dm}{dt}\right)_c}{\left(\frac{dm}{dt}\right)_0} \tag{2.6}$$

Similarly, physical properties of heat and mass transfer allow the effects of forced convection on the rate of heat transfer to be described by the Nusselt number:

$$Nu = 2\,\frac{\left(\ell\ \frac{dm}{dt}\right)_c}{\left(\ell\ \frac{dm}{dt}\right)_0} \tag{2.7}$$

Close examination of equations 2.6 and 2.7 reveals that Sh and Nu are defined as wind factors. One half of these values are multiplication factors used with the motionless rates of transfer to obtain the larger rates experiences with forced convection. When a relative motion between the droplet and the medium does not exist, Sh and Nu are reduced to a constant value of two. This value defines the theoretical lower limit of Sh and Nu.

Chapter 3

Review of Literature

The effects of forced convection on the heat and mass transfer of spherical droplets has been examined at great extent. Theoretical and experimental solutions for the Sherwood and Nusselt numbers have been produced for a wide range of ventilation velocities and droplet diameters. The following review will consider solutions dealing with mass transfer only. Equations similar to these describing the transfer of heat are often presented by authors due to the analogous physical procedures involved.

Limited success has been obtained using strict theoretical solutions to describe the rates of transfer. This limitation is caused by the difficulty in solving the Navier-Stokes equation of fluid flow around the droplet simultaneously with the differential equations of heat and mass transfer. However, several authors have obtained solutions by making assumptions about the physical process. Froessling (4), as cited in Fuchs (5), used a boundary layer theory to obtain equations for a blunt-nosed body of revolution. With this solution, he determined that the Sherwood number could be expressed as a function of two additional dimensionless parameters, the Reynolds (Re) and Schmidt (Sc) numbers. These dimensionless groupings are defined as follows:

$$Re = \frac{2aV\rho_a}{\mu} \qquad Sc = \frac{\mu}{\rho_a D} \qquad (3.1)$$

Specifically, Froessling presented Sh as being proportional to $Re^{1/2}$.

Subsequent experiments using droplets of water, aniline, nitrobenzene, and naphthalene were carried out by Froessling. These experiments were performed with constant ventilation velocities using droplets suspended from glass fibers. An environmental temperature of 20°C was used in every test. In all cases, the data were correlated by:

$$Sh = 2.0 + \beta Re^{1/2} Sc^{1/3} \qquad (3.2)$$

where β, called the mass transfer coefficient, was found to be 0.552. This equation remained consistent for a wide range of Re, from 2.3 to 1280.

Expressions duplicating equation 3.2 have been presented by independent studies. Fuchs, using a similarity principle, determined that the Sherwood number averaged over the entire droplet surface was proportional to $Re^{1/2} Sc^{1/3}$. He combined this result with the limiting case of Sh = 2 when Re = 0 to obtain equation 3.2. The author defines β as a constant to be determined experimentally, but does not include data to calculate a value. Ranz and Marshall (10) also obtained an expression identical to equation 3.2. The authors used Froessling's boundary layer equations in combination with the equations of heat and mass transfer to obtain a set of dimensionless partial differential equations. From these equations, a theoretical and functional form for the Sherwood number was obtained, Sh = Sh(Re, Sc). Experimental data for droplets of water and benzene obtained by Ranz and Marshall were correlated with equation 3.2. The experimental procedure consisted of measuring the rate of feed necessary to maintain a constant diameter droplet suspended on a microburet. Dry air with temperatures up to 220°C was used as the medium. The mass transfer coefficient, β, determined by this data was equal to 0.6.

Kinzer and Gunn (6) developed a theory that considered the transient transfer of vapor to successive packets of fresh environmental air as the droplet moved relative to the medium. In this theory, the authors sum the transfer contributions of all the packets that contact the droplet. In doing so, estimations of the contact area, A, and the time of contact for each packet, t, were required. The vapor transferred to each fresh packet was given by:

$$\text{At} \left(\frac{dx}{dr}\right)_a \tag{3.3}$$

where x is the vapor density ratio and $\left(\frac{dx}{dr}\right)_a$ is the gradient at the droplet surface. The values obtained for each packet by equation 3.3 had to be summed over a time interval, $t_v = 2a/v$, in order to determine the total transfer. The final form of this theoretical approach was given as:

$$Sh = 2.0 \left[1.0 + F(Re\ Sc/4\pi)^{\frac{1}{2}}\right] \tag{3.4}$$

The value of F, called the "ventilation factor", was defined as the ratio of the sum of the terms of equation 3.3 for the ventilated droplet to the same quantity for a droplet at rest. The ventilation factor depended on the ventilation velocity and had to be determined by direct observation. Experiments were performed by Kinzer and Gunn with water droplets using a wide range of temperatures (0 - 40°C) and humidities (10 - 100%) under free fall conditions. Three methods of size measurement were used in these experiments for different ranges of droplet diameters. The method of successive photographs was used to record progressive positions of droplets ranging from 10 to 140 microns in diameter. The droplets were generated at the top end of a well-insulated shaft and allowed to fall freely to the bottom. The terminal settling

velocities were determined using the photographs and the time between each photograph. The droplet diameters were determined from the dependence of diameter to terminal velocity. Similarly, droplets with diameters from 40 to 1000 microns were examined as they fell through a series of inducing rings. Droplets were charged as they were produced and were traced as they fell through the inducing rings. The charged droplets produced an impulse as they passed through each ring. The time between each impulse was used to find the terminal velocities and in turn the droplet diameters. The third method measured droplet diameters from 0.1 to 0.3 cm as a function of height maintained inside a conical tube experiencing a constant velocity. The evaporation rates of the droplets were obtained by measuring the decreasing heights of the droplets at successive time intervals. Comparison of the heights with calibrated data produced diameter versus time data. The results of these experiments were evaluated by equation 3.4 so as to determine values of F for each droplet diameter. The authors presented the results as a plot of F versus $Re^{1/2}$. It should be noted that the results given by Kinzer and Gunn indicate that Sh is not a linear function of $Re^{1/2}$. This is a complete contradiction to the results given by Froessling and Ranz and Marshall correlated by equation 3.2.

Davies (3) reviewed the studies dealing with the transfer of mass from droplets. He presents a step by step procedure used to calculate rates of evaporation in still air and for forced convection. In this procedure, equation 3.2 was used to describe the effects of forced convection. Davies also presented experimental data performed at an air temperature of $20^{o}C$ using droplets of furfural and water. These

droplets were suspended on a fine glass spill in a constant air stream. The author used equation 3.2 with $\beta = 0.552$ to compare with the results of the experiments. Errors up to 13% were obtained in this comparison.

Beard and Pruppacher (1) developed a unique experimental procedure to determine the mass transfer from droplets under free fall conditions. Experiments with water droplets were performed using a limited range of temperatures (22 - 24°C) and humidities (27 - 65%). Droplets ranging in diameter from 100 - 375 microns were held stationary by a vertical tunnel air stream. The velocities of the air stream required to maintain the stationary position of the droplet were recorded over time. The velocity record was then used to determine the rate of change of droplet size. The data were correlated with an equation similar to equation 3.2. Two distinct linear curves were found over the range of $Re^{1/2}\ Sc^{1/3}$ tested. For $1.43 \leq Re^{1/2}\ Sc^{1/3} \leq 12.0$, the authors found that:

$$Sh = 1.56 + 0.616\ Re^{1/2}\ Sc^{1/3} \tag{3.5}$$

Values of $Re^{1/2}\ Sc^{1/3}$ below 1.43 were described by the relation:

$$Sh = 2.0 + 0.216\ Re^{1/2}\ Sc^{1/3} \tag{3.6}$$

Equation 3.6 was obtained to satisfy the theoretical lower limit, $Sh = 2.0$, along with the experimental data.

Chapter 4

SCOPE OF STUDY

The present study was to determine time rate evaporation histories for fourteen solutions. These solutions include thirteen mixtures of pesticides or pesticide components used today and water as a reference. The Evaporation Rate Facility of the Aerosol Science Laboratory at Colorado State University utilized a microscope coupled to a solid state camera to measure the droplet diameter directly at each present time step. A microcomputer programmed by Aerosol Science Laboratory personnel calculated the droplet diameter from the image of the pendant droplet as seen by the camera. The microcomputer then calculated the terminal settling velocity and adjusted the wind tunnel velocity to equal this terminal velocity. The droplet was sized and velocity adjusted continuously at each second of the test.

The test condition variables for each of the 14 solutions included environmental temperature, relative humidity of the air, and nominal initial droplet diameter. The testing values used in this study for these variables can be seen in Table 1. By changing these conditions, the relative effects on the mass transfer from the droplets was ascertained.

Varying the initial droplet diameters allowed the mass transfer process of each solution to be described for different sized droplets falling at terminal velocities. The wide range of test parameters used

Table 1

Experimental Testing Conditions

Environmental Temperatures
$5^{o}C$
$10^{o}C$
$15^{o}C$
$20^{o}C$

Environmental Relative Humidities
20%
60%
90%

Initial Droplet Diameters
50 microns
100 microns
250 microns
400 microns

in the study allowed most common environmental conditions to be matched. Thus, the results produced by this study could be applied directly to a proposed spray operation. For a given pesticide, nozzle spray droplet distribution, environmental temperature and relative humidity, and spray height the mass of pesticide that reaches the intended target could be approximated, if one neglects the added effects of mixing from the aircraft wake and atmospheric turbulence. This would assist in the determination of the effect of the pesticide on the target insect population. The total mass that reaches the intended target will increase or decrease with variations of the environmental conditions. Optimum conditions can then be determined that allow the maximum effect of the pesticide on the insect population. A cost and effect evaluation could also be applied to optimize the entire procedure. Therefore, the knowledge afforded by the present study can contribute greatly to the effective use of aerially disseminated pesticide sprays.

Chapter 5

EVAPORATION RATE FACILITY DESCRIPTION

5.1 General Overview

The experimental facility utilized in the evaporation rate study is shown schematically in Figure 1. For purposes of illustration, the microscope and Reticon camera are shown above the tunnel along with the traverse and aerosol generator. The microscope and camera were actually mounted beneath the test section during testing. The tunnel consisted of a blower-driven closed circuit wind tunnel powered by a DC motor and controller. The tunnel air temperature and relative humidity were altered separately with individually controlled equipment. A vibrating reed aerosol generator, a specially designed and fabricated long focal length microscope, a Reticon solid state camera and camera controller, and a Texas Instruments microcomputer completed the system. The evaporation rate histories of virtually any solution ranging in aerodynamic size from 50 - 1000 microns, ambient temperatures from 5 - 30^{o}C, and relative humidities from 20 - 90% could be obtained with the use of this facility. The data could be accumulated with a constant test section velocity or with a continually adjusted velocity equal to the settling velocity of the observed droplet.

The testing procedure will be described in detail later. A short description is given here for clarification. First, the moving air stream was conditioned to the desired value for temperature and

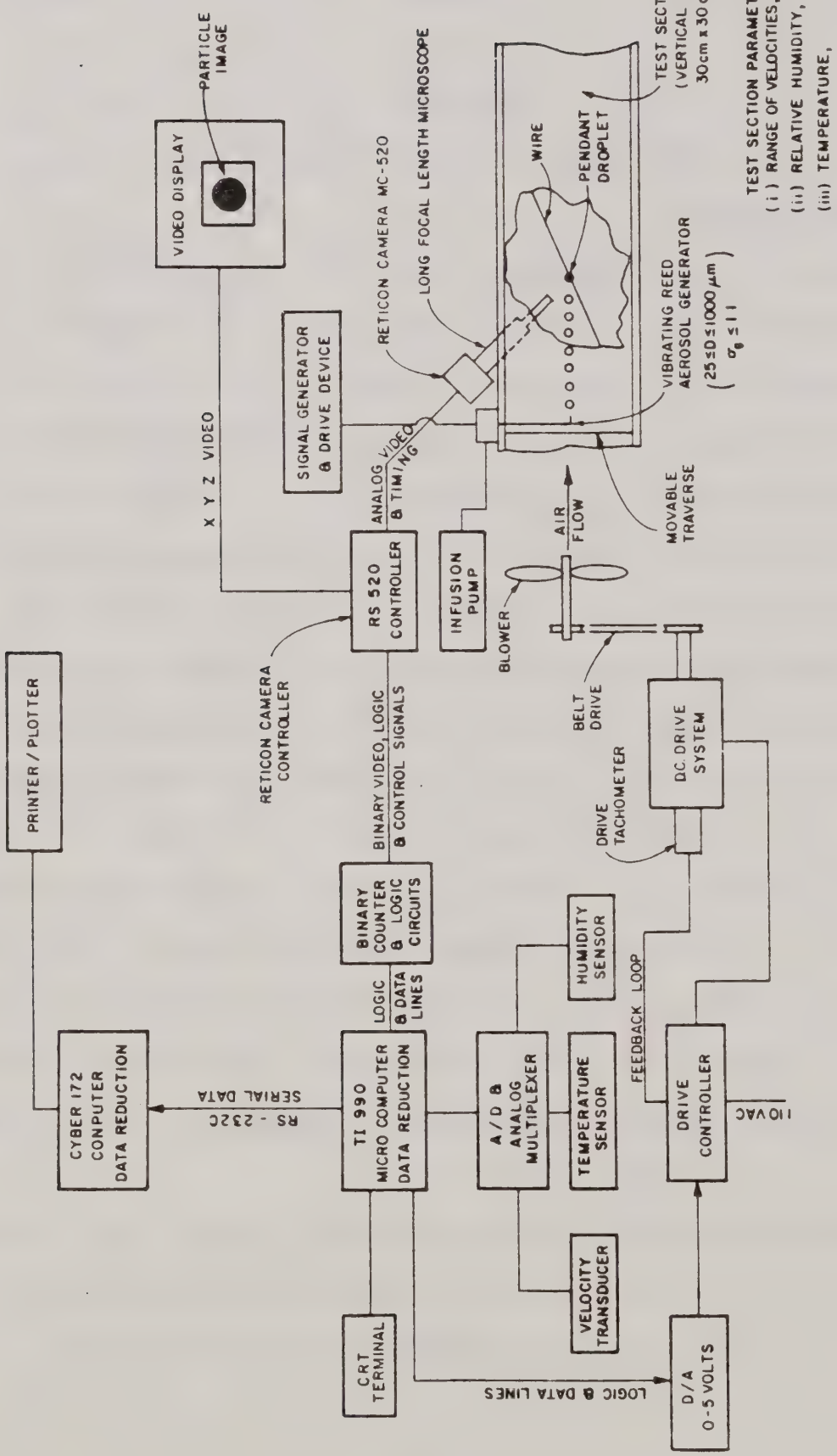

DATA ACQUISITION SYSTEM FOR EVAPORATION RATE FACILITY
AEROSOL SCIENCE LABORATORY

Figure 1

relative humidity. Then a droplet of the desired aerodynamic size was generated and collected on a small wire (5 - 25 microns in diameter) held perpendicular to the airflow. When a pendant droplet was captured within the field of view of the microscope, Reticon camera and data acquisition were started manually. The data acquisition consisted of determining the diameter of the observed droplet at each time step. The following section will discuss each component of the Evaporation Rate Facility separately.

5.2 Aerosol Generator

A vibrating reed aerosol generator was developed for the purpose of producing droplets of a range of sizes between 50 and 1000 microns. The vibrating reed aerosol generator was selected for use in this facility as it is capable of generating large, predictable droplet sizes and because of its flexibility in controlling the placement of the droplets generated. This system allowed the operator to place a stream of droplets throughout the test section. The collection of a single droplet on a supporting wire was facilitated greatly with the use of this areosol system. The vibrating reed system presented by Wolf (14) was used as the basis in the production of the present system.

The entire generating system, depicted in Figure 2, was mounted on a traverse that allowed the generator to be moved longitudinally as well as laterally. The traverse consisted of four 3/4 inch diameter steel bars with two sets of four SPB-12 pillow blocks. A hand crank connected to a threaded vertical bar provided the needed vertical movement. The combination of these three movements allowed the direct placement of the generating system at any desired location within the test section. Four additional adjustments were contained in this generating system to

Figure 2. The Vibrating Reed Aerosol Generator

a) Schematic diagram of the vibrating reed aerosol generator.

b) Detailed drawing of the vibrating reed aerosol generator, scale 1/6" = 1"

a)

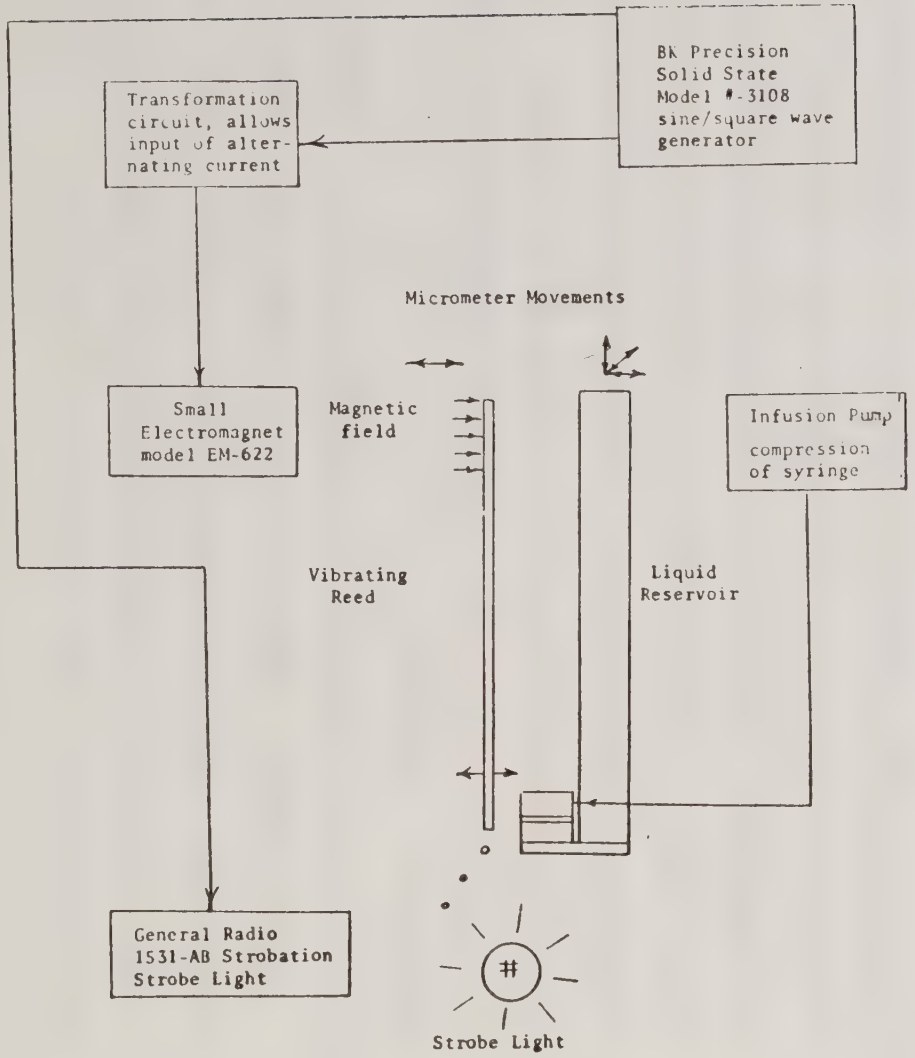
BK Precision
Solid State
Model #-3108
sine/square wave
generator
Transformation
circuit, allows
input of alter-
nating current
Micrometer Movements
Small
Electromagnet
model EM-622
Magnetic
field
Infusion Pump
compression
of syringe
Vibrating
Reed
Liquid
Reservoir
General Radio
1531-AB Strobation
Strobe Light
Strobe Light

b)

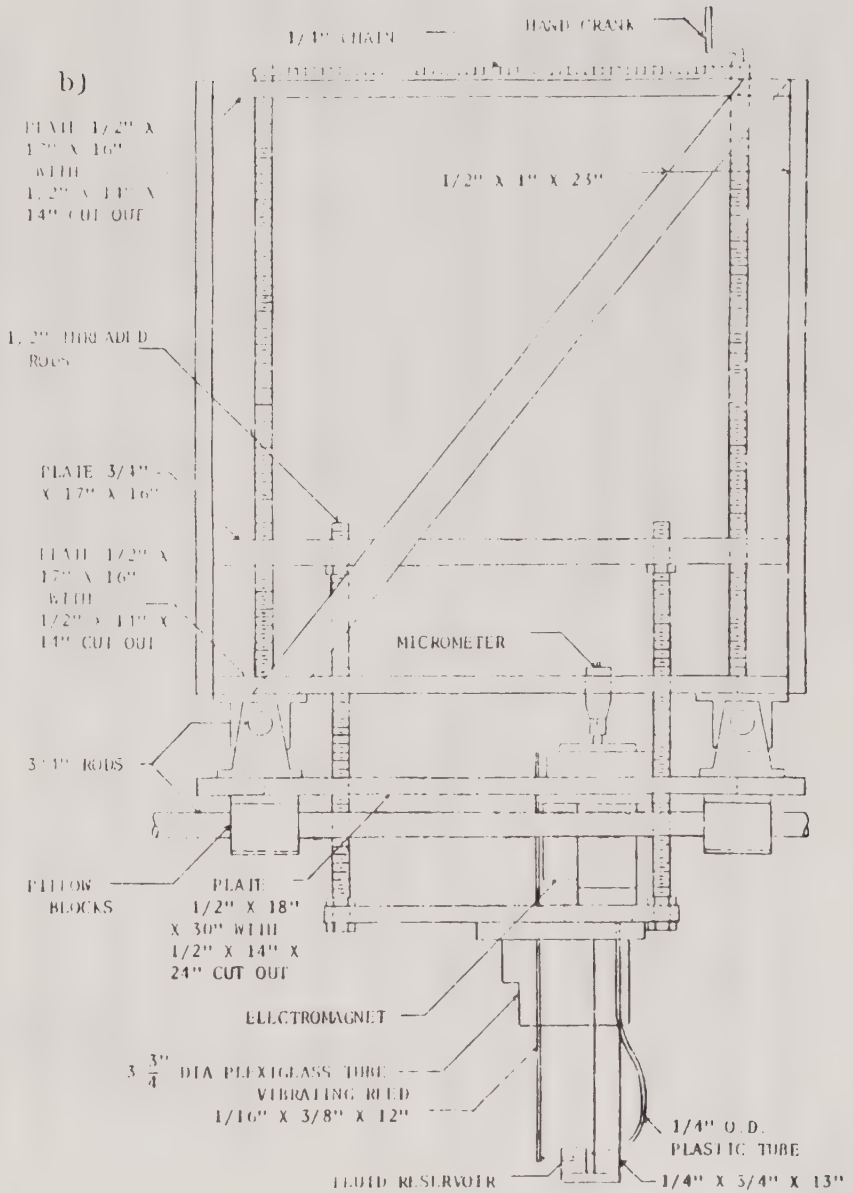
1/4" CHAIN
HAND CRANK
1/2" X 1" X 23"
MICROMETER
PILLOW
BLOCKS
PLATE
1/2" X 18"
X 30" WITH
1/2" X 14" X
24" CUT OUT
ELECTROMAGNET
VIBRATING REED
1/16" X 3/8" X 12"
1/4" O.D.
PLASTIC TUBE
1/4" X 3/4" X 13"

enable a change in the aerodynamic droplet size. Three micrometer adjustments modified the placement of the fluid reservoir with respect to the vibrating reed. The fourth micrometer changed the distance between the magnet causing the motion in the upper portion of the vibrating reed's shaft. This provided for adjustment of swing amplitude of the vibrating reed, enabling the adjustment of the generator to any desired aerodynamic size.

The reed consisted of a 12 inch long stainless steel plate with a thickness of 1/16 inch. The upper portion was fixed, while the lower end was free to move. At this lower end, a small connector was used to support the desired wire size which acted as the reed. Selection of wire diameter was contingent upon the required droplet size.

The fluid reservoir in which the reed vibrated consisted of a slot cut in a 1 X 3/4 X 1 inch piece of plexiglass. Two such reservoirs with different slot thicknesses were used in this study. Larger droplets were easily generated using a reservoir with a 1/8 inch slot, while a 1/16 inch slot thickness was used to obtain the smaller droplet sizes. The reservoir was held in place by a 3/4 X 1/8 inch aluminum bar approximately 13 inches long. The upper portion of this bar was connected to the aforementioned three positioning micrometers. As these micrometers were adjusted, the entire bar holding the reservoir was moved.

The fluid reservoir had a small diameter hole drilled from the downstream side through the solid plexiglass above the slot. This hole terminated in the center of the slot and was used to provide a path between the slot and the infusion pump. The infusion pump

compressed a syringe, thereby generating a continuous stream of fluid into the fluid reservoir. A long plastic tube with the appropriate fittings provided the connection of the syringe and the fluid reservoir.

A small rectangular flat faced electromagnet, model EM-622, was used as the device causing the vibrating motion. The magnet was driven by an alternating current signal. This caused the magnet to change polarity, and thus the shaft of the reed was forced to vibrate. A circuit was developed to allow the input of the alternating current to the magnet. The alternating current was supplied by a BK Precision solid state model E-3108 sine/square wave generator. This wave generator allowed the frequency to be adjusted so as to also optimize the droplet generation. A General Radio 1531-AB strobe light was tied into the signal generator, allowing the operator to observe the motion of the reed and the path of the droplets being generated. A delay was connected to the strobe so that both the generated droplets and the vibrating reed could be seen at any location of the continuous cycle. Liquid droplets ranging in aerodynamic size from 50 to 1000 microns could be generated with this system.

5.3 Humidity and Temperature Control

A wide range of temperatures and relative humidities were attained with the equipment installed in this facility. The tunnel air temperature and humidity were controlled with the aid of sensors located just upstream of the test section. The temperature sensor was a thermistor which registered relative values via changes in internal resistance. A lithium chloride temperature compensated sensor was used to control and

detect changes in relative humidity. The exact test section temperature and relative humidity were monitored with a psychometer located downstream of the test section. Both the temperature and humidity sensors were wired into a control circuit housed in a metal cabinet. Set controls for the temperature and humidity were contained in the control circuitry and were mounted on this cabinet. The desired values of temperature and humidity were obtained by manually adjusting the set controls until the conditions were met. The controlling circuitry maintained the values of temperature and humidity at the set values. If the temperature drifted below the required value, the circuitry activated the heat exchangers. Similarly, if the temperature was too hot, the air compressor and refrigeration unit was activated and cooling initiated. The relative humidity was maintained in an analogous manner.

To provide a greater control in the temperature and relative humidity, each of the systems were provided with toggle switches. The heating and cooling systems had two-way toggle switches that allowed each to be either a part of the controlling system or completely shut off. The humidifier and dehumidifier had three-way toggle switches, the first two options being identical to those of the temperature controls. The third option allowed the system to remain on constantly, independent of the sensor's signal to the controlling circuit.

The heat used in the facility was supplied by an electrical heating coil that covered the entire flow area. The air was cooled using a compressor, condensor and receiver system that used 45 ounces of Freon-12 flowing through an evaporator coil design. Both systems were located just upstream from the test section to allow better control of the temperature. The control circuitry mentioned above alternately activated

the heating and cooling systems depending on the temperature of the wind tunnel air as compared with the desired testing temperature.

The system used to maintain the humidity was somewhat different from the system used for the temperature control. When the air humidity was higher than the required test humidity, the air was diverted through a Dryomatic Model R-150 Dehumidifier. This dehumidifier continually regenerated 50% of its desicant by way of a rotating bed. The air was diverted from the closed loop wind tunnel by using two large, automatically controlled butterfly-type valves. One of the valves was located at the diverted section entrance and the other was located downstream in the main tunnel. Both valves rotated $\pm 90^{\circ}$ at their center and were spring-loaded to remain closed unless they were forced to rotate. A rope and pulley were attached to the center axis of these valves and were interfaced to electromagnets. These electromagnets were supplied current by the controlling circuit, thereby forcing the valves open. When the humidity level exceeded the desired level, the air flow was diverted by closing the main tunnel valve and opening the diversion tunnel valve. The opening and closing of these valves was performed by the controlling circuitry by supplying current to one of the two electromagnets interfaced with the valves. The third toggle switch configuration mentioned earlier forced the appropriate valve to remain open continuously. As with the temperature system, the sensor's reading was used by the controlling circuitry to maintain the humidity. When the humidity level was too low, a water atomizer was used to raise the humidity. This atomizer was fitted with a heater to allow large amounts of water to be supplied to the air. The atomizer was located

in the section upstream of the test section and delivered the water through a four-way manifold to allow uniform humidity across the tunnel test section.

5.4 Velocity Monitoring

Determination of the test section velocity was accomplished with the aid of a temperature compensated hot film anemometer. The sensor was placed in a reduced cross section area in the facility, with 10^{o} maximum converging angles to prevent separation and allow accurate calculation of the low velocities realized in the test section.

5.5 Microscope

Magnification of the image of the pendant droplet was necessary to simplify the acquisition of the evaporation rate data. A microscope developed by Dick Rossmiller Company of Boulder, Colorado was used to produce an image of workable size. The microscope's specifications included a range of magnification of 2.5X through 2500X and a working distance of .700 to 7.000 inches. It was mounted on a stage that allowed limited movement in three directions, twelve inches vertically and two inches both longitudinally and laterally. The back lighting for the microscope was provided by fiber optics. A Dolan-Jenner Fiber-Lite illuminator, model 170-D, was used as the light source. The light was also provided with movements both horizontally and laterally to allow it to be positioned directly over the microscope. Three leveling adjustments were also used to ensure the acquisition of uniform illumination. A columnating system of lenses was used with the back light to supply uniform parallel lighting. The inside of the microscope as well as its various attachments were lined with black felt or painted black to reduce reflection.

5.6 Camera and Microcomputer Description

To determine the evaporation rates of droplets under free fall conditions it was necessary to acquire data on: (1) the droplet size, and thus allow computation of the corresponding settling velocity; (2) the wind tunnel velocity, and the correction of the wind tunnel velocity to the calculated value. A measurement and control scheme of this complex operation required the use of a microcomputer. The Evaporation Rate Facility at Colorado State University Aerosol Science Laboratory used a microscope fitted with a Reticon solid state camera to measure the droplet size. A Texas Instruments TI-990 microcomputer was used to perform the necessary computations and control operations.

5.6.1 System Operation

A pendant droplet, held stationary in the microscope viewing field by a small stainless steel, tungsten or platinum wire, was imaged on a 100 X 100 detector array within the Reticon camera. The Reticon camera controller provided the timing and video signal processing necessary to form an image on a video monitor. The resulting binary video output was obtained by comparing the signals from the camera to a threshold set by the operator. The droplet size was determined by the number of photodiodes occluded above the threshold. This count was proportional to the average projected area of the pendant droplet. The computer read the data from the counters and calculated the droplet size using calibration data stored in memory and a simple mathematical algorithm. The settling velocity corresponding to the measured droplet size was calculated and compared to the actual tunnel velocity as determined by the air meter, analog multiplexer, and analog to digital converter (see Figure 1). The measured droplet size, wind tunnel velocity, and

elapsed time from the start of the test were displayed on the CRT terminal and simultaneously transmitted to the Colorado State University Cyber computer for storage.

Two modes of operation were required of the data acquisition system, the time measurement and the calibration mode. The typical time step used in the data acquisition was approximately one second. The count mode or calibration mode was used to determine the calibration factors each day. While operating in this mode, the microcomputer displayed on the terminal the number of photodiodes not illuminated above the threshold during the previous frame scan. This was done by subtracting the diodes illuminated above the threshold from the total number, ten thousand. No other calculation or control operation were performed in this mode.

5.6.2 Reticon Camera and Controller

The Reticon MC520 camera was based on a solid state image detector formed by a 100 X 100 photodiode array (10,000 pixels). Center-to-center spacing of the pixels was 60 microns. The electronic circuitry needed for scanning the diode array was contained within the camera. The RS520 camera controller provided the camera power and the circuitry used in the synchronizing of clock signals for scanning. The photodiode scanning rate was determined from controller settings and could vary from 25 - 500 frames/second (250 kHz - 5 MHz). Camera focusing was achieved manually by observing the video monitor driven by the x,y,z display monitor drive signals from the controller. Necessary adjustments with the microscope were then made until the image on the video monitor was focused. As each pixel was scanned, the camera output to the controller a voltage pulse proportional to the light intensity on that

pixel integrated over one frame period (1/25 - 1/500 second). The amplitude of each voltage pulse was compared to the voltage level of an adjustable threshold in the controller. The threshold voltage level produced a bi-level digital video, the same as the pixels above the threshold voltage. Counting the number of true pulses, pixels above the threshold, for one frame scan provided a number proportional to the droplet size during that frame period.

5.6.3 Computer Configuration

The TI-990 microcomputer components included:

1) TM 990/101M Microcomputer Board
2) TM 990/201 and TM 990/206 Expansion Memory Boards
3) TM 990/302 Softward Development Board
4) TM 990/310 48 Bit I/O Board
5) TM 990/512 Prototype Board

The TM 990/512 prototype board served to interface the microcomputer to the velocity and droplet size sensors. This board consisted of specialized circuits wired by Aerosol Science Laboratory personnel. Digital counters and their associated control circuits interfaced with the Reticon RS520 camera controls. An analog multiplexer and analog to digital converter (A/D) allowed the measurement of wind tunnel velocity by the computer, and a digital to analog converter allowed computer control of this velocity. Transfer of data from the counters and A/D to the microcomputer board was facilitated by the TM 990/310 48 bit I/O board. Software, written by Aerosol Science Laboratory personnel, resided in RAM on the 101M and 206 boards and in RAM and EPROM on the 201 board. The computer operating system resided in the 302 software

development board. The Cyber interface and overall system operation was controlled by the 101M board.

5.6.4 Calibration Procedure

The Reticon camera was calibrated daily by determining the number of photodiodes occluded by a known area. The step-by-step procedure for calibration follows:

1) Illumination intensity and uniformity were adjusted while monitoring the z axis video on an oscilloscope. The intensity was set at approximately 90% of saturation.

2) The data threshold in the camera controller was set at approximately 80% of saturation.

3) An opaque ink stained dot of known diameter was observed by the microscope. The count of the number of diodes occluded by this dot was obtained with the computer in the calibration mode. This count was taken several times with the dot at random locations in the viewing field. The count was averaged and labeled NCAL. The incremental area corresponding to a single diode was determined by

$$\Delta A = \frac{\pi(\text{Diam})^2}{4\text{NCAL}} \tag{5.1}$$

where Diam was the diameter of the ink dot.

4) A stainless steel, tungsten or platinum wire of appropriate diameter was positioned in the viewing field. The count of diodes occluded by the image of the wire alone was taken several times and averaged. This average value is named NWIRE.

Chapter 6

REAGENTS

Time history evaporation rates for 13 mixtures along with water were to be studied. The solutions correspond to common pesticides and pesticide components used today. These solutions and their densities in grams per cubic centimeters can be seen in Table 2.

Table 2

Solutions and Their Densities

Mix Index	Mixture	Density (gm/cc)
1	0.5 gallons of Sevin-4 oil 0.48 gallons of No. 2 Fuel oil 0.02 gallons of Automate Red B dye	0.88062
2	½ ounce of Polyhedra Douglas Fir Tussock Moth Nucleopolyhedrosis Virus ½ gallons of Molasses 0.7 gallons of water NaOH-amount sufficient to make ph of mixture between 6.0 and 7.2	1.03551
3	0.80 gallons of Sevin-4 oil 0.48 gallons of No. 2 Fuel oil 0.02 gallons of Automate Red B dye	0.98770
4	0.98 gallons of No. 2 Fuel oil 0.02 gallons of Automate Red B dye	0.86090
5	0.50 gallons of Thuricide 16B 0.50 gallons of water	1.12600
6	½ pounds of Orthene 75S 1 gallon of water	1.02004
7	1 pound of Orthene 75S 1 gallon of water	1.0428
8	2 quarts of Dow Esteron (2,4,5,-T) 10 gallons of water	1.01224

Table 2 (Cont'd.)

Mix Index	Mixture	Density (gm/cc)
9	2 quarts of Dow Esteron 99 10 gallons of water	1.00882
10	½ pound of Dipel ½ pound of Shade 1 gallon of water 0.016692 pounds Rhodamine B extra	1.05404
11	½ pound of Dipel 1 gallon of water 0.016692 pounds Rhodamine B extra	1.03008
12	water	1.00000
13	5 ounces of Nalco-Trol 100 gallons of water	1.00070
14	10 ounces of Nalco-Trol 100 gallons of water	1.00140

Chapter 7

EXPERIMENTAL PROCEDURE

7.1 Testing Procedure

The experimental test conditions used in this study are given in Table 1. All combinations of the three variables were obtained by holding two constant and performing tests for the different values of the third. Once the conditions of the test were selected, the wind tunnel was sealed and the desired temperature, humidity and initial velocity of the tunnel air were set and allowed to stabilize. The initial wind tunnel velocity corresponded to the settling velocity of the droplet to be generated.

Once the temperature and humidity had stabilized at the desired values, droplets of the given solution were generated by the vibrating reed aerosol generator. A single droplet was collected on the suspended wire within the viewing field of the microscope. Droplet diameters within a range of ±10% of the nominal diameters were deemed acceptable for the tests. Data collection and wind tunnel velocity control was initiated with a single command to the microcomputer and continued until stopped by the operator. The researcher based the decision to stop a test by viewing data displayed on the CRT terminal. At every second the droplet diameter, wind tunnel velocity and elapsed time were displayed on the terminal. The general criteria used by the researcher to stop the test are listed in Table 3. These general test-ending criteria

Table 3

General Test-Ending Criteria

The time interval of any test was to be the minimum of the following:

1) The time required for the droplet to undergo a 90% change in original diameter.
2) The droplet diameter becomes less than 10 microns.
3) The time it takes for the droplet to fall 300 feet.
4) 30 minutes.

were contractually predetermined and represented limits that occur in actual spraying operations. The behavior of the individual solutions could also dictate separate test-end rationale for each solution. These individual criteria became apparent during the collection of data and will be discussed when appropriate.

7.2 Adjustments in Facility Equipment

Several adjustments of the facility equipment were required when the initial droplet diameter was varied. Different sizes of reed diameters, ranging from 25 - 250 microns, were used for the vibrating reed aerosol generator. The diameter of the reed depended on the droplet diameter to be generated and the pesticide solution. The physical properties of each solution varied considerably. This required the use of different reed sizes and micrometer settings to generate droplets of the same diameter between different solutions. In general, a reed diameter of approximately one half of the proposed droplet diameter was used by the aerosol generator. The micrometer settings were then varied until a droplet within the respective range was generated.

The magnification of the microscope was also changed as the droplet diameters were varied. This was accomplished by changing the eyepiece of the microscope. During tests of the large initial droplet diameters, 250 and 400 microns, a 10X eyepiece and a 10X objective lens were used with the microscope. A 20X eyepiece was used with the 10X objective lens in those tests which required observation of the smaller initial droplet diameters. This change was necessitated to eliminate sizing errors that would occur by viewing the small droplets with the original magnifications.

The last required adjustment was the choice of the diameter to be used for the supporting wire. Three different wire materials and sizes were utilized throughout this study. A platinum wire with a diameter of 17.3 microns and a stainless steel wire measuring 25 microns in diameter were used arbitrarily while performing the 250 and 400 micron tests. A 5 micron tunsten wire was used to collect the smaller diameter droplets. The reason for the change in supporting wires for the smaller droplet diameters was to reduce the pixel count due to the presence of the wire. The count of the larger wires promised to be approximately the same as the count of the smaller diameter droplets. This was felt to produce significant errors in measuring these droplet diameters. The use of the smaller wires eliminated this problem as well as facilitating the collection of the smaller droplets.

7.3 Time Delay

One additional comment concerning the experimental procedure must be made. An increment of time existed between the actual collection of the droplet on the wire and the start of a given test. This time delay was unavoidable when using the described experimental procedure. In order to account for this delay, a stop watch was used to record this difference in time. The stop watch was started the instant the droplet settled on the supporting wire. The difference between the elapsed time recorded by the test and the time recorded by the stop watch was found to be the time delay. An average value of approximately six seconds was used for those tests in which a time delay was not recorded. This time delay was required in order to determine the actual initial droplet diameter.

7.4 Transparent Solutions

Some of the pesticide solutions used in this study were transparent. A problem became apparent when droplets of these solutions were observed with the microscope. The back lighting required by the microscope caused the center portion of the droplet to be too light to occlude the pixels. This glare exceeded the threshold level set in the Reticon Camera Controller, thereby producing an erroneous droplet diameter to be calculated. To eliminate this problem, Rhodamine B dye was added in small amounts to the transparent solutions. This addition increased the opacity of the droplet and enabled the actual droplet diameter to be measured. Great care was taken to add negligible amounts of dye to preclude any effect on the evaporation process. Concentrations less than 0.2% were used.

7.5 Data Collection and Reduction

The values of NCAL and NWIRE, described in Section 5.6.4, were used by the microcomputer to determine the evaporating droplet's size at each time step. The pixel count due to the evaporating droplet and its supporting wire was taken at each time step when the computer was in the testing mode. Each of the counts was proportional to the area covered by the evaporating droplet and the wire. Therefore, the field-of-view area covered by the evaporating droplet and wire was:

$$(\text{count})\ \Delta A = \text{AREA} \tag{7.1}$$

The methodology used for the diameter calculation is best seen by referring to Figure 1 and noting that the area occluded by the droplet and wire in the viewing field can be divided into three sub-areas:

1) The cross-sectional area of the droplet not common to the wire.

2) The area common to both wire and droplet.

3) The total cross-sectional area of the wire.

Also note that the width of the wire can be approximated by:

$$W = (NWIRE)/100)(\Delta A)^{1/2} \tag{7.2}$$

The assumption that the wire diameter was small in comparison to the droplet diameter yields the following quadratic:

$$AREA = \frac{\pi Diam^2}{4} - (W)(Diam) + NWIRE\ \Delta A$$

$$(Count)\Delta A = \frac{\pi Diam^2}{4} - \frac{(Diam)(NWIRE)}{100}\ (\Delta A)^{1/2} + NWIRE\ \Delta A \tag{7.3}$$

In the equation, count refers to the number of diodes occluded by the evaporating droplet and wire. The ΔA and NWIRE values were determined with the calibration procedure each day. Therefore, the resulting equation could be solved yielding a droplet diameter, Diam, at each time step. This diameter was used in the following equations for drag coefficient and settling velocity to obtain the required wind tunnel velocity.

$$C_D = \frac{24}{Re} + \frac{6}{1 + \sqrt{Re}} + 0.4 \qquad \text{(Taken from Reference 12.)}$$

$$V_T = \left[\frac{4/3(Diam)\ g(\rho_p - \rho_a)}{C_D \rho_a} \right]^{1/2} \tag{7.4}$$

The wind tunnel velocity was adjusted to this value by the microcomputer at each time step. The value of ρ_p, or the density of the droplet, was assumed to remain constant throughout the test. This simplifying assumption was used to avoid the complex relation of the droplet density as a function of time. This relation was unknown and would require extensive research to determine. For this reason, the assumption of a constant density was believed to represent a reasonable approximation of the actual physical process.

Chapter 8

RESULTS AND DISCUSSIONS

8.1 Experimental Data

The data obtained in the study consisted of the droplet diameter recorded at a time step equal to one second. In addition to this diameter, the actual wind tunnel velocity was recorded. Each set of data was curve fitted to a third order polynomial derived to present an averaged but accurate result. Along with the third order equations, values of the average errors between the actual data and the third order functions were calculated. These terms, called Delta, represented a closeness of fit value for the third order smoothing. The third order functions were used over a limited range for some of the highly volatile solutions tested at the small droplet diameters. This limited range was necessitated by large errors encountered by forcing the entire test to fit a polynomial constant after the evaporation process had ended. For these cases, the range of time in which the third order function was applied accompanies the equation. The complete set of raw data obtained in this study was stored on a magnetic tape. The order of tests and the required accessing procedures are listed in Appendix 5.

8.2 Elimination of Tests

8.2.1 Solutions of Low Volatility

Among all of the 14 pesticides and pesticide components, two distinct groups of solutions were prevalent. The first group contained

water as part of the total mixture and had a tendency to evaporate relatively fast. The second group, solutions 1, 3 and 4, contained oil and evaporated at a much slower rate. Close examination of the data obtained for the second group of solutions revealed two notable tendencies. First, when working with the larger diameter droplets, 250 and 400 microns, the total change in droplet diameter was less than 5%. The initial tests were performed at the extreme conditions felt to produce the greatest amount of mass transfer--i.e., high temperatures and low humidities. Since the change in diameter at these critical conditions was small, the change in diameter using low temperatures or high humidity values could also be assumed to be small. Therefore, tests that were to be performed at low temperatures or high humidities were eliminated.

Examination of the smaller diameter tests, 50 and 100 micron initial diameters, revealed the second trends. Tests were performed using these solutions over the time interval required for the droplet to fall 300 feet. Examination and comparison of the tests performed at 20 and 60% relative humidities showed little or no difference. It was concluded that raising the relative humidity to 90% would produce results not achieving the minimum criteria of Table 3. Therefore, the tests were eliminated with 90% relative humidity at all temperatures. Tables showing the rationale used to eliminate the tests for solutions 1, 3, and 4 can be seen in Appendix 1.

8.2.2 Solutions of High Volatility

Time rate evaporation histories were to be obtained for solutions 13 and 14 which contained different concentrations of Nalco-Trol and water. After acquiring data under a variety of test conditions, the

Nalco-Trol additive was found to have no significant effect on the rates of evaporation of the droplets. The result was that the time rate histories were essentially identical to the previous data determined for water. To ensure this result, a new solution was mixed which increased the amount of Nalco-Trol added to the water by a factor of ten. Examination of the data corresponding to this new solution produced similar results--the Nalco-Trol did not detectably retard the evaporation process.

Another test was developed and performed to support the results obtained using the evaporation rate facility. Approximately 10 cubic centimeters each of water, solution 13 and solution 14 were measured into 100 ml beakers. These beakers were set side by side and weighed at prescribed time intervals. The mass lost by free evaporation from the beakers was then compared. The mass loss of each solution was normalized to a percentage by dividing by the total mass. These percent mass losses were then plotted as a function of time and compared (see Appendix 2). The comparison showed a negligible difference in the loss of mass between the solutions at all times. Therefore, the conclusion was sustained--solutions 13 and 14 evaporated at the same rate as water. The remaining tests were then eliminated for solutions 13 and 14.

It should be mentioned that the addition of the Nalco-Trol did significantly affect the generation of the droplets. The Nalco-Trol additive greatly increased the surface tension or "elasticity" of the solution. The result was that the solution would stretch considerably before the filament of fluid would relax and form a droplet. This indicates that the Nalco-Trol additive may serve to reduce the number of

fine droplets formed, thus reducing drift loss and perhaps narrow the resulting size distribution of droplets formed by presently used atomization systems.

8.3 Small Droplets of Volatile Solutions

8.3.1 Length of Tests

Tests performed on solutions 2 and 5 - 11 that contained large amounts of water were seen to evaporate rapidly using the small initial droplet diameters. Most of the change in droplet diameters occured in the time required for crystallization to begin. In tests involving these solutions, a relitively constant diameter particle remained on the wire after the first minute of the test. To insure no additional change would be experienced, each test was performed over a period of 200 seconds. In all cases none of the test-ending criteria of Table 3 were met during this interval. However, it was assumed that the evaporation process had been completed and the tests could be ended.

8.3.2 Approximation of Tests

An empirically calculated technique was used for solutions 2 and 5 - 11 with initial diameters of 50 microns and additionally an initial droplet diameter of 100 microns for solution 5. The rapid evaporation and difficulty found in generating and collecting small droplets required for these tests necessitated the application of this technique. The parameters, assumptions, and calculations used in this approximating technique can be found in Appendix 3.

The technique used to approximate the small diameter tests relied on four assumptions. Application of this technique also required the evaporation process of a given solution to be divided into three separate stages: normal evaporation, transition and crystallization. The first

stage, normal evaporation, was the portion of the process in which most of the mass was transferred. It was this stage of evaporation that was determined using the first assumption. This assumption stated that a water-based solution evaporated at the same rate as water until the inert material contained in the solution began to crystallize. Direct observation of the present data supported this assumption. This tendency remained consistent for all temperatures and relative humidities. Several authors, including Ranz and Marshall and recently Picot, Chitrangad, and Henderson (9) have reported data that also supports this assumption. Therefore, the first stage of evaporation can be approximated by using the water data obtained by this study. The second-by-second droplet diameters used in the approximated tests were taken from the water data with the appropriate environmental conditions. This was continued until the crystallization stage began.

Determination of the droplet diameter at which the crystallization started (called the critical droplet diameter) required the application of the second assumption. This assumption stated that the crystallization droplet diameter depended on the solution concentration and initial droplet size alone. The ratio of the volumes of the critical droplet to the initial droplet, as stated in assumption three, should then be a constant value for any initial size. This was to remain consistent for any temperature and relative humidity combination. The data obtained for the initial droplet diameters of 100 microns were used to obtain an average ratio of volumes for critical to initial droplet diameters. Therefore, the critical diameter for an original diameter of 50 microns could be approximated. This critical diameter used in combination with

the first assumption and the appropriate water data was used to approximate the first stage of evaporation.

At the point of crystallization the rate of evaporation reduced significantly. This rate reduction was a result of the decreasing amount of volatile material present. As the evaporation progressed, the volume of the volatile material was continuously reduced and more inert material crystallized. As more and more material crystallized, the rate of evaporation reduced accordingly. The process of reducing the rate of evaporation gradually was seen to be the cause of a curved transition between the first and second, or crystallization, stages of evaporation. This curved transition represents the transition stage of evaporation and will be explored later.

In approximating the second stage of evaporation, a fourth assumption was needed. This assumption was simply a direct observation obtained by examining several tests. The second stage of evaporation, the process in which the critical diameter reduces to a final constant diameter, was seen to be closely approximated by a constant slope line. This slope was seen to be relatively invariant to changes of temperature, humidity and initial droplet size. Therefore, once a value for the slope had been found, it could be used for all droplet sizes and environmental conditions. An average value of this second stage slope was taken directly from the 100 micron tests for each solution. The second stage slope was continued until the evaporation process had ended, or the final droplet diameter was obtained. The final droplet diameter, like the critical droplet diameter, was considered to be dependent upon the original diameter and solution concentration alone. A ratio of the

final diameter to original diameter for each solution was found by averaging the values given by the 100 micron tests. A volumetric concentration relationship could also be used, however the volume of inert material must be known to implement this approach.

Combining the approximation techniques for the first and crystallization stages produced an approximation for the entire evaporation process. The application of these two techniques required the use of the data obtained for water and the given solution with initial diameters of 100 microns. Once the parameters used by this technique were obtained, two sets of diameter-versus-time approximated data were determined and combined. The transition stage of the curve was then found by applying a numerical smoothing subroutine. The subroutine changed the sharp transition between the first and second stages to a smooth gradual curve. This was consistent with the gradual transition between the two stages as seen in actual tests.

Appendix 3 also contains tables listing tests and calculations required to determine the various parameters used in the technique. Statistical values for the mean absolute and probable errors obtained in this technique are given for each solution. Plots of the critical versus original diameters are also shown. Summarizing the errors produced by the approximation technique reveals all are less than 9%. The maximum change in the critical diameter corresponding to this error would be $\pm$ 2 microns. This is equivalent to a volume difference of less than 25%. Therefore, application of this technique enabled data that could not be obtained experimentally to be calculated empirically with confidence in the accuracy of predictions.

8.3.3 50 Micron Tests for Solution 12

Included in the tests using an initial diameter of 100 microns were the data with an original diameter of 50 microns. Since solutions 12, water, was a homogeneous solution, the evaporation should continue uniformly throughout the test until the substance has completely evaporated. The dye needed to view and perform tests for water at 500 and 250 microns was not required for the small diameters. Hence, the tests performed with the original diameter of 100 microns represented pure water. The required data with an original diameter of 50 microns could then be taken directly from the 100 micron tests performed.

8.4 Simulation of Terminal Velocities

The experimental facility used in this study was to determine the rates of mass transfer of droplets falling at their terminal velocities. Droplet diameters were measured at each second and their corresponding settling velocities calculated with equation 7.4. The wind tunnel velocity was then adjusted to the terminal velocities by the microcomputer as detailed in section 5.6.1. The actual test velocity was recorded along with the droplet diameter and elapsed time.

Figure 3 shows a comparison of the calculated and the actual test velocities for a representative test. Examination of this plot reveals that the two velocities were very close at each step. There was a slight deviation in the velocities at the beginning of the test. This was a direct result of the time required for the computer to initiate control of the velocity. The test velocity also tended to be a little larger than the calculated velocity. This indicated that there was a time delay between the determination of the droplet diameter and the adjustment of the wind tunnel velocity. This resulted in the test

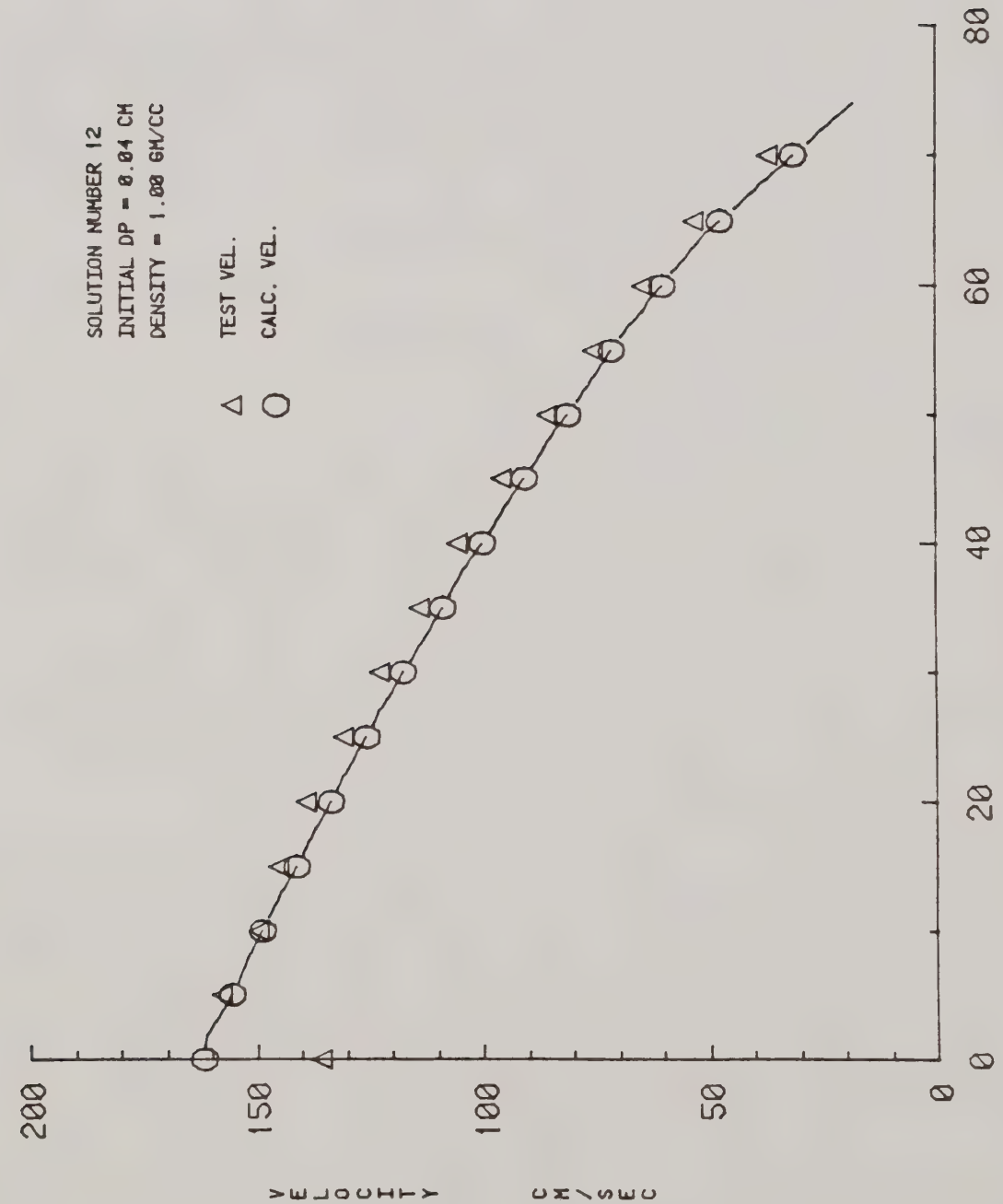

Figure 3. Comparison of Test and Calculated Velocities

wind velocity lagging behind the calculated velocity by approximately one second. However, it is assumed that the differences between the actual test and calculated velocities were negligible. Therefore, the terminal velocities of the droplets simulated in this facility were felt to be accurate.

8.5 Evaluation of Data

8.5.1 Water Data

Of all the solutions examined in this study only one, solution 12, can be explored in the traditional manner presented by Froessling, Ranz and Marshall, and others. The determination of an equation which presents the Sherwood number as a function of Re and Sc required the use of several little known physical properties. Values of the diffusion coefficient and the saturation vapor pressure are not easily obtained for all solutions. These physical properties have been explored at great extent for water, solution 12. Therefore, this solution was used to determine a relationship between the Sherwood number and Re and Sc. This allowed direct comparison of the resulting relationship with those presented by previous authors.

The parameters and equations required to obtain an equation relating Sh with Re and Sc are given in detail in Chapters 2 and 3. Equation 2.6 must be used to determine values of the Sherwood number at every time step. Values for Re and Sc, given by equation 3.1, must also be determined at each time step. The physical properties required to determine these values are shown in Table 4.

In order to use equation 2.6 the temperature at the droplet surface must be known. Ranz and Marshall, Kinzer and Gunn, and Fuchs all state that this temperature is basically equal to the ventialted wet bulb

Table 4

Physical Properties for a Water
Droplet Evaporating into Air

Air Temperature (^{o}C)	Diffusion Coefficient (cm^2/sec)	Dry Air Density (g/cm^3)	Saturation Vapor Pressure (bars)
-5	0.210	0.001088	0.0041
0	0.216	0.001068	0.0061
5	0.222	0.001049	0.0114
10	0.227	0.001031	0.0123
15	0.234	0.001013	0.0171
20	0.240	0.000995	0.0234
30	0.254	0.000962	0.0250

Diffusion coefficients taken from Davies.

Values for the dry air density were calculated from the ideal gas equation.

Values for the saturation vapor pressure were taken from the Steam Tables of Van Wylen and Sonntag (11).

temperature. Experiments have shown that this is true within about 0.2^{o}. Thus, the surface temperature of the droplet was taken as the wet bulb temperature. The vapor pressure at the surface, P_0, was taken to be the saturated vapor pressure at the surface temperature. The free stream vapor pressure, P_∞, was determined by multiplying the air humidity times the saturation vapor pressure at the air temperature. A geometric mean value for the diffusion coefficient was used in this equation, as suggested by Fuchs. This value was obtained using equation 8.1.

$$D = \sqrt{D_0 \, D_\infty} \tag{8.1}$$

The denominator of equation 2.6 could then be calculated. At each step the only change in this value would be the radius of the droplet.

The numerator of equation 2.6 was determined with the data obtained in this study. A higher order central difference method was employed to find the time rate of change of the diameter at each step. The data was first smoothed by a spline and then equation 8.2 was used to determine $\left(\frac{dm}{dt}\right)_c$.

$$\left(\frac{dm}{dt}\right)_c = 4\pi\rho_p \, a^2 \left(\frac{da}{dt}\right)_c \tag{8.2}$$

This mass derivative was calculated at each time step and divided by the denominator to obtain a value for the Sherwood number for each second.

Most authors have related the Sherwood number as a function of Re and Sc. The most commonly published of these relationships has been $Re^{1/2}Sc^{1/3}$. The value of $Sc^{1/3}$ remained constant for a given temperature using water. $Re^{1/2}$ varied as the droplet diameter decreased. Because the described facility simulated terminal velocities, both a and V_T varied in the equation for Re. This value was calculated at each second and used to obtain a value of $C = Re^{1/2}Sc^{1/3}$.

Values for Sh and C were determined for solution 12 using tests with every variation of temperature, relative humidity and initial diameter. Examination of tests using the high humidities indicated that at 20°C and 15°C the actual humidity attained was somewhat less than the desired 90%. The reason for this discrepancy was the difficulty in sustaining the required amount of moisture in the air at these higher temperatures. Great difficulty was found while attempting to stabilize the humidity at high temperatures. The stabilization of these high humidities was also hindered with the small diameter droplets. The wind tunnel was operated at low velocities in order to match the terminal velocities of these small droplets. These low ventilation velocities resulted in slight alterations in the wind tunnel air humidity. Because the velocities were so low, a consistent value of relative humidity was not easily maintained using the high humidities, 90%. For these reasons, none of the tests requiring 90% relative humidity were included in the analysis to find Sh as a function of C.

The values of Sh and C were plotted over the ranges obtained in this study. A linear regression was performed over these ranges of Sh and C. The plot and resulting regression equation are shown in Figure 4. The equation representing the results obtained by this study is given in equation 8.3.

$$Sh = 1.755 + 0.535\ Re^{1/2} Sc^{1/3} \qquad (8.3)$$

A significant amount of scatter was shown by the plot and the value given for the average percent error. This scatter was a result of the variety of initial conditions used. Four temperatures, two humidities, and three initial droplet diameters were used to obtain the

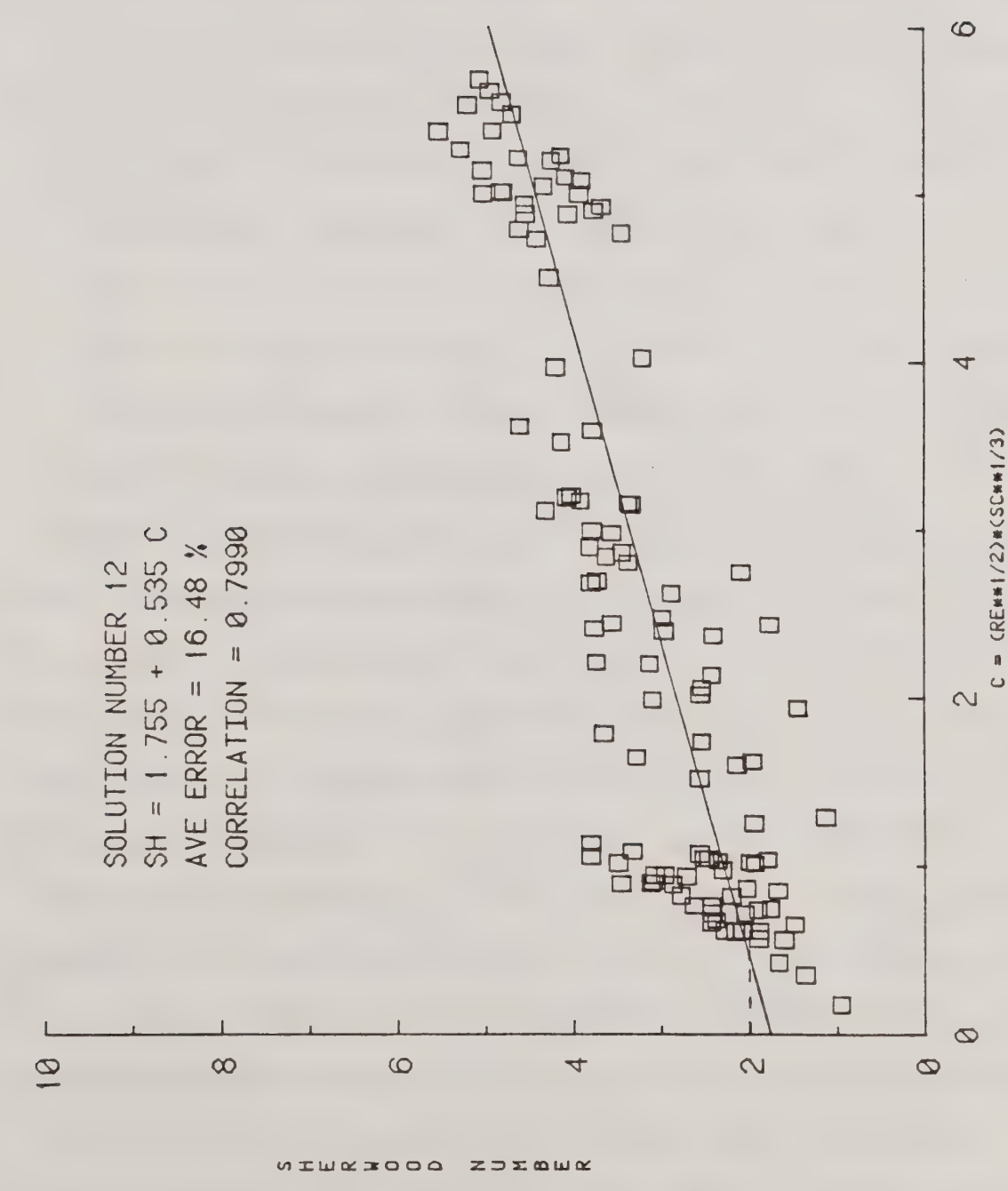

Figure 4. Sherwood Number as a Function of Re and Sc

results. The regression equation given correlated to the data fairly well. A correlation coefficient of about 0.8 was found and indicated a relatively close fit. The outer lying data points shown in Figure 4 were produced by actual test conditions different from those recorded. The outer points lying below the regression line correspond to low temperature and low humidity tests, or tests performed at 5^{o} C and 20% humidity. Similarily, the outer most points above the line were obtained with tests using the higher temperatures and humidities.

The representative equation, 8.3, agreed well with previous results. The mass transfer coefficient, β=0.535, was very close to those obtained in other works. However, the intercept term, α, obtained in this study differed from those reported previously. Previous authors have determined this intercept value to be equal to the theoretical lower limit of Sh=2. Ranz and Marshall determined an intercept of 1.79 experimentally using water. The authors believed that the low value was caused by neglecting the change in vapor concentration at the surface of the drop. Beard and Pruppacher have also reported an intercept below the theoretical lower limit. However, the authors described the convective mass transfer with two equations for two seperate ranges of $C=Re^{1/2}Sc^{1/3}$. A straight line was drawn from the last data point to the lower limit of Sh=2. In this way, the data was represented in two ranges in order to conform to the theoretical requirements as well as the data obtained experimentally.

The present study established an intercept of α=1.755. This value is below the theoretical lower limit of Sh=2, shown in Figure 4 by the dashed line. Limited data were obtained in the lower range of

C. Therefore, an actual description of the regression curve in this lower region was not possible. However, the trend of experimental data justified the continuation of the regression line to C=0. Values below the theoretical lower limit of Sherwood number equal to two could be obtained using the model representing the present experimental data. This indicates that a discrepancy exists between the theory discribed in Chapter 2 and the experimental data aquired in this study.

8.5.2 Effects due to Changes in Experimental Conditions

The effects of relative changes in temperature, relative humidity, and initial droplet diameter can easily be seen with the use of plots. Plotting every combination of condition and comparing them would require a great amount of time and space. For this reason, a representative set of conditions were chosen. Plots comparing the relative effects were performed by holding two of the conditions constant and varying the third. Therefore, three plots of multiple curves were obtained for each solution. The elimination of some of the tests reduced the amount of curves on some of the plots. The representative conditions were set at $20^{\circ}C$, 20% relative humidity, and an initial droplet diameter of 100 microns. Again, this condition represented the highest rate of volatility.

In order to allow the direct application of the data obtained, the cumulative percent of mass lost was plotted as a function of time. In order to determine the actual percent loss of mass at each time step, the original droplet diameter needed to be determined. This was found by using a relationship of the droplet's surface area at constant velocities. At a constant velocity, the slope of the surface area versus time curve can be seen to be constant.

$$\frac{da^2}{dt} = \frac{-2D}{\rho_p} (C_a - C_\infty) = \text{constant} \qquad (8.4)$$

During the delay time between the collection of the droplet and the start of the data acquisition, the wind tunnel velocity remained constant. Therefore, equation 8.4 could be used to find the original droplet diameter. The constant slope of the surface area versus time was approximated from the first three data points. This slope was then multiplied by the delay time and added to the surface area of the first data point. The resultant initial surface area was used to find the initial droplet diameter. The percent loss of mass at each time step can then be calculated using the initial diameter with the diameter at each step. Again, the assumption of a constant droplet solution density must be made. As stated previously, this assumption is incorrect, but allows a close approximation. Using the assumption of a constant density of the droplet, the cumulative loss of mass at each time step was found by equation 8.5.

$$\text{percent mass loss} = \frac{(a_{int})^3 - (a)^3}{(a_{int})^3} \qquad (8.5)$$

where a_{int} is the initial droplet radius. Solving equation 8.5 for each time step allowed the curves of mass loss over time to be obtained.

As mentioned in section 8.2, two distinct groups of solutions can be seen -- water-based and oil-based pesticides. Generally, the solutions in each group behave similarly. The results of the procedure given above will be examined in these general groups. Distinct individual characteristics of each solution will be detailed during these discussions.

The plots of percent loss of mass as a function of time given in this study can easily be used for direct application. Knowing the temperature and relative humidity of the surrounding air and the average droplet size produced by a spray nozzle, allows the operator to determine the approximate total loss of mass occurred over a specific time. The percent loss of mass for a single droplet as given by this study could be used to approximate the percent of mass lost in a spraying operation. The spraying height of the operation and the terminal settling velocities of the droplets can be used to determine the time interval of the operation. The average droplet diameter produced by a spray nozzle could be used with the appropriate plot to give an approximate percent of mass lost for the given time interval. This could then be used with the total starting mass to determine the amount of pesticide remaining. Thus, the mass of pesticide reaching the intended target is approximated. This result would be conservative as the effects of aircraft wake and atmospheric turbulence have not been considered. A more involved procedure could be used to find a closer approximation if the droplet distribution produced by the nozzle was known. Summing the loss of mass from the

different droplet sizes would yield a total percent of mass lost. Again, the pesticide remaining could be determined. This remaining mass of pesticide would give an idea of the effect on the insect population produced by the spraying operation.

Using combinations of the resulting plots of this study would allow the acquisition of the percent of mass lost for conditions not shown. The relative differences between curves with varying temperatures, humidities, and droplet sizes can be used to determine the percent loss of mass of a given condition. A simple example will illustrate this point clearly. The percent of mass lost after five seconds of solution 12 at $20^{o}C$ and 60% relative humidity with an initial diameter of 240 microns is desired. Using Figure 22, the percent loss of mass of the same droplet with a 20% relative humidity was about 20% after five seconds. A droplet whose diameter was 100 microns in the $20^{o}C$ and 20% humidity air lost about 75% of its mass after five seconds. From Figure 44, the same droplet with a 60% humidity lost only 40% of its mass after five seconds. Using these three conditions, the mass loss of the 240 micron droplet at $20^{o}C$ and 60% relative humidity after five seconds can be approximated by:

$$\text{mass loss } (240\ \mu m,\ 20^{o}C,\ 60\%) = \frac{0.20}{0.75}\ (0.40) = .106 = 10.6\%$$

An actual test of a droplet with a diameter of 240 microns at $20^{o}C$ and 60% relative humidity lost 10% of its mass after five seconds. Therefore, this procedure will allow a close estimate of the percentage of mass lost for conditions not included in the plots.

8.5.3 Solutions of Low Volatility

Solutions 1, 3 and 4 were included in this group of solutions. Each was composed of varying amounts of Sevin-4 and No. 2 fuel oil. The relative effects caused by changes in droplet diameter, temperature, and relative humidity can be seen in Figures 5 - 13.

8.5.3.1 Change in Initial Droplet Diameter

Figures 5 - 7 show the mass loss of solutions 1, 3 and 4 respectively for four different initial droplet diameters. The actual initial diameters are also given. The rate of mass loss can be seen to increase as the initial diameter decreases. At successively smaller droplet diameters the rate of percent loss of mass increases. Figure 6, corresponding to solution 3, shows a variation to this observation. The two larger droplet diameters have near identical curves for very different initial diameters, 420 and 240 microns. This may be a result of the increased amount of Sevin-4 oil used in this solution. Figure 7 also shows near identical curves for the two larger droplet diameters. However, these initial diameters are fairly close, 330 and 280 microns, so that near identical curves could be expected. In these figures, the curves corresponding to an initial diameter of 50 microns have a great deal of scatter. Small variations in the droplet diameter measurements become more evident using these small initial diameters. Therefore, the resulting curves of percent loss of mass versus time show some scatter. A smooth curve was drawn through the points to represent the data. With the solutions of low volatility a decrease in the initial diameter from about 400 to 50 microns will increase the percent loss of mass from approximately four to close to 20% after 50 seconds. This is an increase

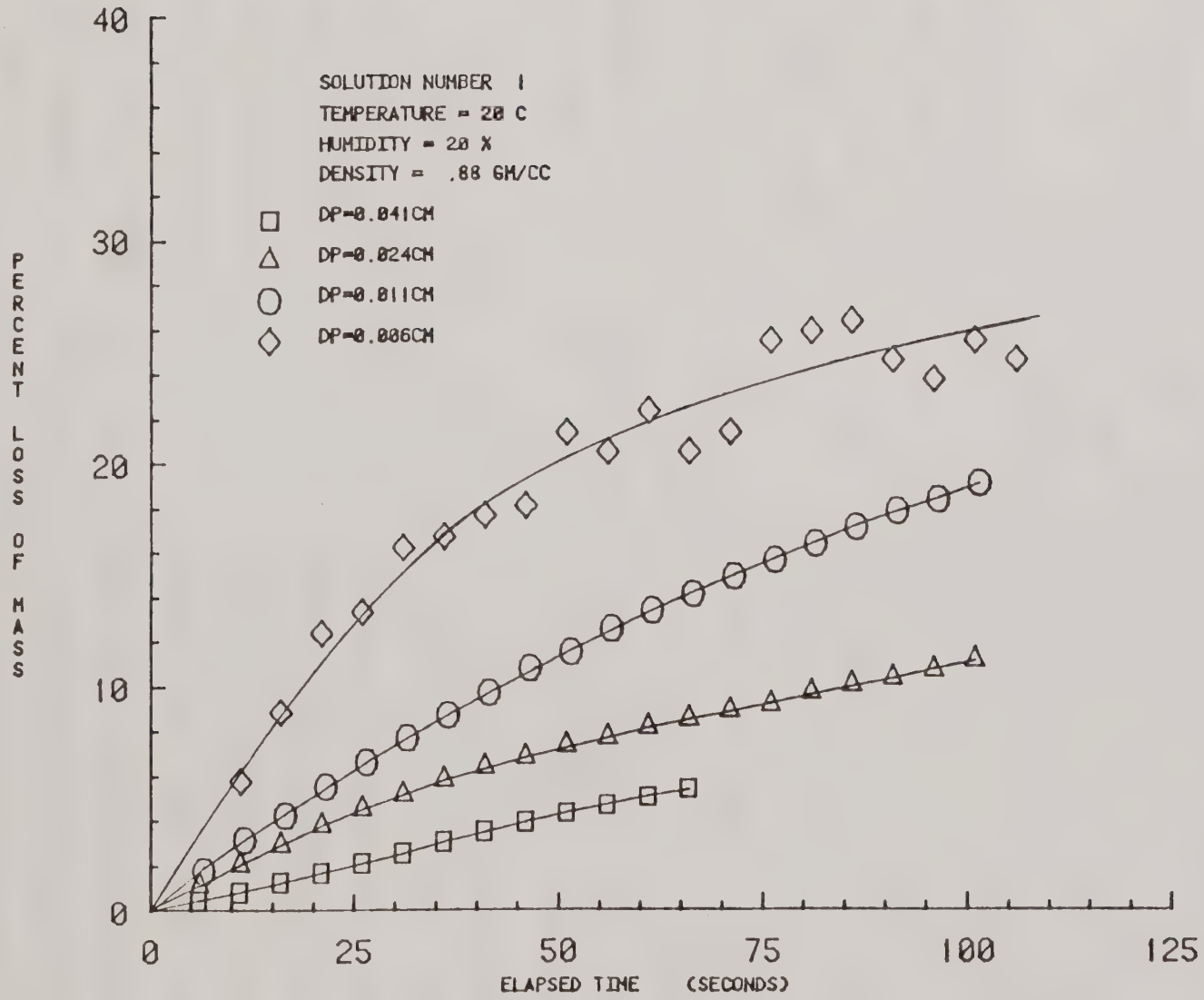

Figure 5. Relative Effects of Percent of Mass Loss by a Change in Initial Diameter for Solution 1.

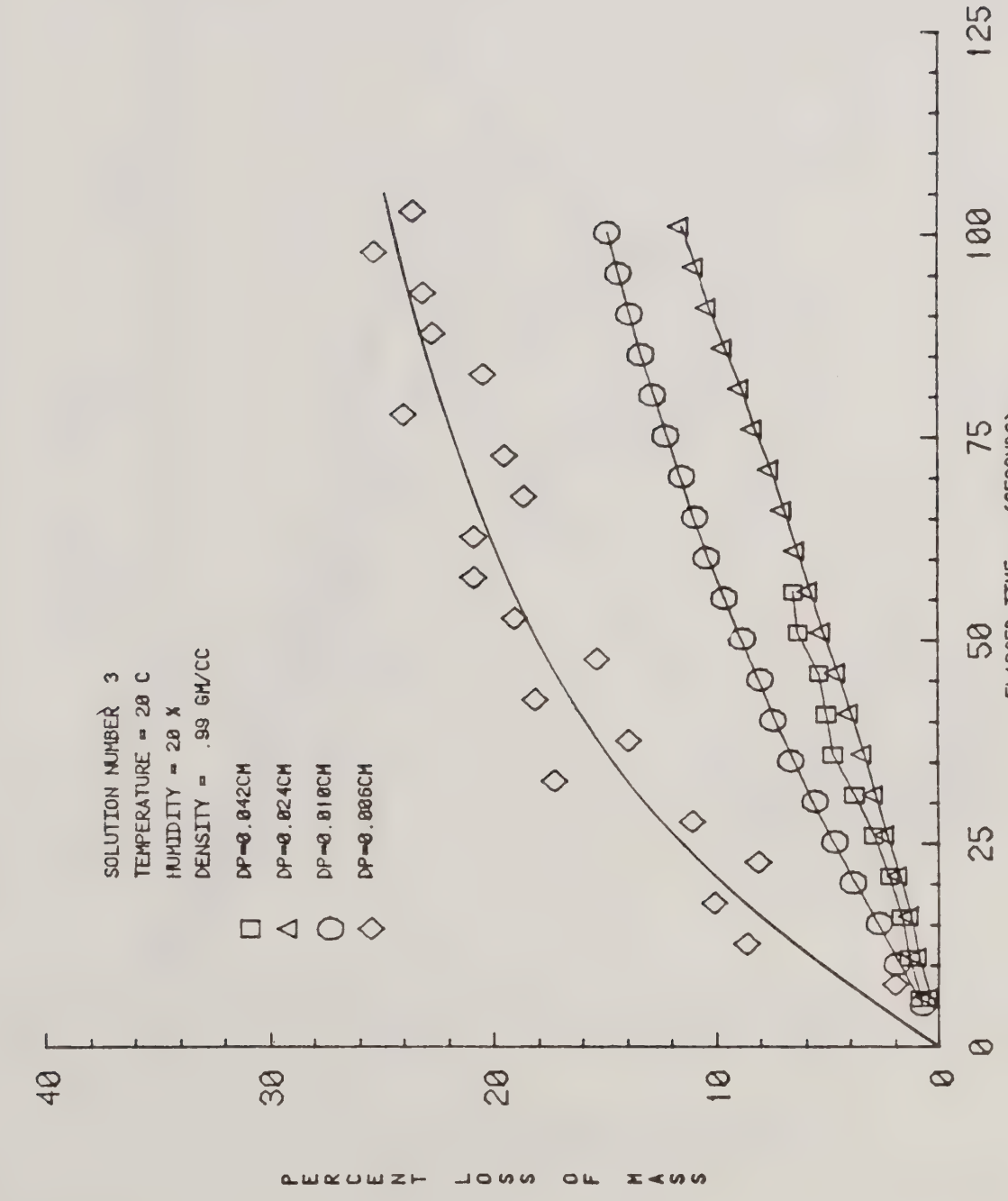

Figure 6. Relative Effects of Percent of Mass Loss by a Change in Initial Diameter for Solution 3.

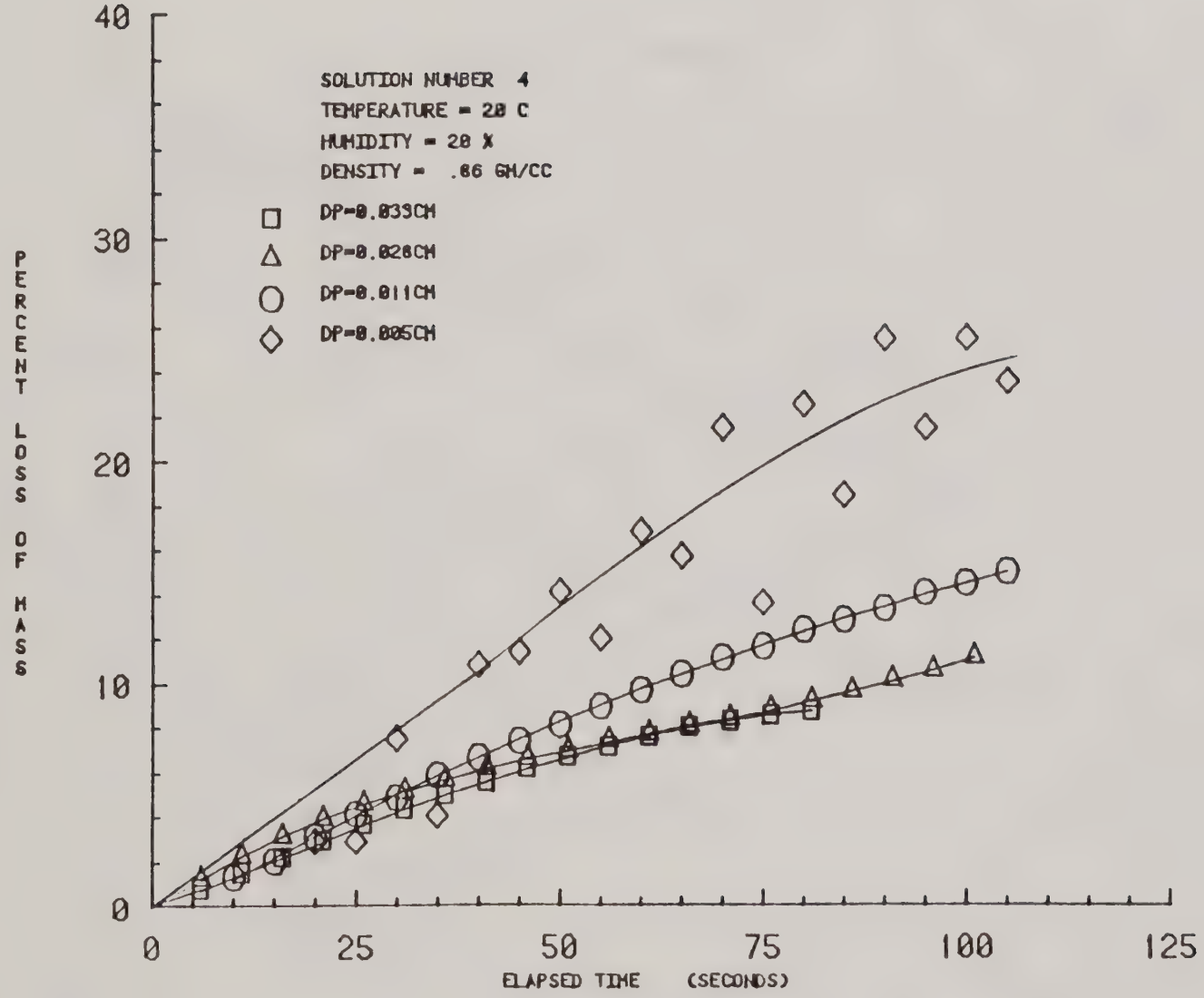

Figure 7. Relative Effects of Percent of Mass Loss by a Change in Initial Diameter for Solution 4.

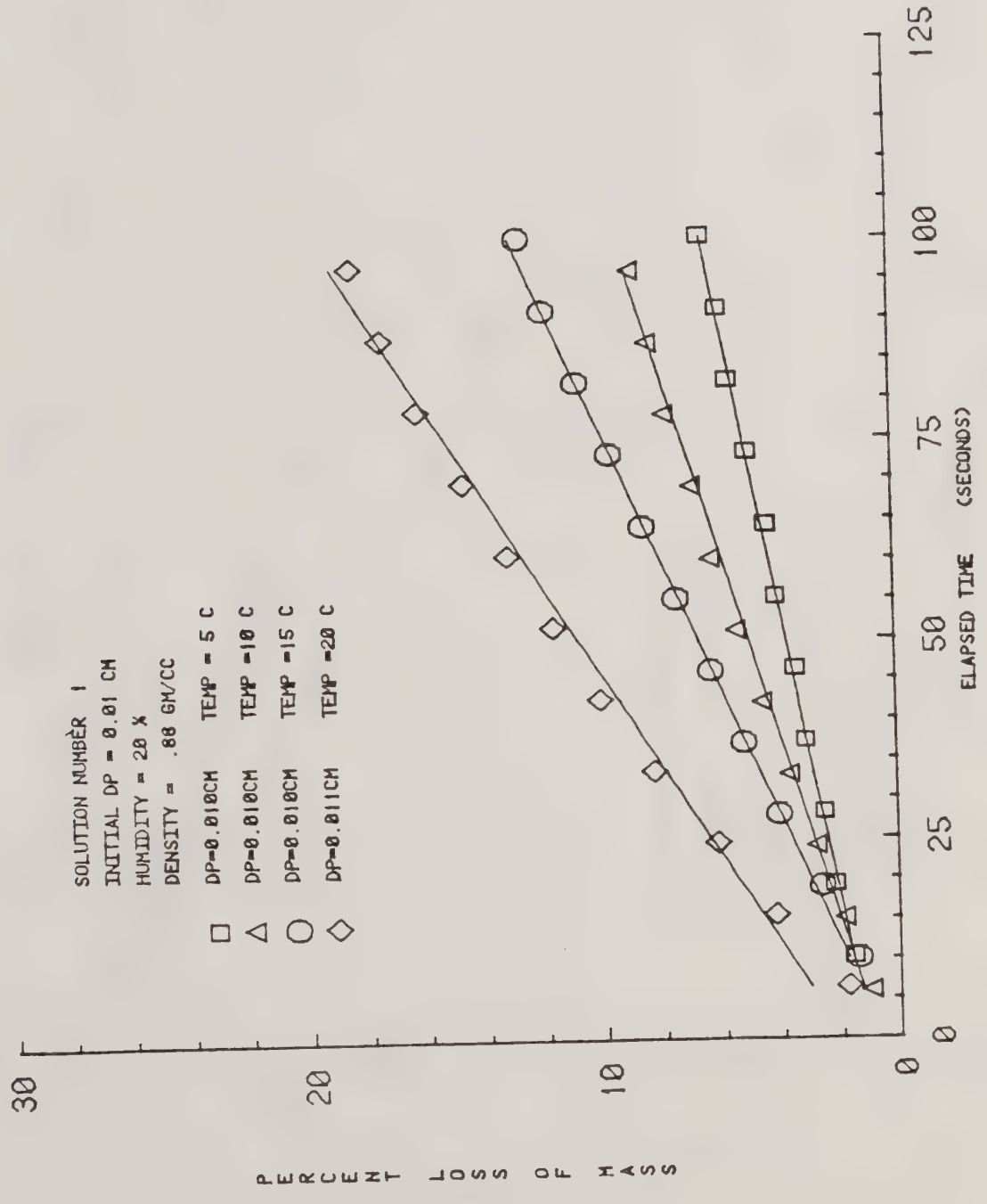

Figure 8. Relative Effects of Percent of Mass Loss by a Change in Air Temperature for Solution 1.

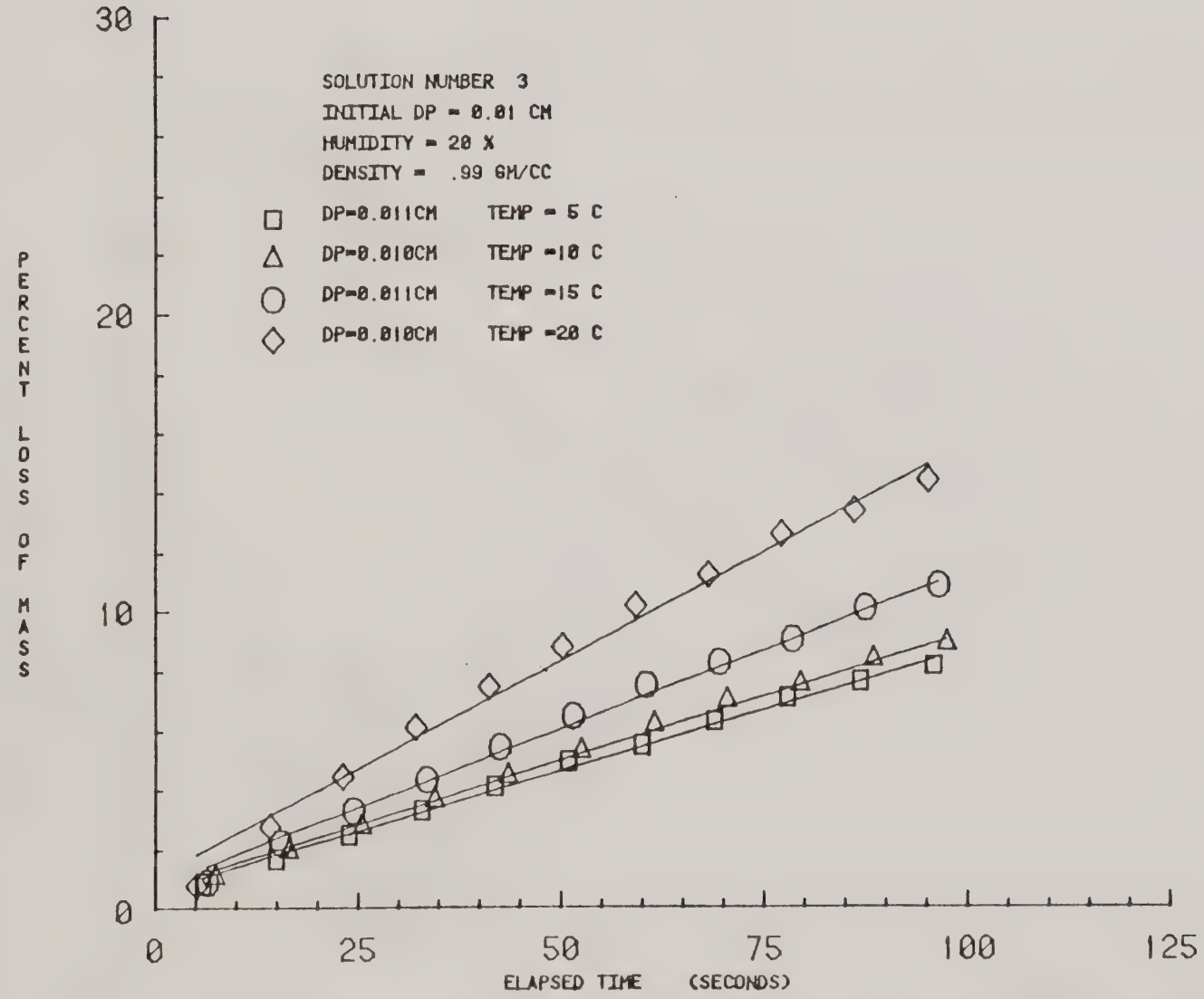

Figure 9. Relative Effects of Percent of Mass Loss by a Change in Air Temperature for Solution 3.

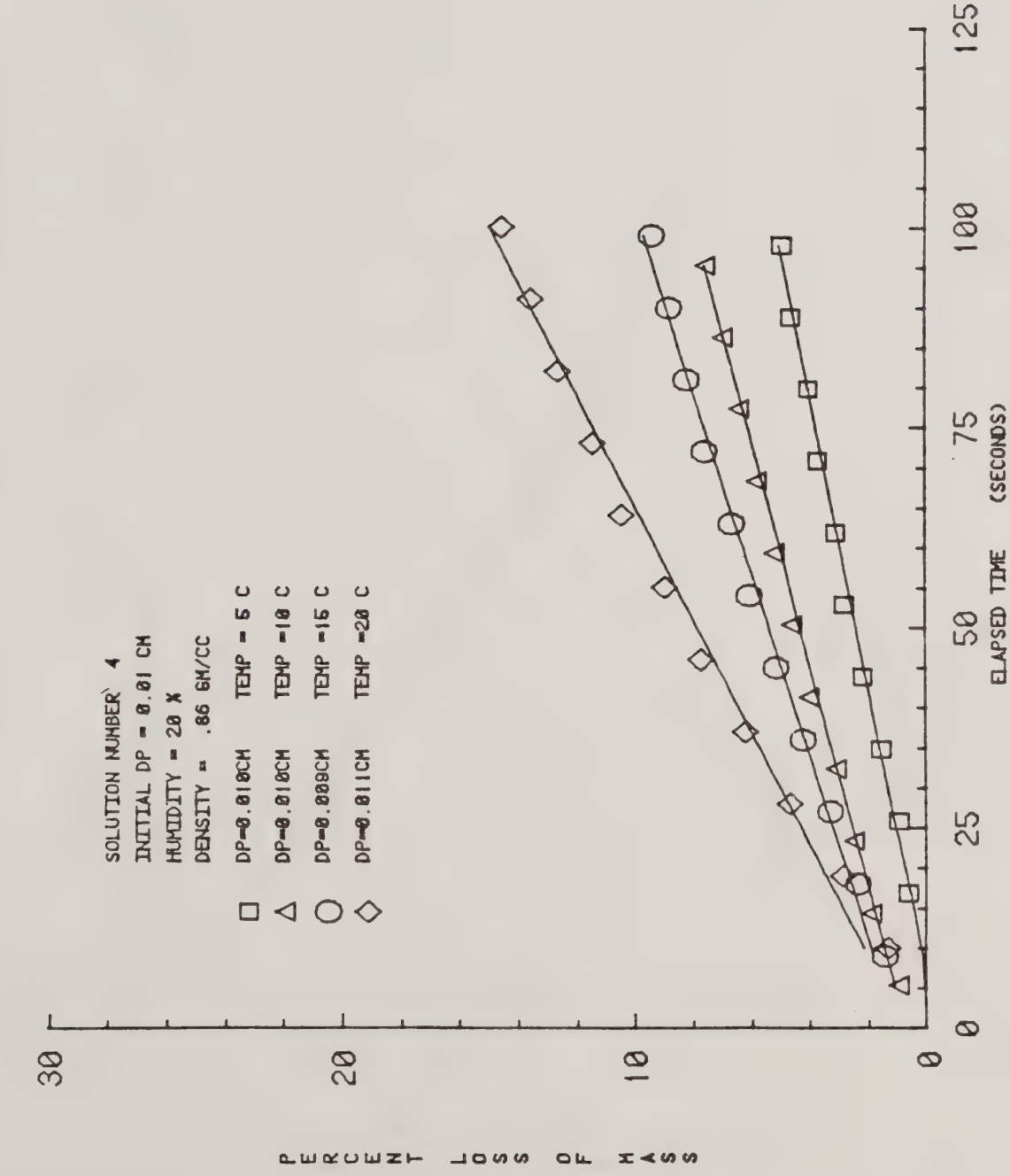

Figure 10. Relative Effects of Percent of Mass Loss by a Change in Air Temperature for Solution 4.

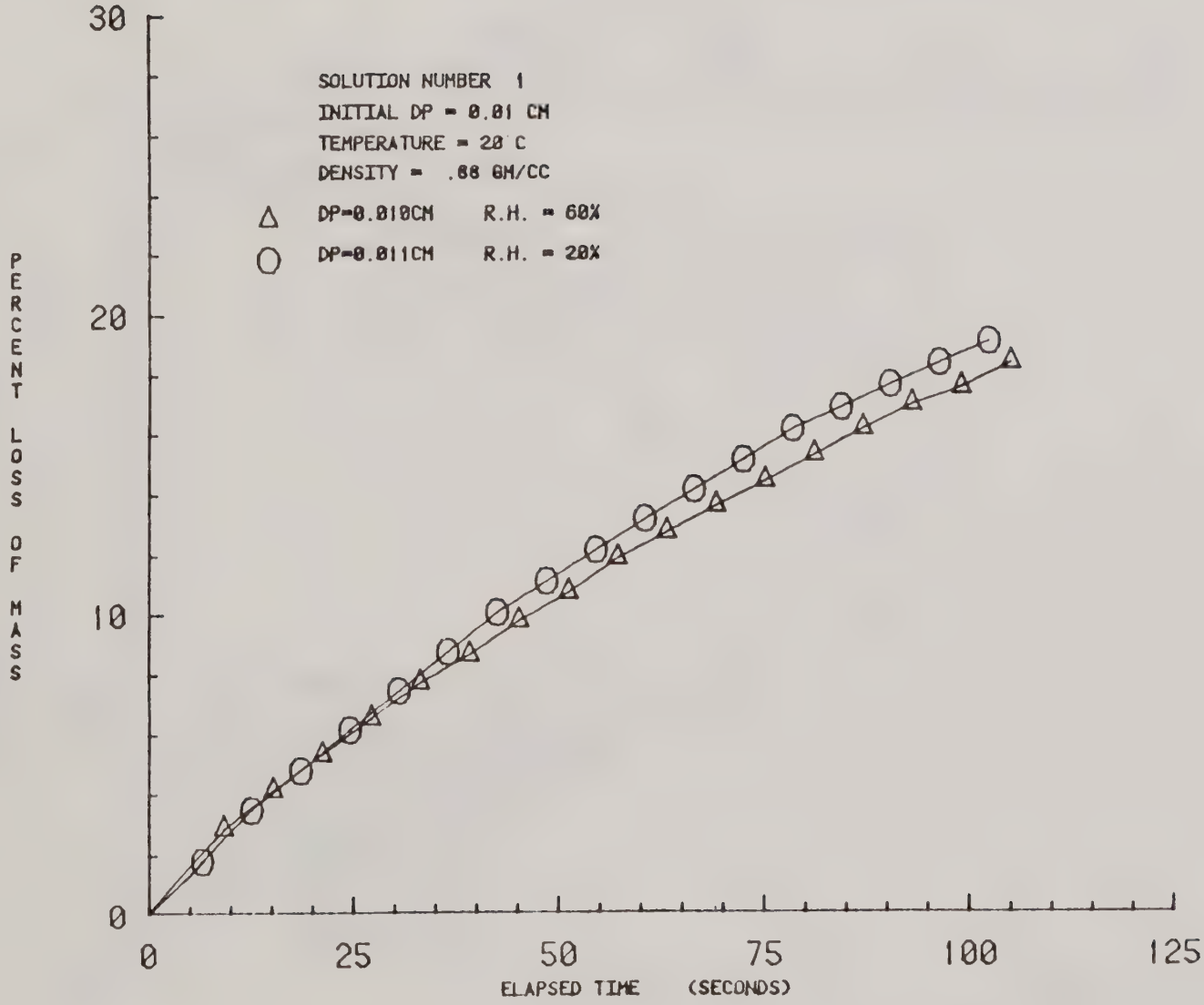

Figure 11. Relative Effects of Percent of Mass Loss by a Change in Air Humidity for Solution 1.

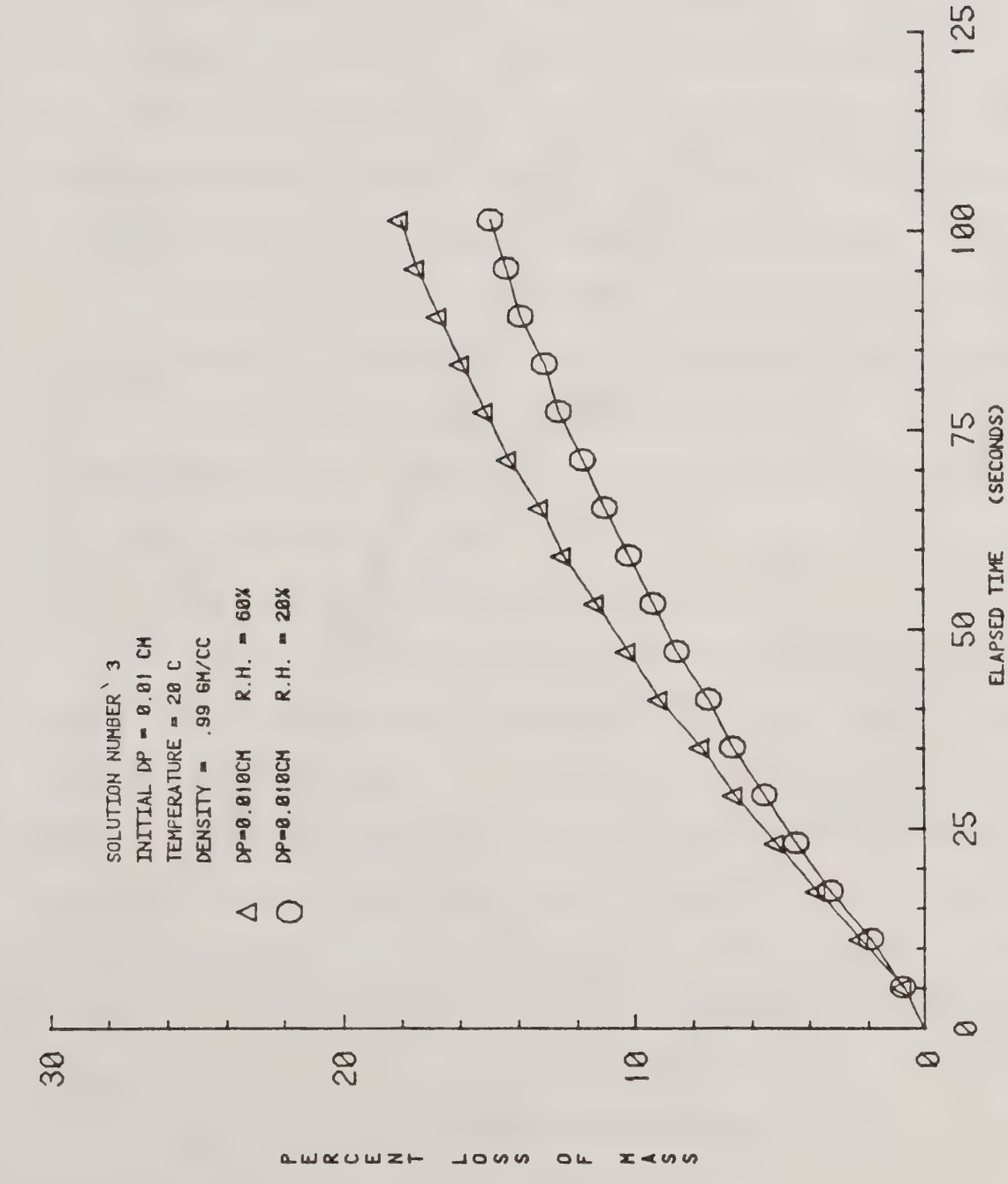

Figure 12. Relative Effects of Percent of Mass Loss by a Change in Air Humidity for Solution 3.

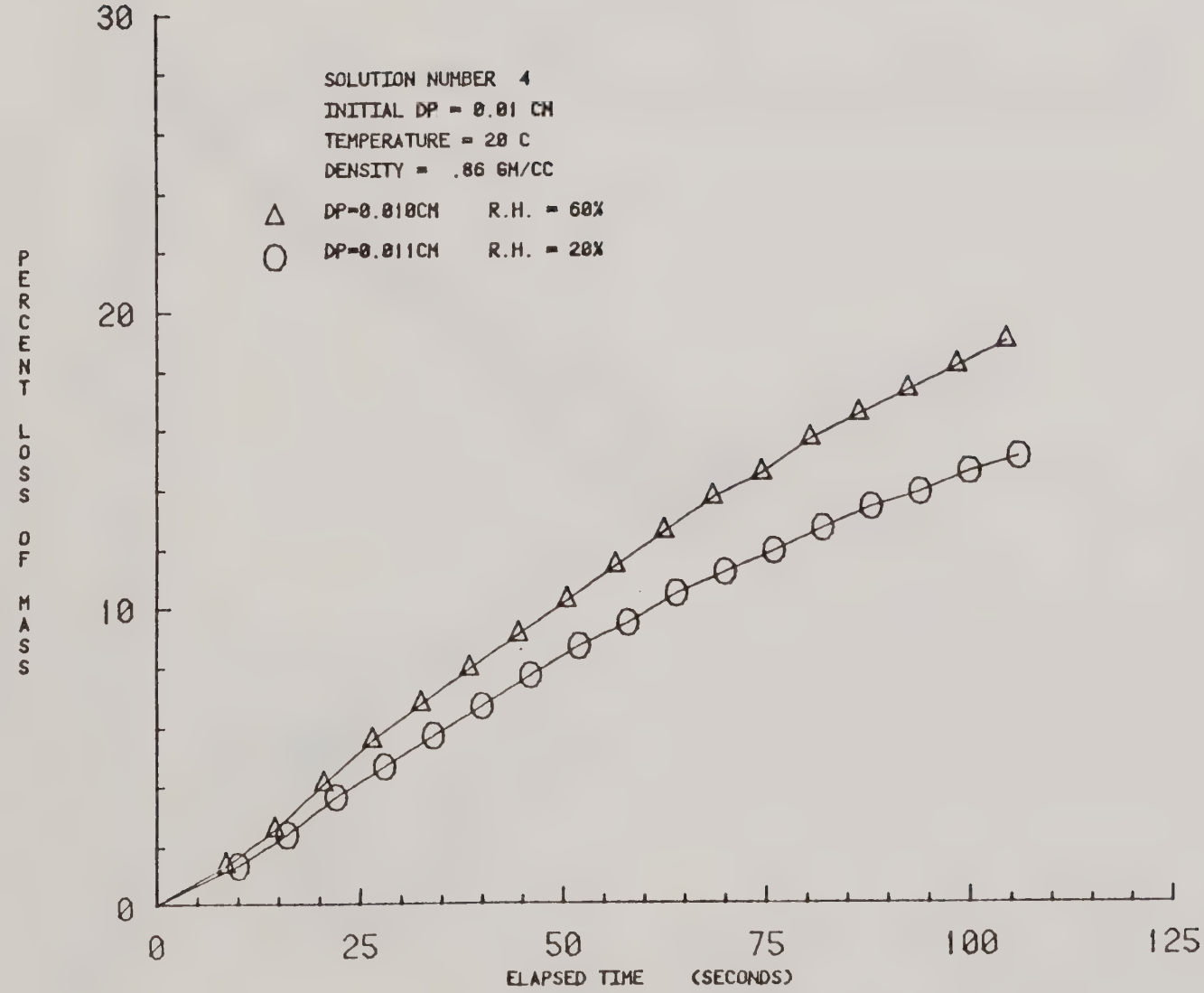

Figure 13. Relative Effects of Percent of Mass Loss by a Change in Air Humidity for Solution 4.

of a factor of five in the percent mass loss for the range of droplets used in this study.

8.5.3.2 Change in Air Temperature

The effect due to the change in air temperature for solutions 1, 3 and 4 are shown in Figures 8, 9 and 10. As expected, the rate of mass loss increases as the temperature of the medium increases. In these figures, the initial droplet diameter accompanied the air temperature. In some instances this may become a factor in examining the plots. In each of the plots, the curves of increasing temperature generally increase gradually. The percent of mass lost using $5^{o}C$ was about 3% after 30 seconds. For the same length of time, the $20^{o}C$ curve loses approximately 9%. The percent loss of mass increased by a factor of three for the temperatures used in this study.

8.5.3.3 Change in Air Relative Humidity

Figures 11 - 13 display the effects of change in relative humidity in the mass loss of droplets of solutions 1, 3 and 4. Again, the diameter of the initial droplet was also given. These plots show that there are negligible effects on these solutions due to a change in humidity. This was given earlier as a criteria for eliminating tests. In each figure, the differences between the curves of varying humidity were small. An explanation for this can be shown by examining the equation for stationary evaporation, equation 2.4. The driving force in this equation was the difference of the vapor concentration between the droplet and surrounding air, equation 8.6.

$$D.F. = \frac{M_{\ell}}{R}\left(\frac{P_0}{T_0} - \frac{P_{\infty}}{T_{\infty}}\right) = (C_0 - C_{\infty}) \qquad (8.6)$$

Quantities for the vapor pressures, or concentrations, are not known for these solutions. However, since the vapor of the evaporating droplet was basically composed of oil, the addition of water in the form of humidity should have little effect on the concentration gradient of this vapor. Therefore, the entire evaporation process using droplets of these solutions should change very little for changes in air humidity. This relatively small change applies to the limited ranges used in this study. Over longer periods of time, the effective differences may become significant.

8.5.4 Solutions of High Volatility

Solutions that contain water as the basic component are included in this group. Solutions 2 and 5 - 14 belong in this high volatility group. Figures 14 - 46 show the effects on the percent mass loss as a function of time due to changes in the experimental conditions. It should be noted that each of the curves was continued past the start of crystallization. This was done to show the different stages of evaporation described earlier. Examination of all the plots revealed that the critical point, detailed in 8.3.2, was in fact dependent on the initial diameter and solution concentration alone. In nearly all the plots, crystalization starts at the same level of percent loss of mass for the varied initial conditions. This was a basic assumption used in the approximation of the 50 micron data for these solutions.

8.5.4.1 Change in Initial Droplet Diameter

Figures 14 - 24 display the effects of changing the initial droplet diameter for each of the solutions. As with the low volatility solutions, the smaller droplet diameters lose mass at a faster rate than the larger. The curves used for the 50 micron initial diameter were obtained from the

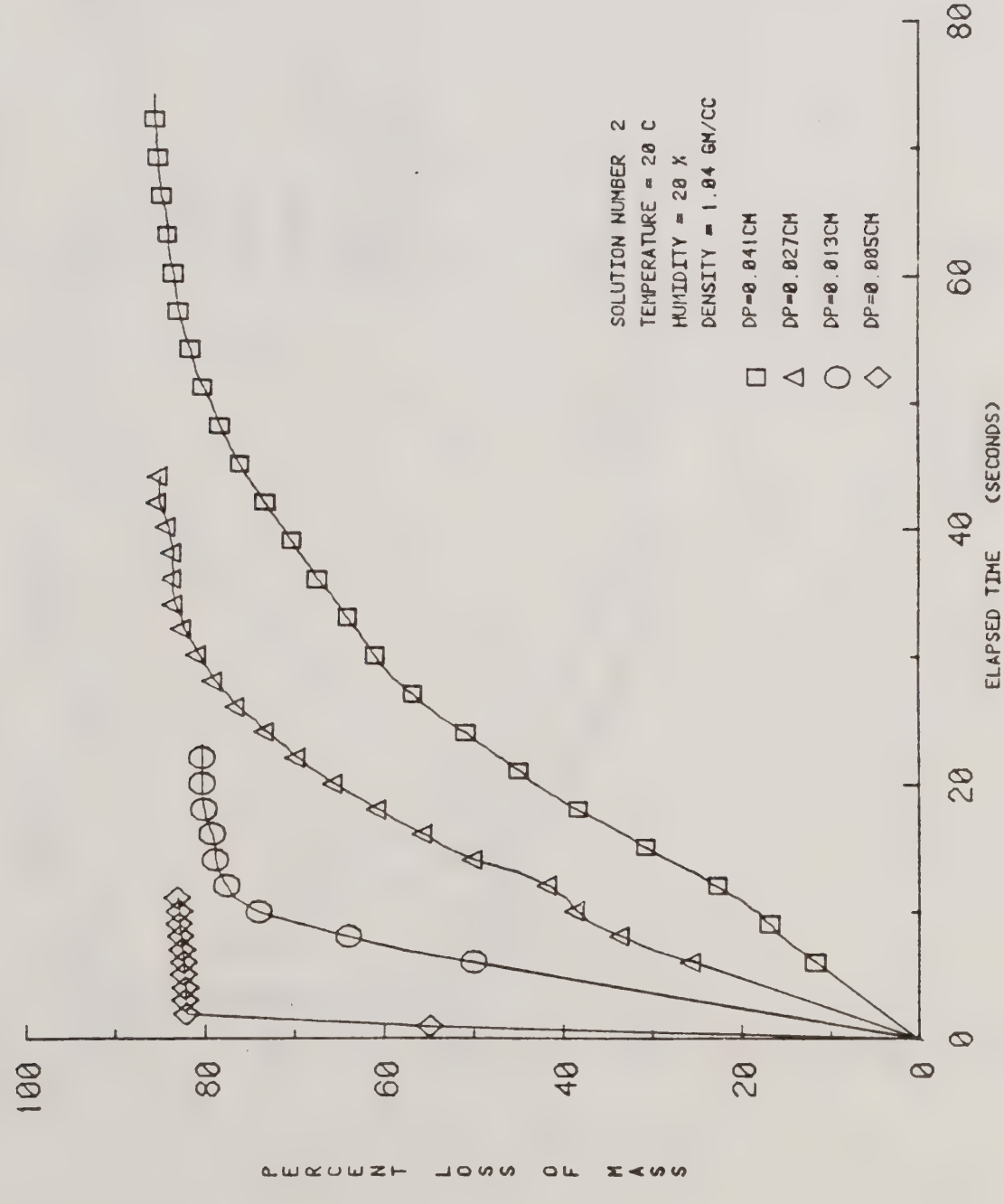

Figure 14. Relative Effects of Percent of Mass Loss by a Change in Initial Diameter for Solution 2

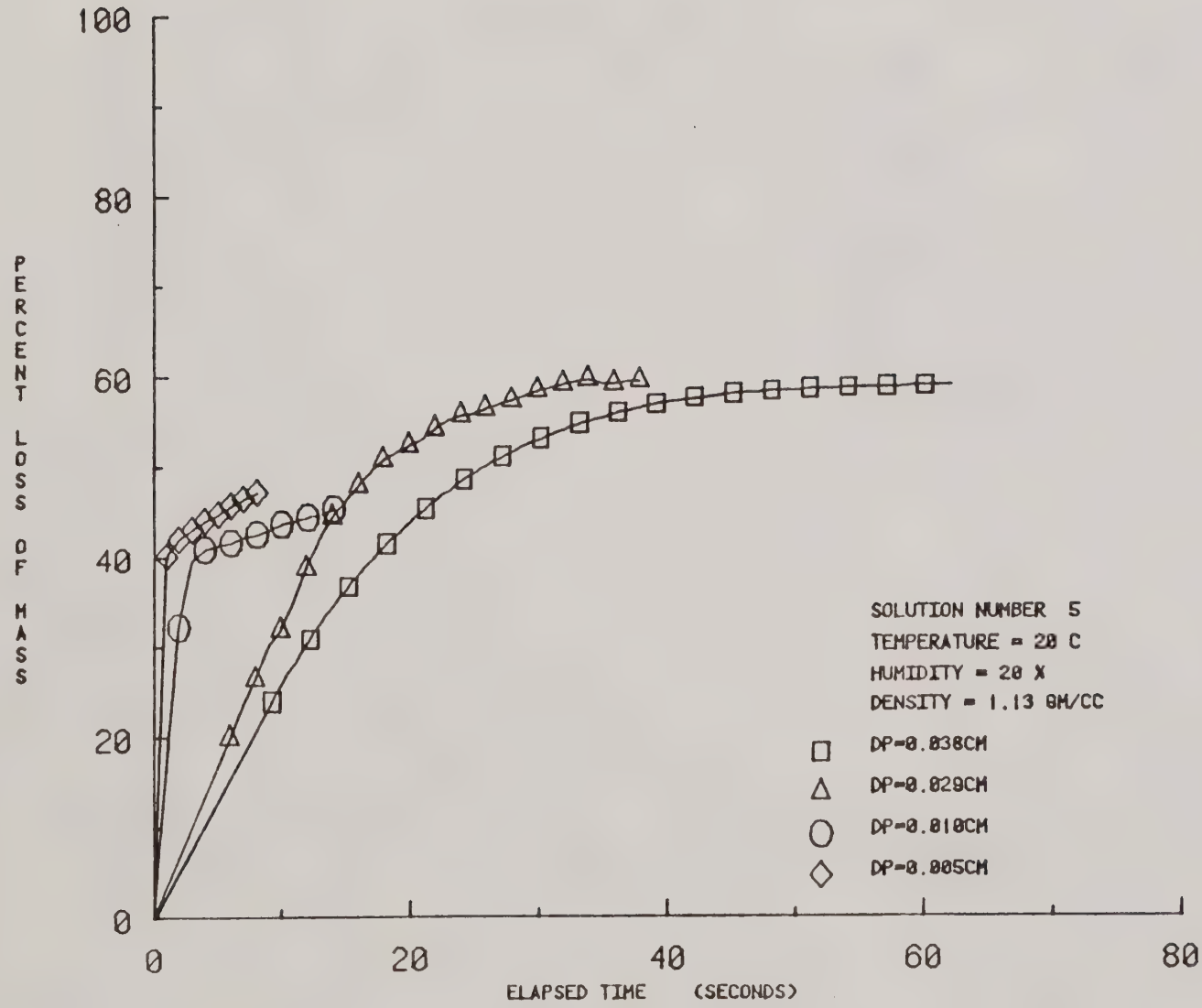

Figure 15. Relative Effects of Percent of Mass Loss by a Change in Initial Diameter for Solution 5

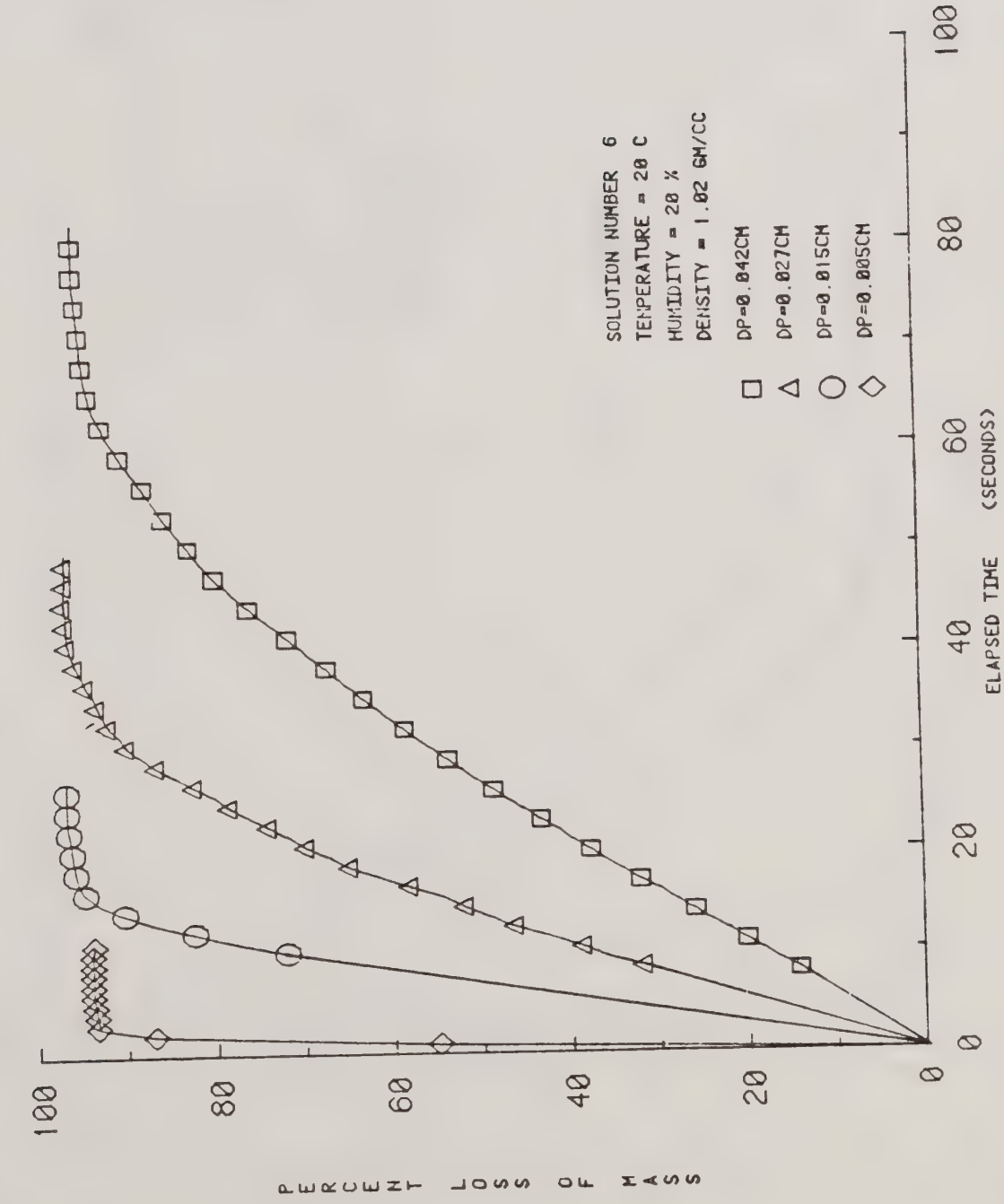

Figure 16. Relative Effects of Percent of Mass Loss by a Change in Initial Diameter for Solution 6

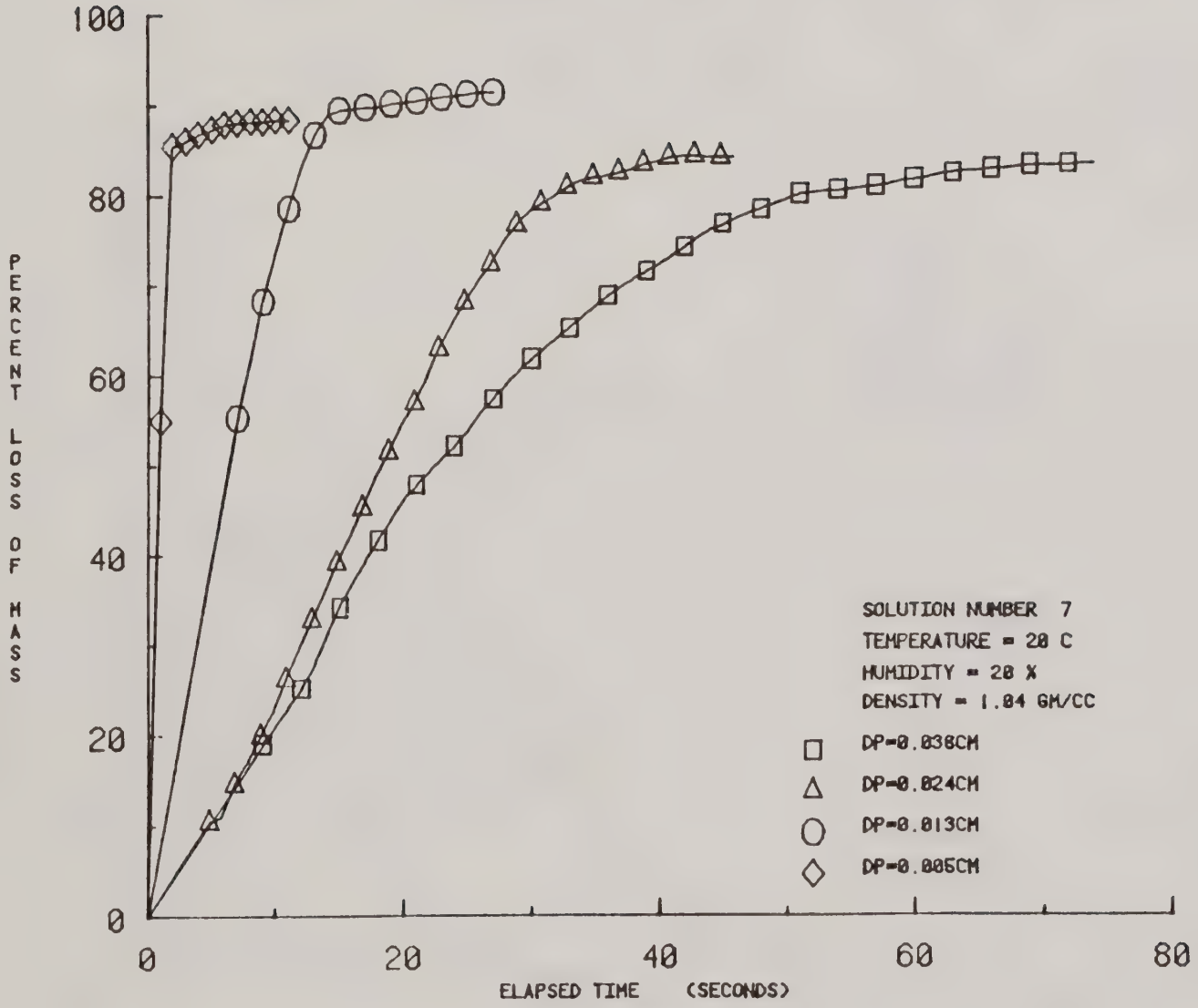

Figure 17. Relative Effects of Percent of Mass Loss by a Change in Initial Diameter for Solution 7.

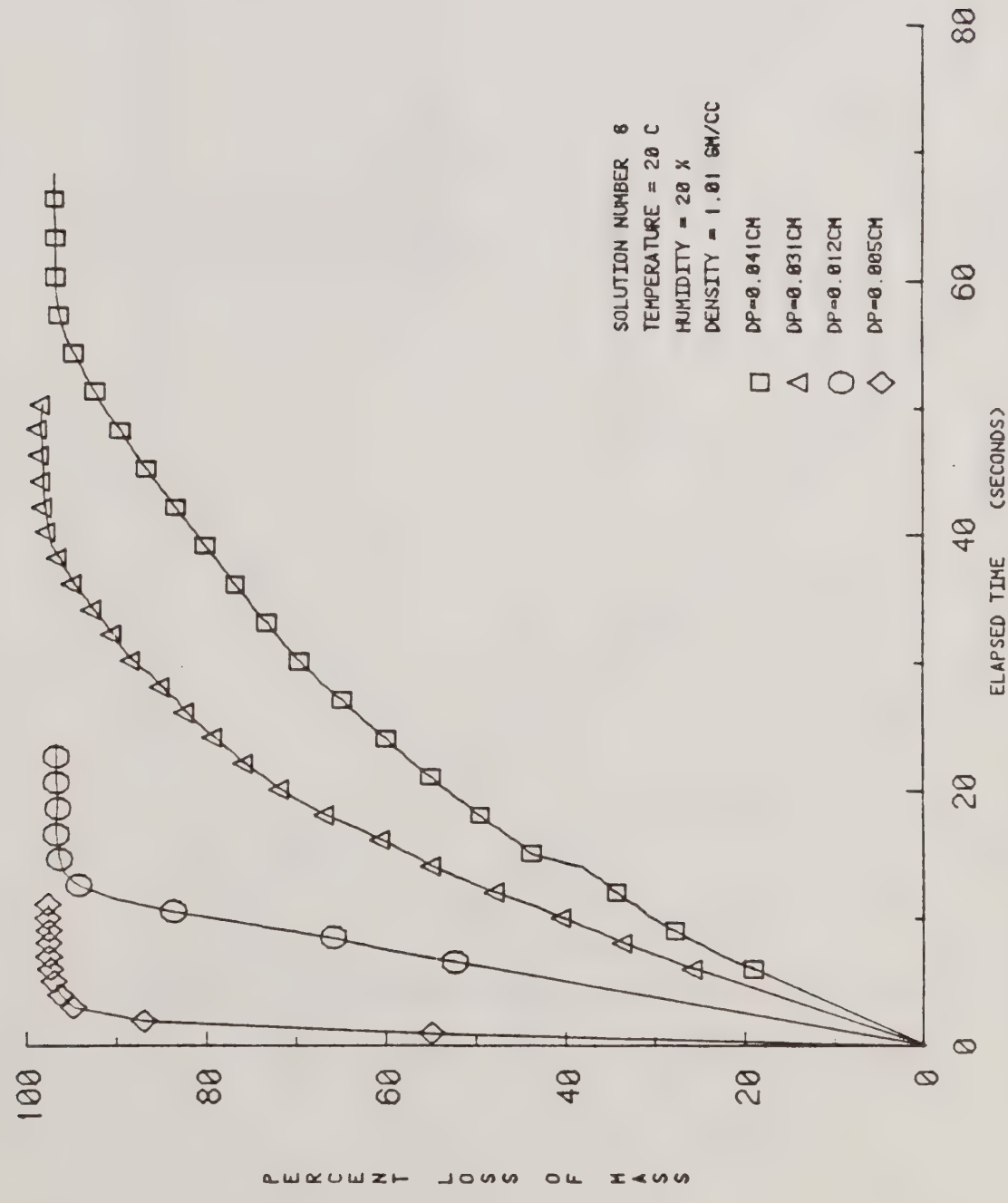

Figure 18. Relative Effects of Percent of Mass Loss by a Change in Initial Diameter for Solution 8.

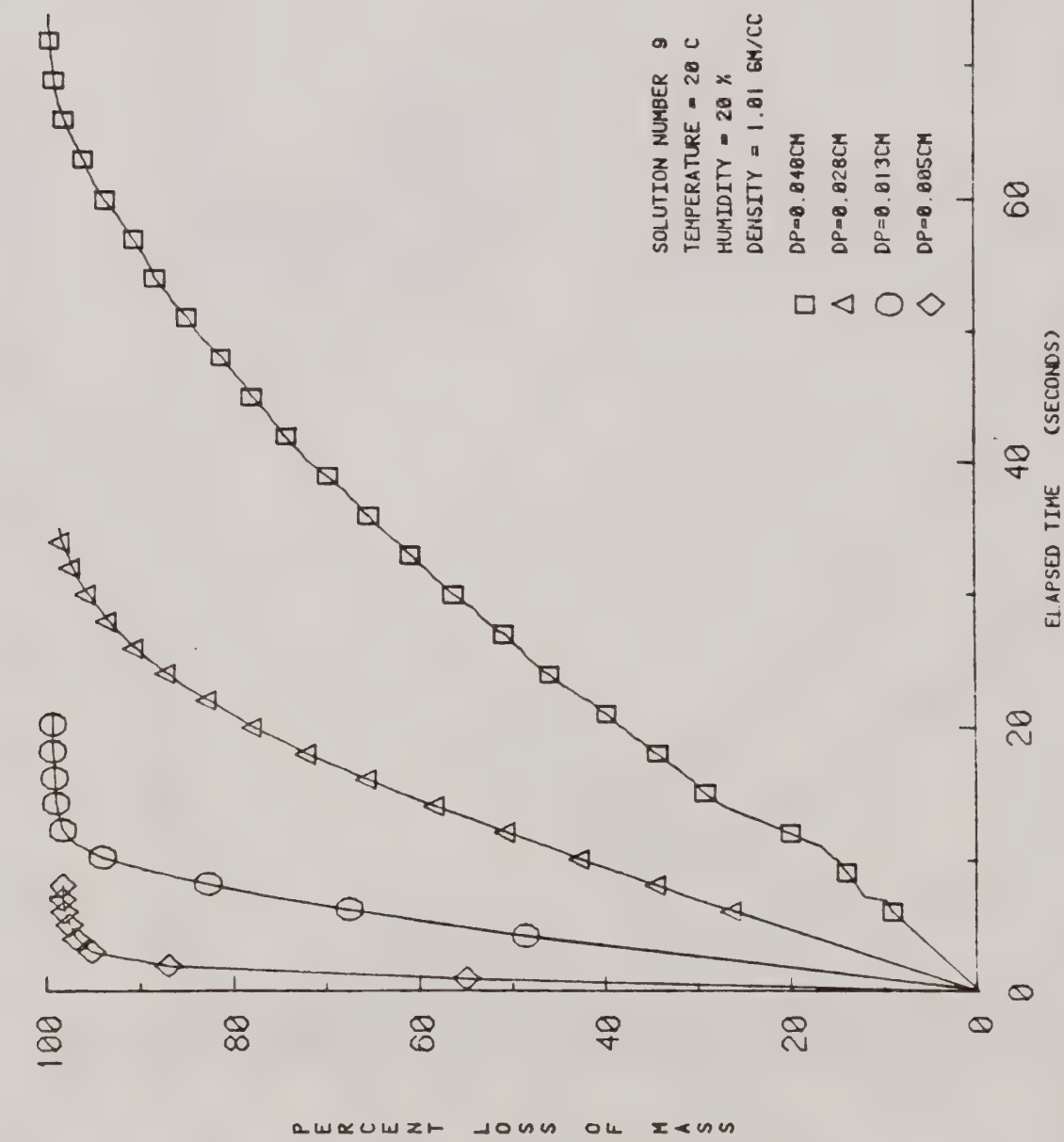

Figure 19. Relative Effects of Percent of Mass Loss by a Change in Initial Diameter for Solution 9.

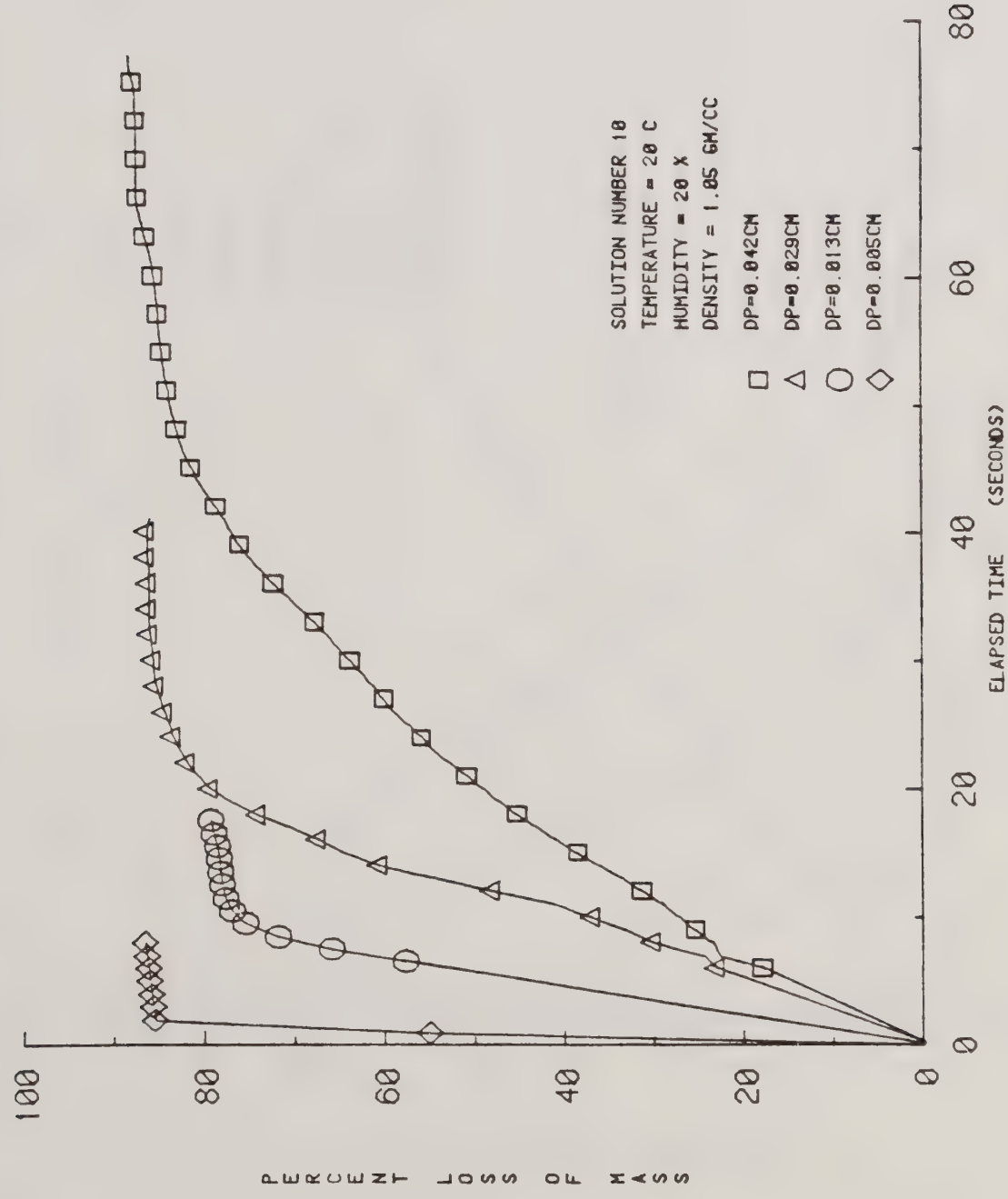

Figure 20. Relative Effects of Percent of Mass Loss by a Change in Initial Diameter for Solution 10.

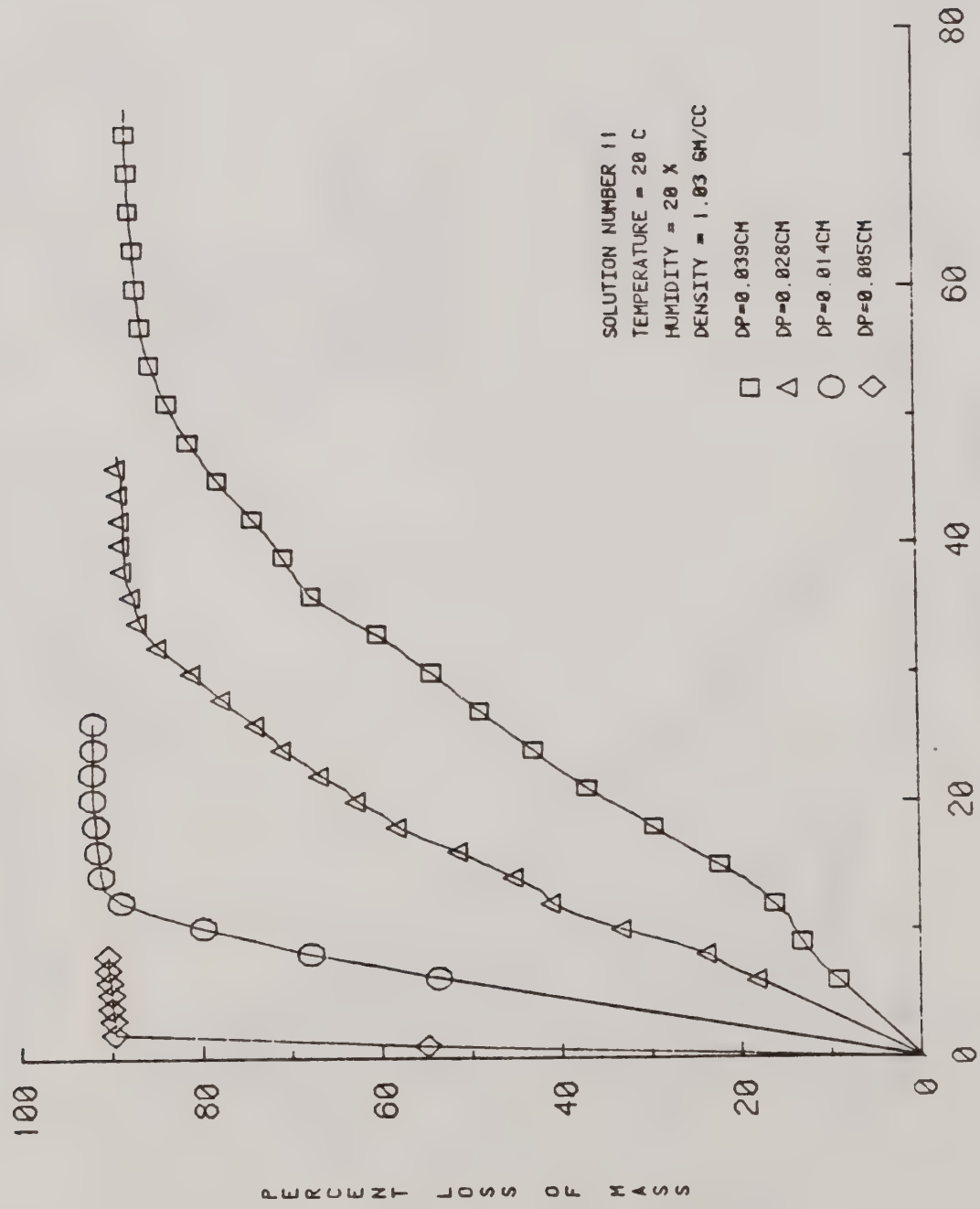

Figure 21. Relative Effects of Percent of Mass Loss by a Change in Initial Diameter for Solution 11.

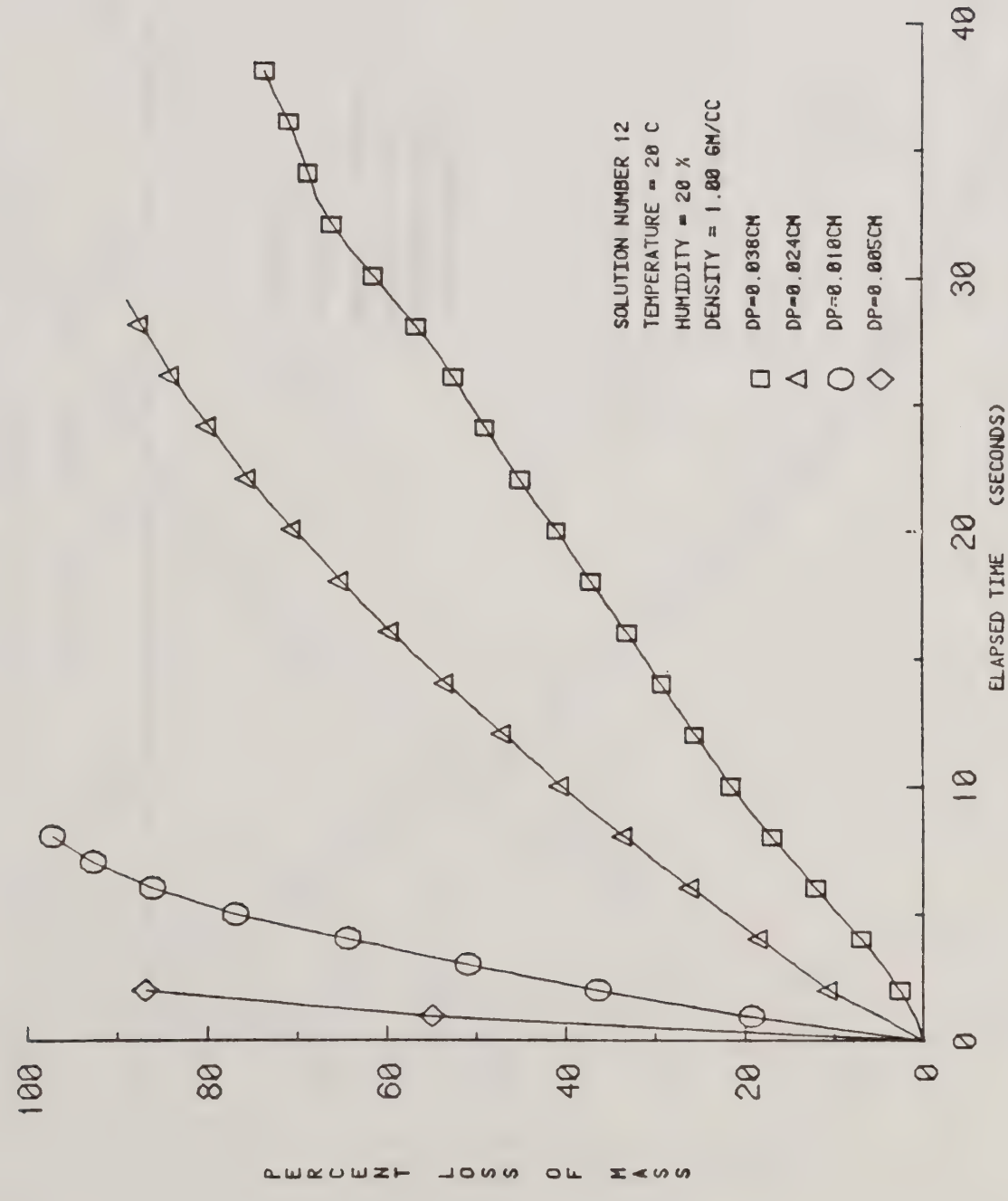

Figure 22. Relative Effects of Percent of Mass Loss by a Change in Initial Diameter for Solution 12.

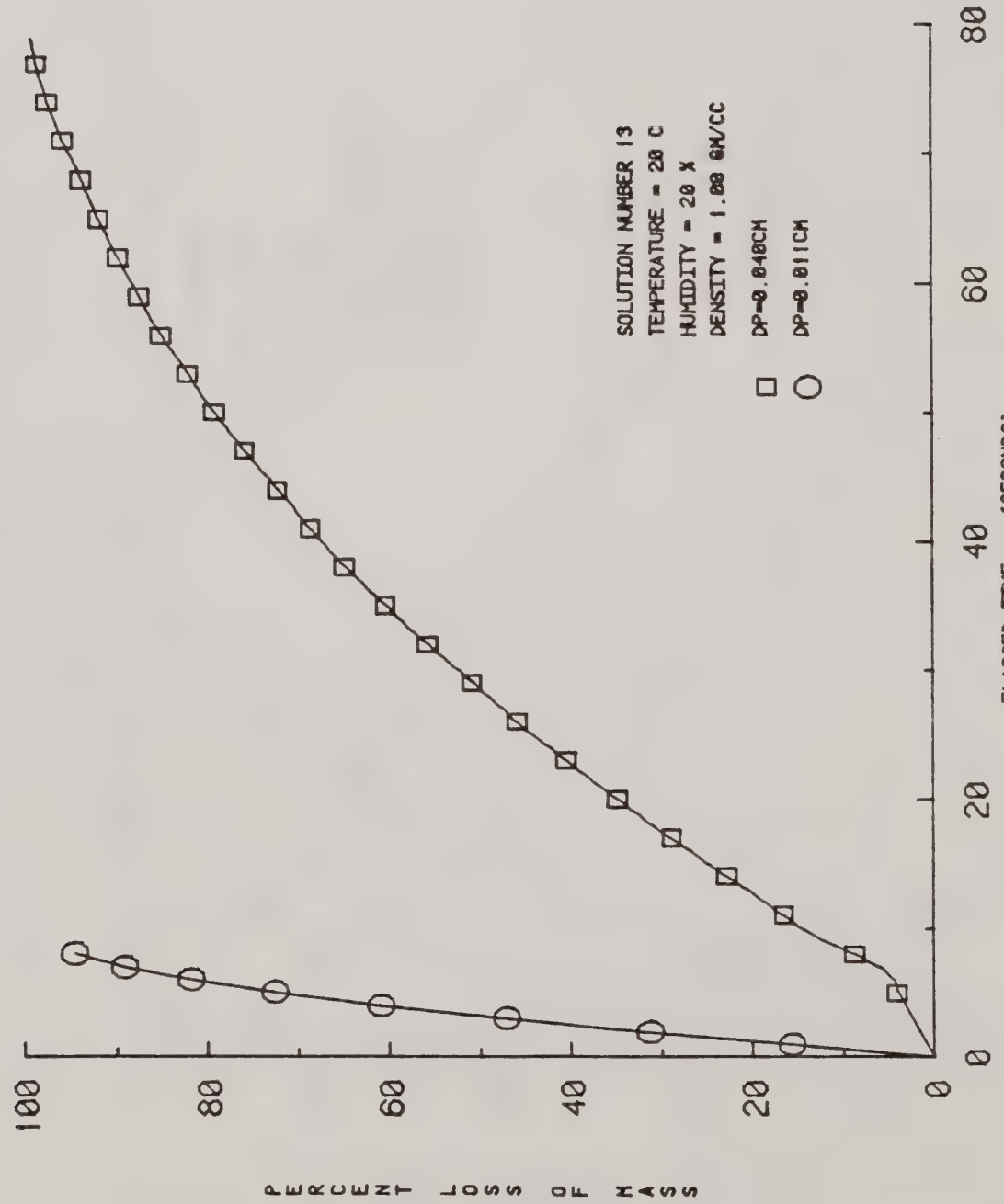

Figure 23. Relative Effects of Percent of Mass Loss by a Change in Initial Diameter for Solution 13.

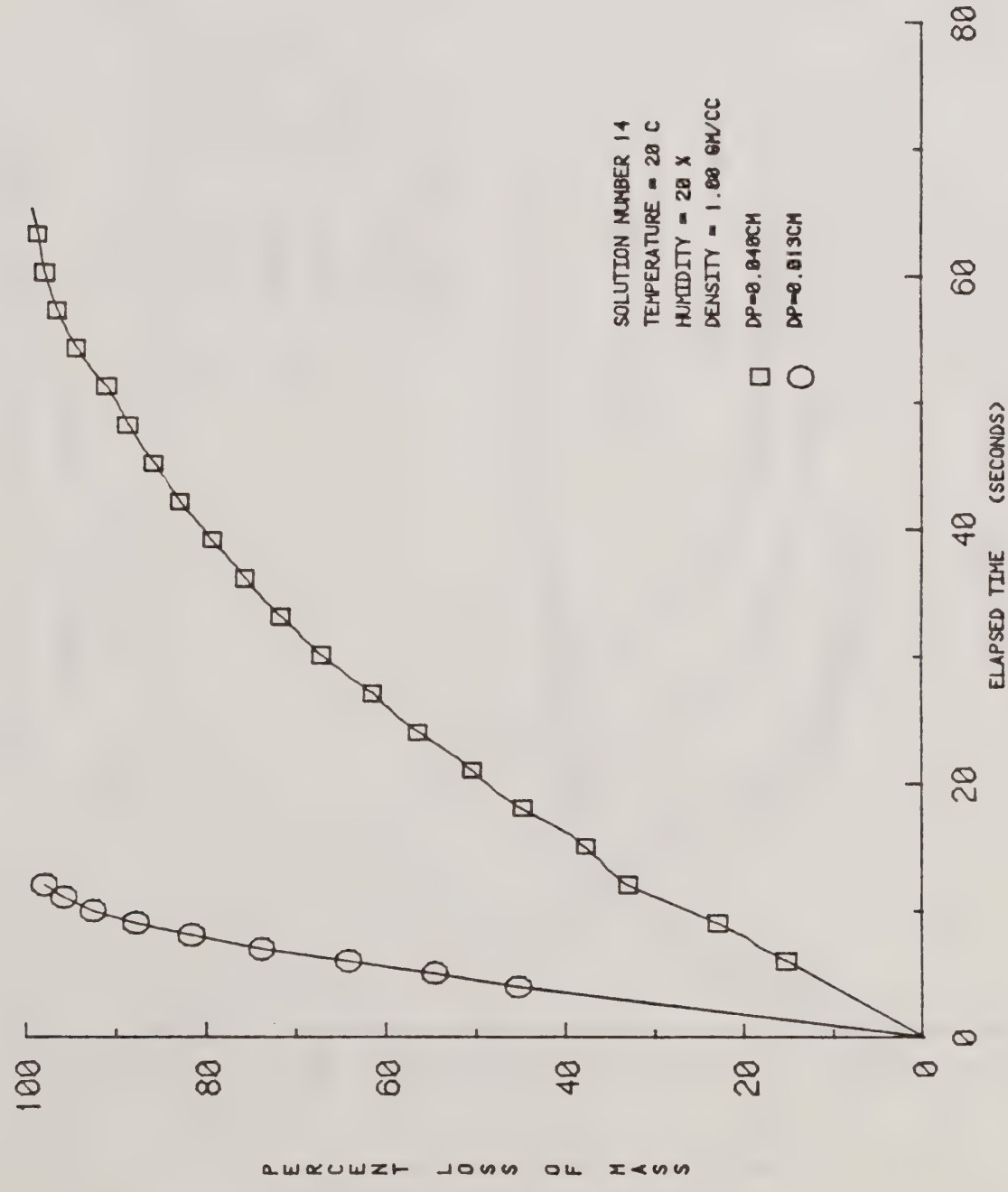

Figure 24. Relative Effects of Percent of Mass Loss by a Change in Initial Diameter for Solution 14.

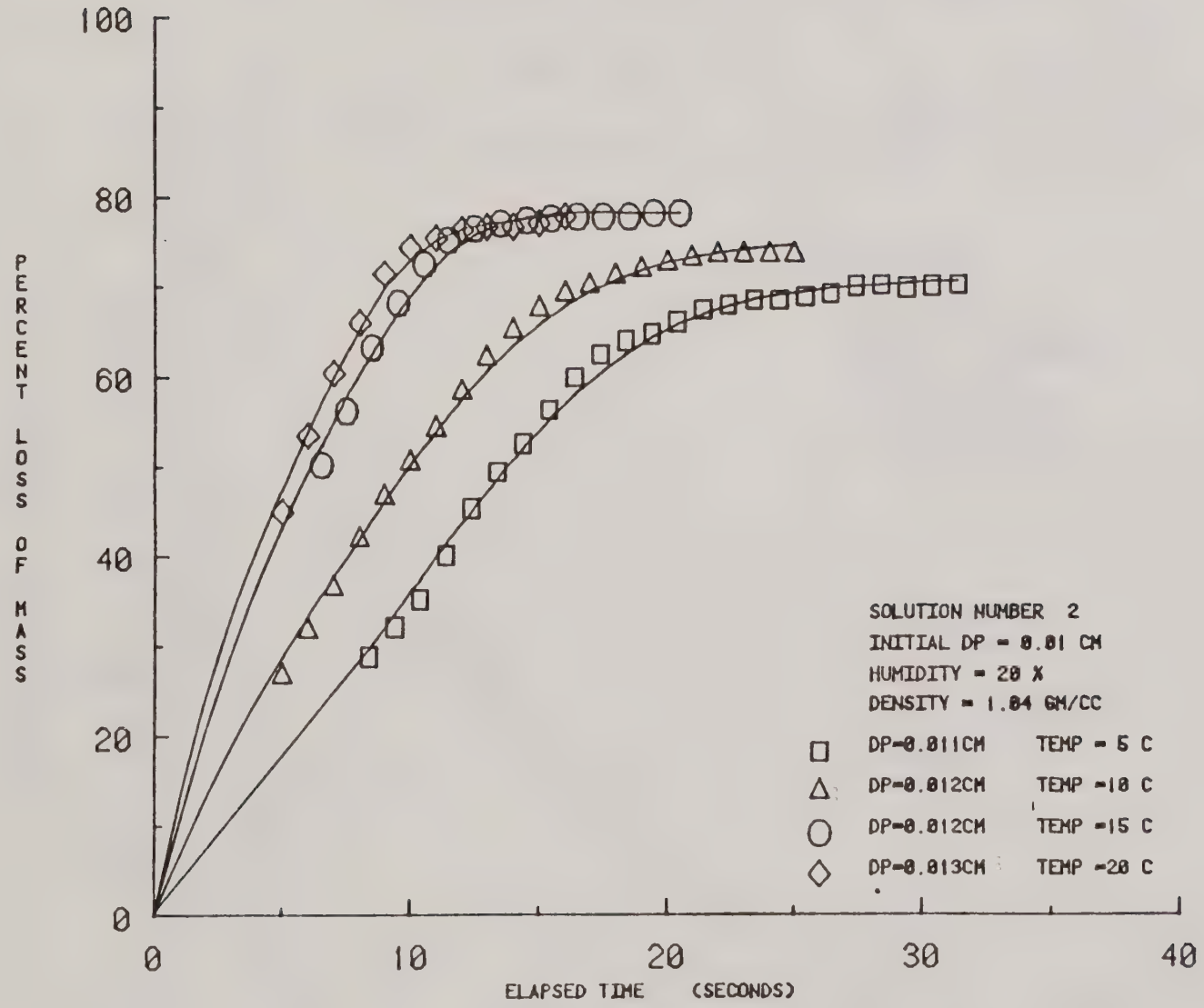

Figure 25. Relative Effects of Percent of Mass Loss by a Change in Air Temperature for Solution 2.

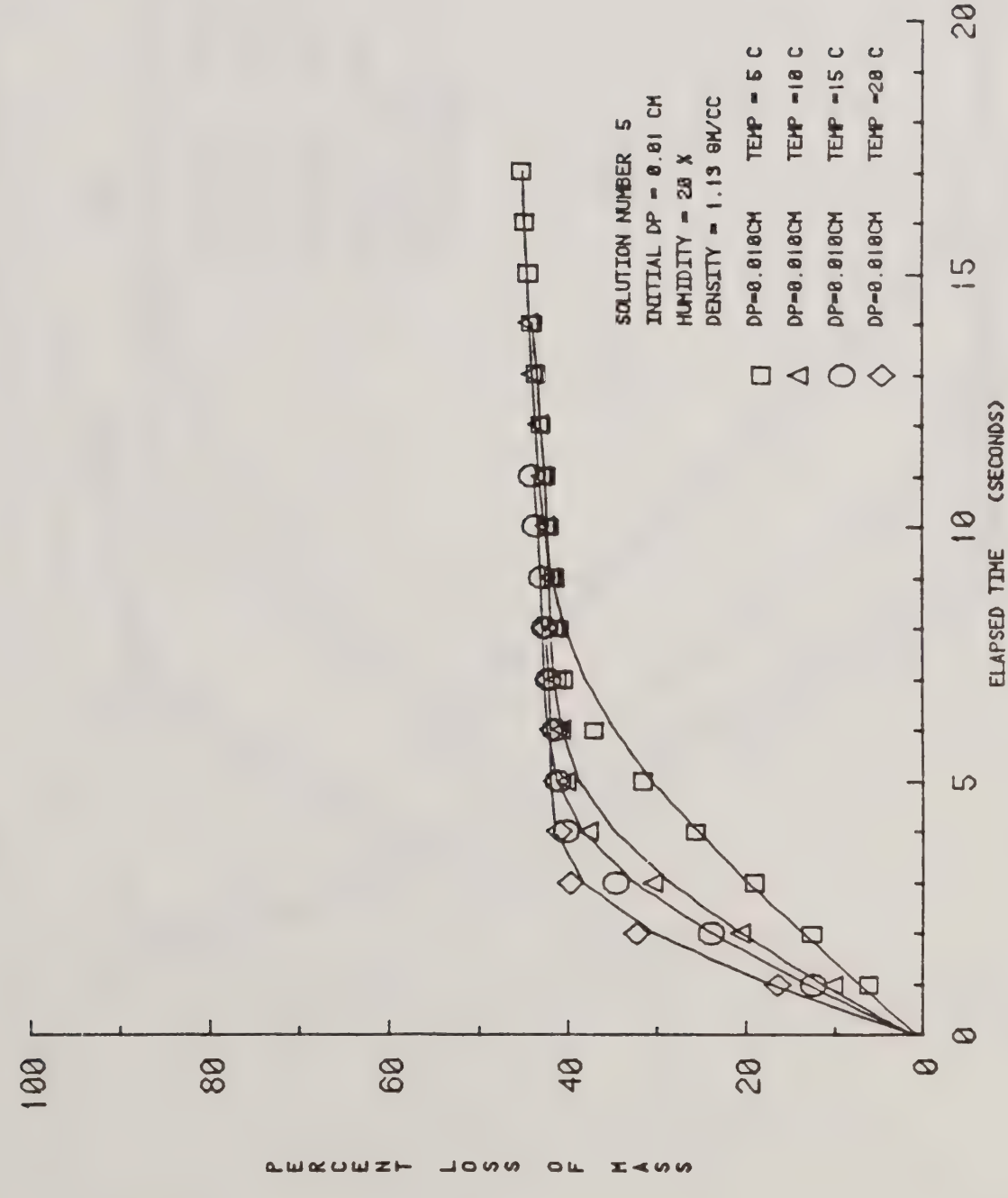

Figure 26. Relative Effects of Percent of Mass Loss by a Change in Air Temperature for Solution 5.

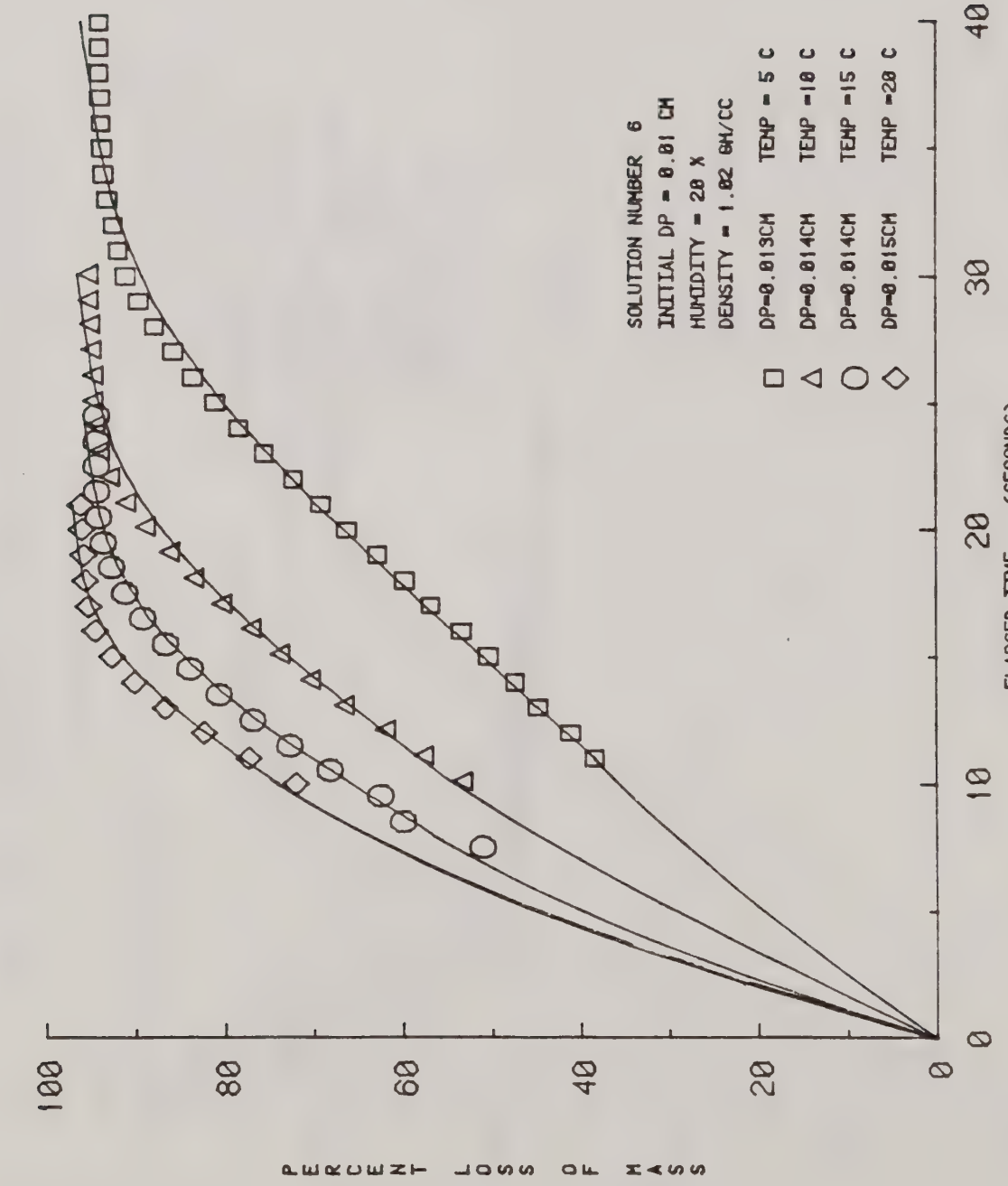

Figure 27. Relative Effects of Percent of Mass Loss by a Change in Air Temperature for Solution 6.

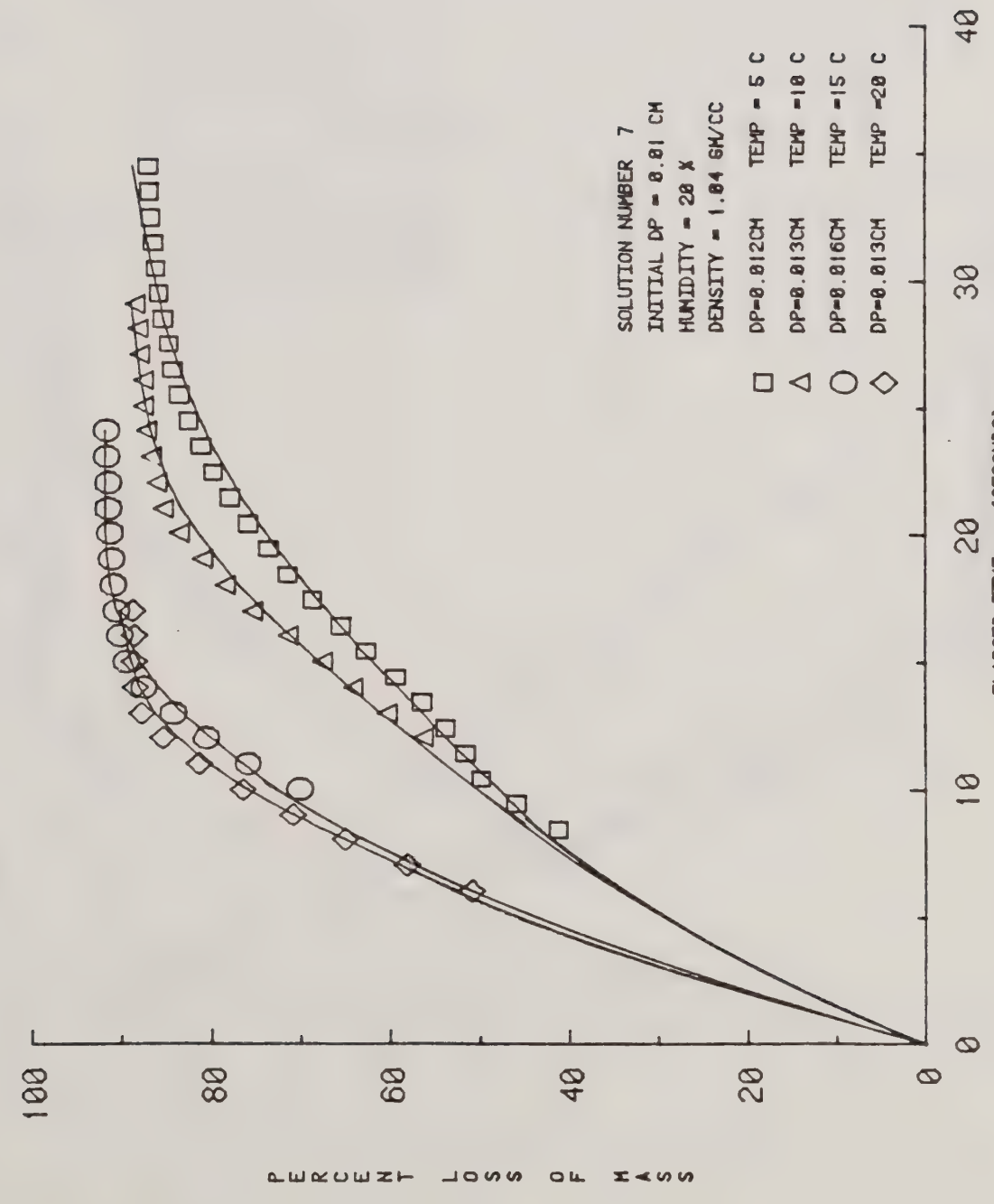

Figure 28. Relative Effects of Percent of Mass Loss by a Change in Air Temperature for Solution 7.

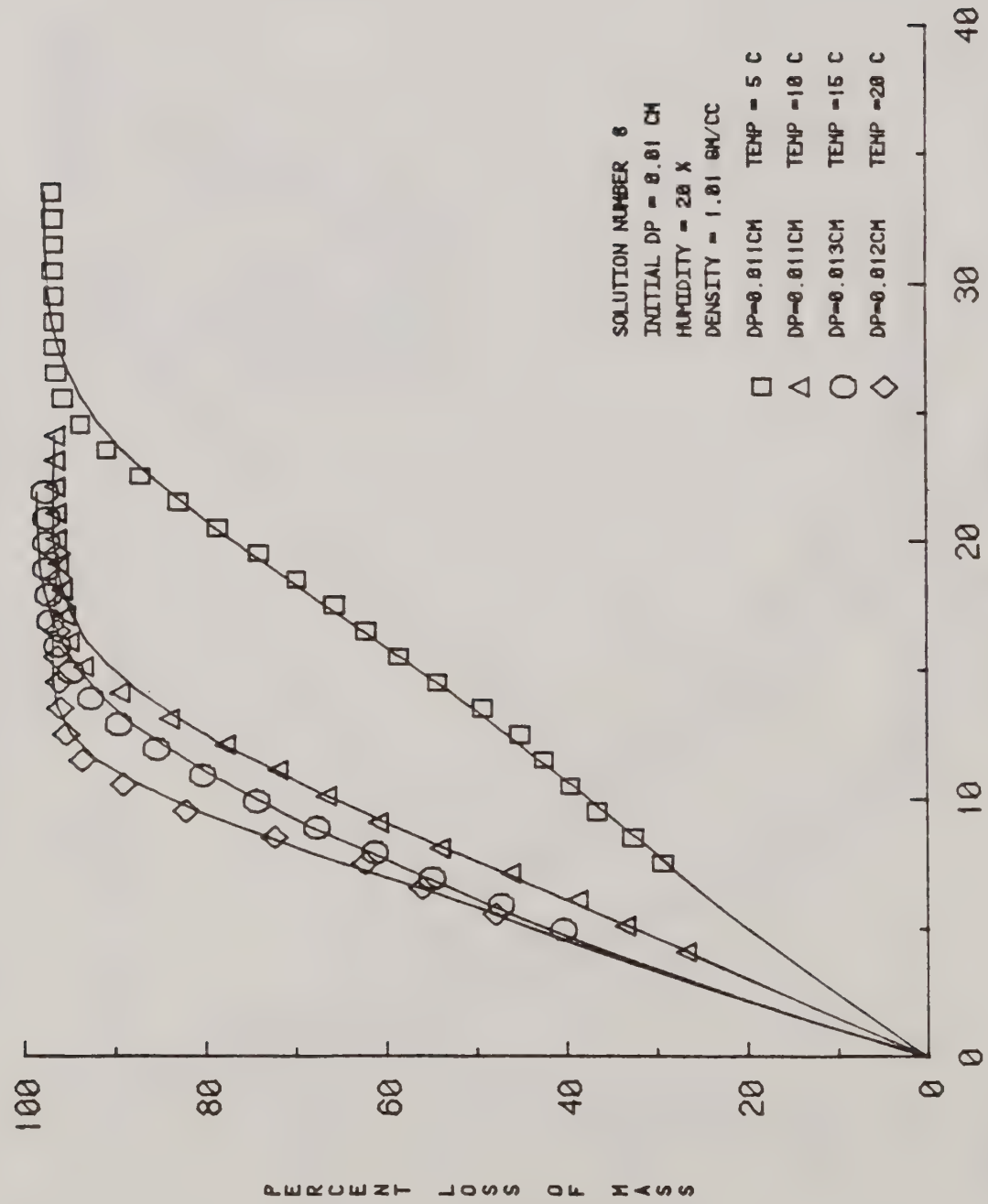

Figure 29. Relative Effects of Percent of Mass Loss by a Change in Air Temperature for Solution 8.

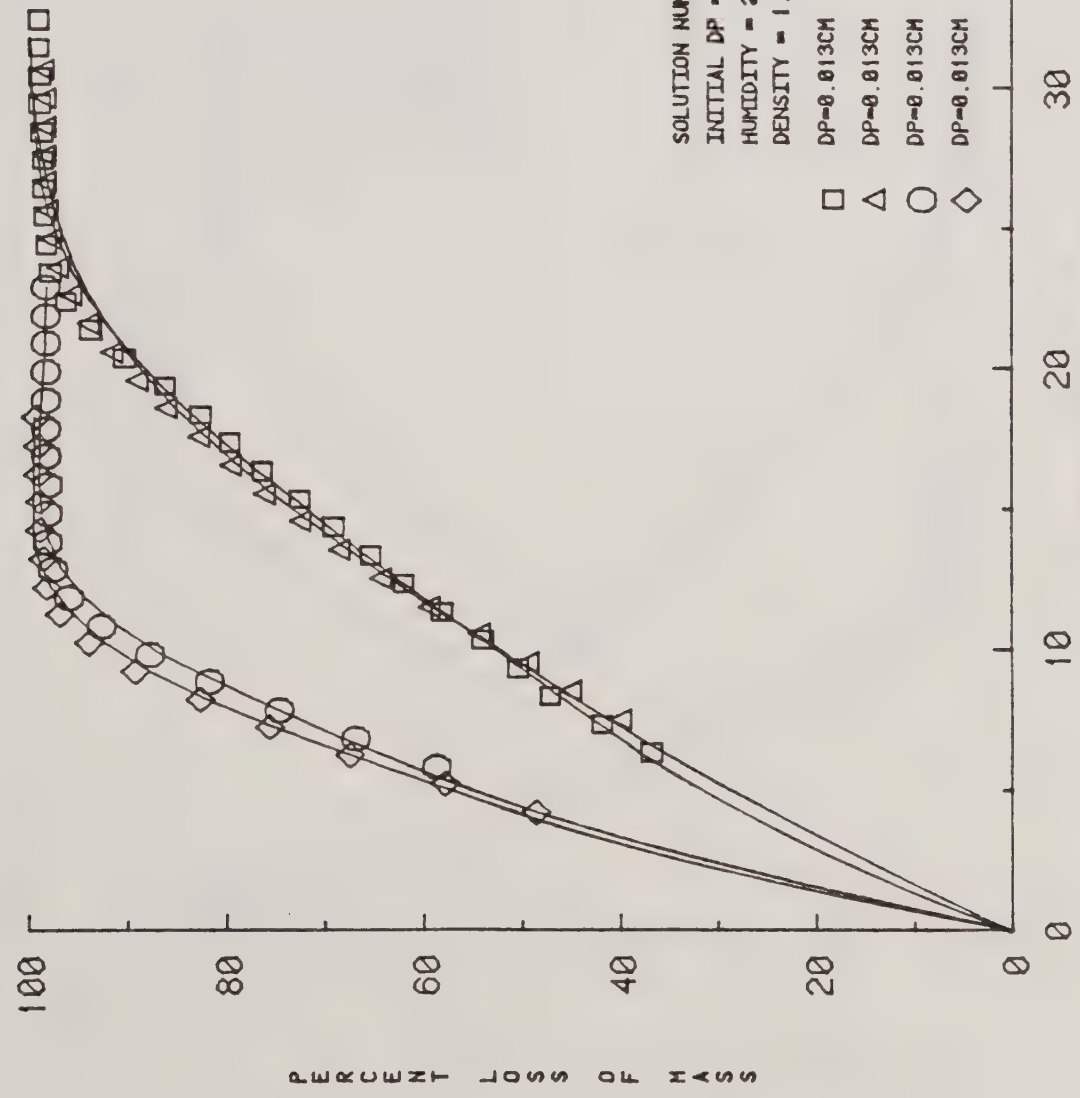

Figure 30. Relative Effects of Percent of Mass Loss by a Change in Air Temperature for Solution 9.

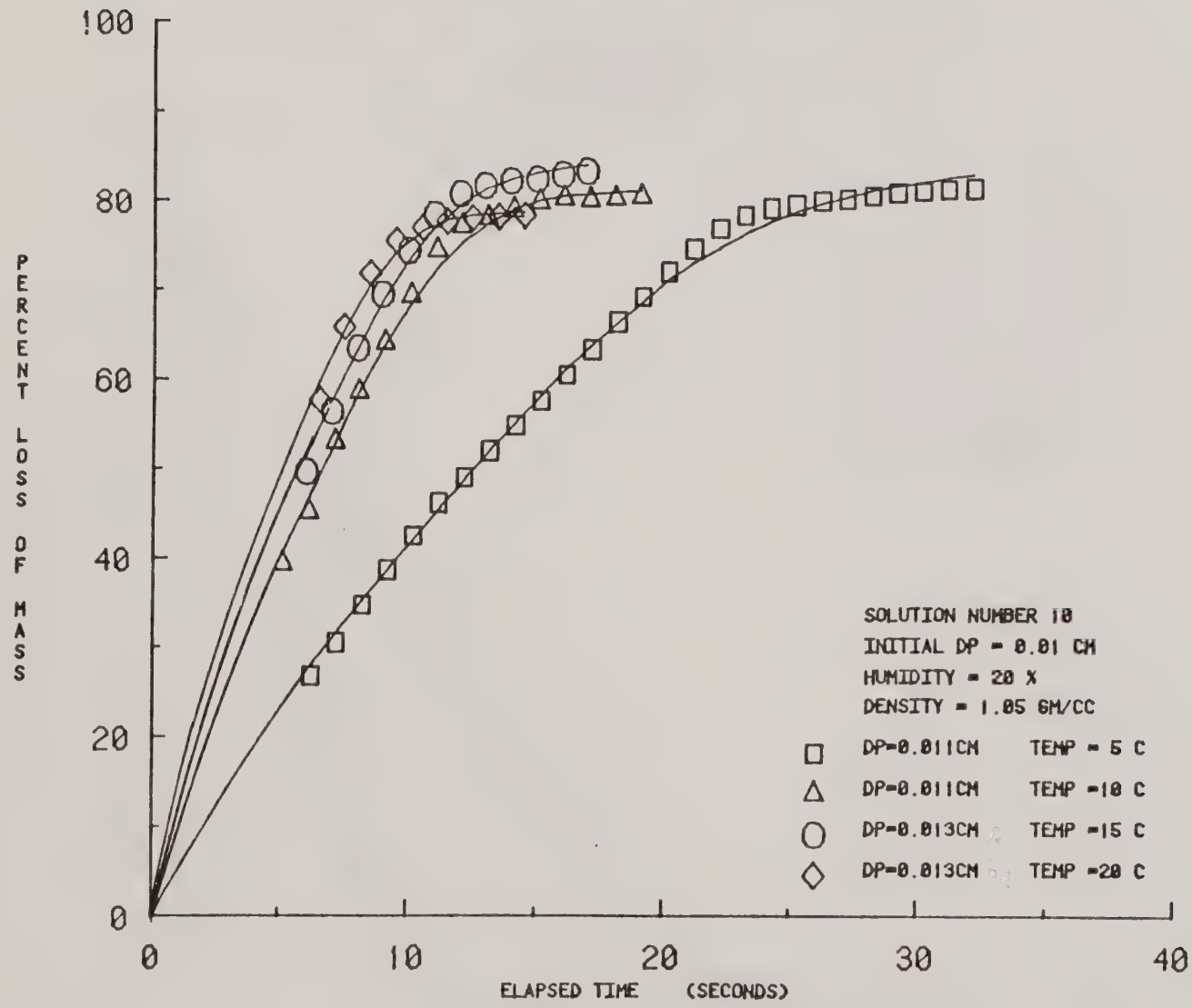

Figure 31. Relative Effects of Percent of Mass Loss by a Change in Air Temperature for Solution 10.

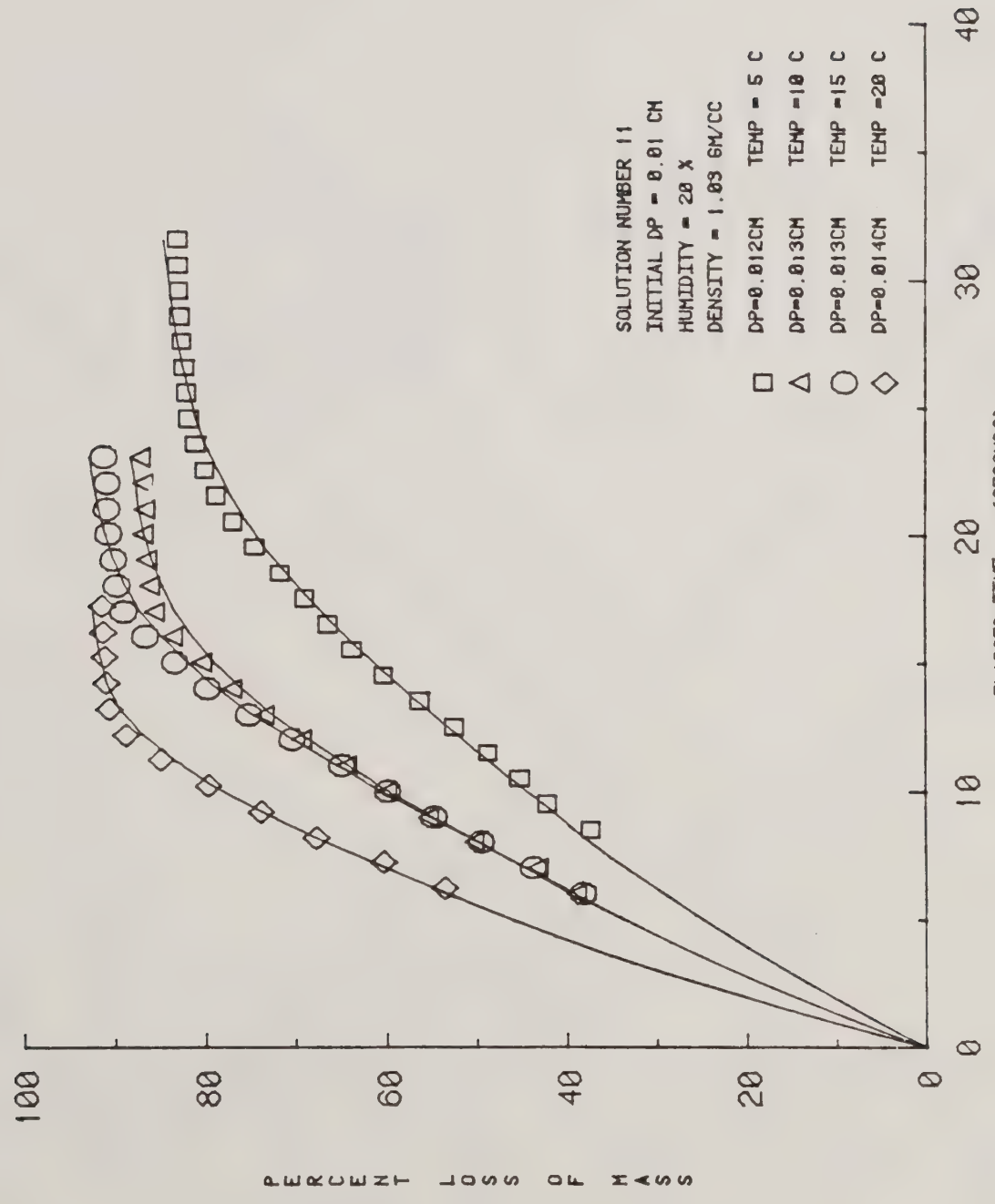

Figure 32. Relative Effects of Percent of Mass Loss by a Change in Air Temperature for Solution 11.

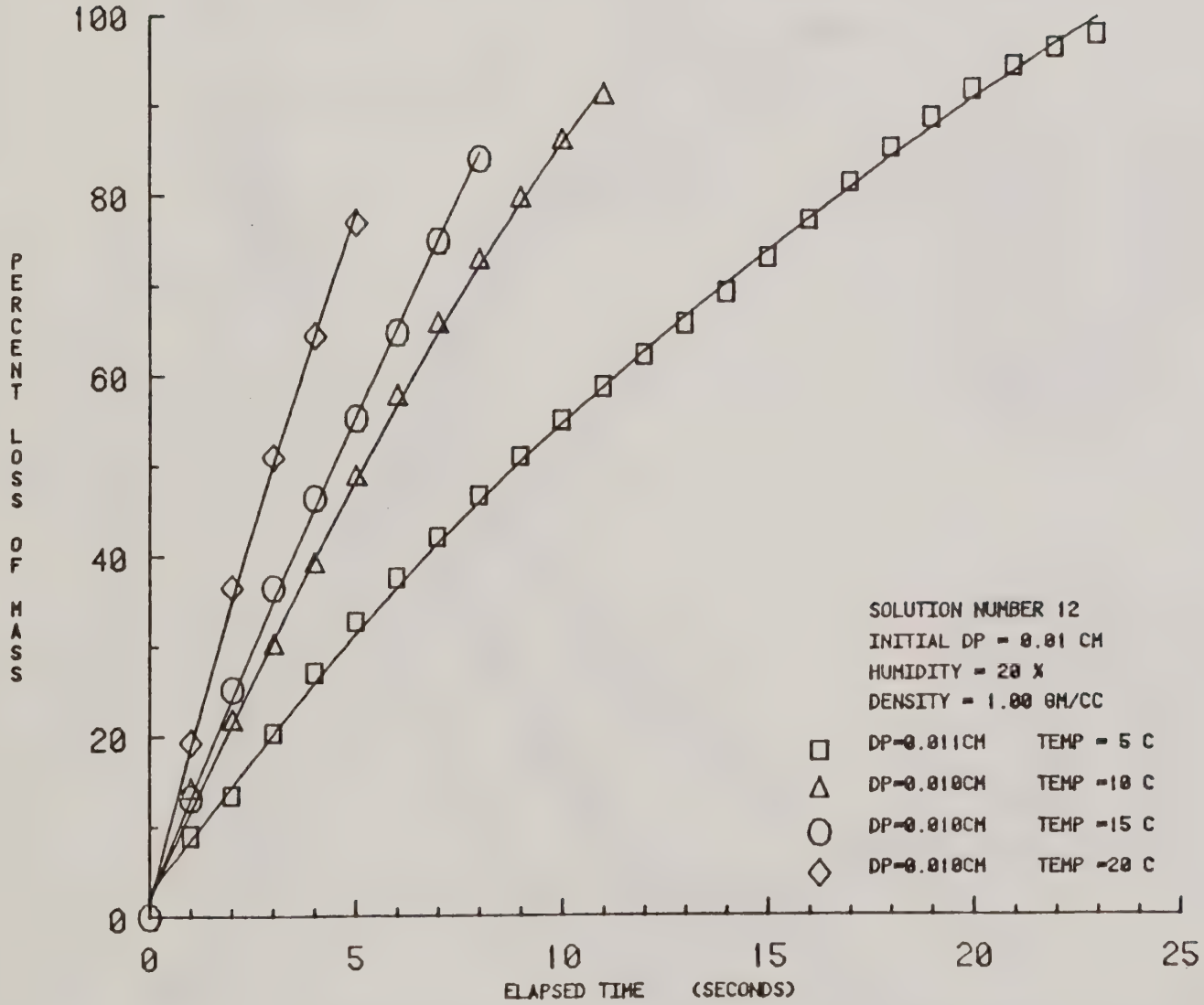

Figure 33. Relative Effects of Percent of Mass Loss by a Change in Air Temperature for Solution 12.

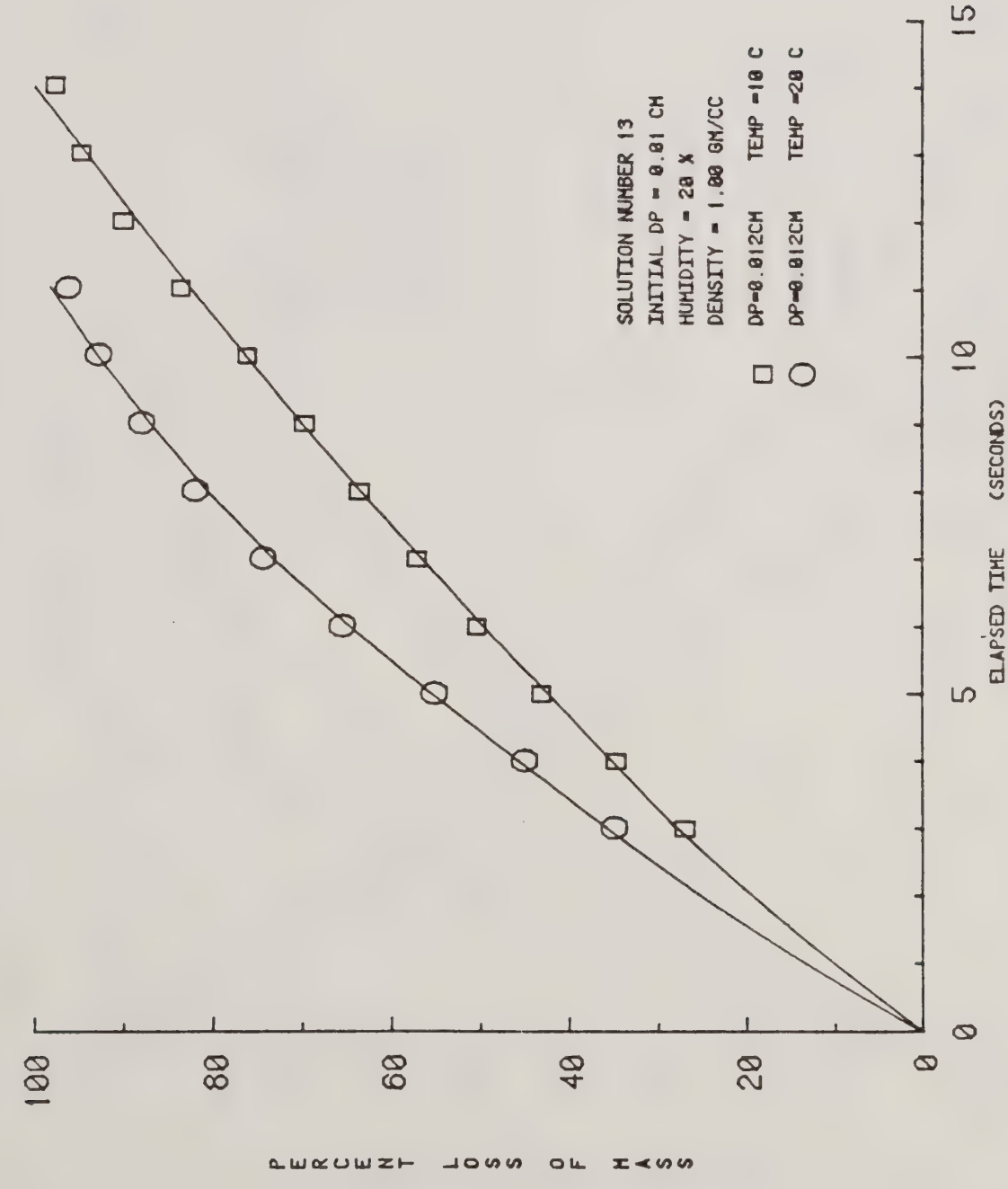

Figure 34. Relative Effects of Percent of Mass Loss by a Change in Air Temperature for Solution 13.

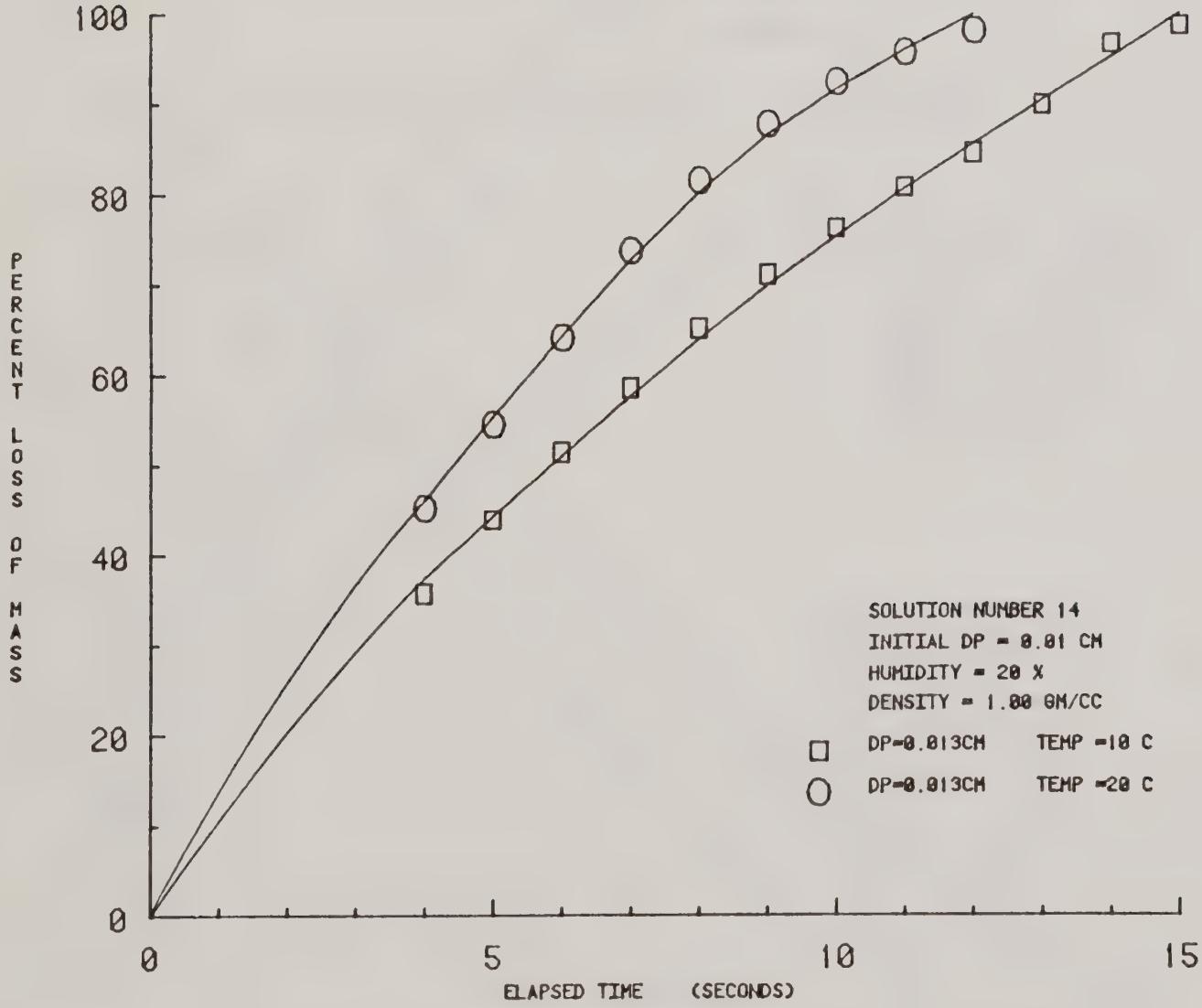

Figure 35. Relative Effects of Percent of Mass Loss by a Change in Air Temperature for Solution 14.

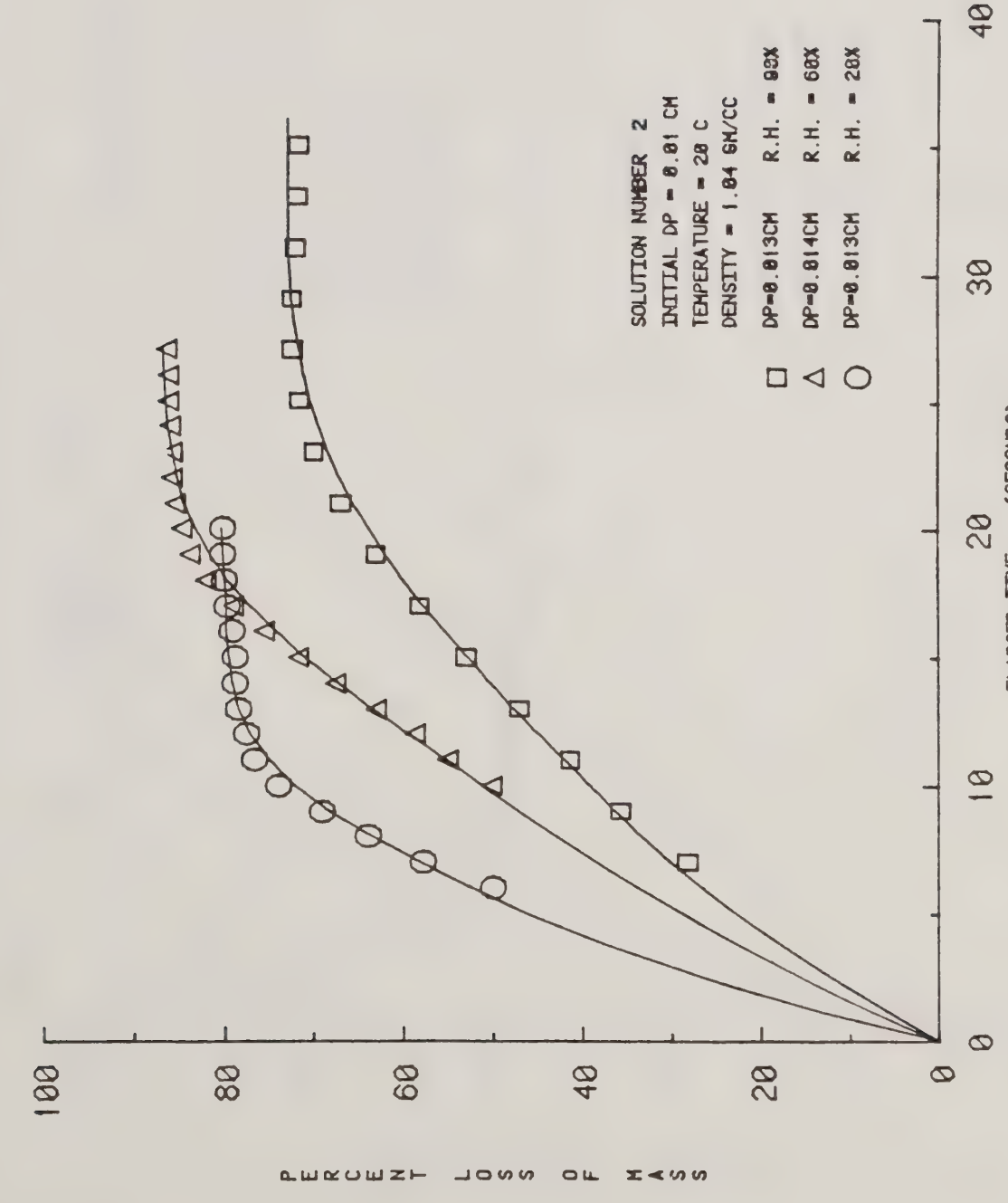

Figure 36. Relative Effects of Percent of Mass Loss by a Change in Air Humidity for Solution 2.

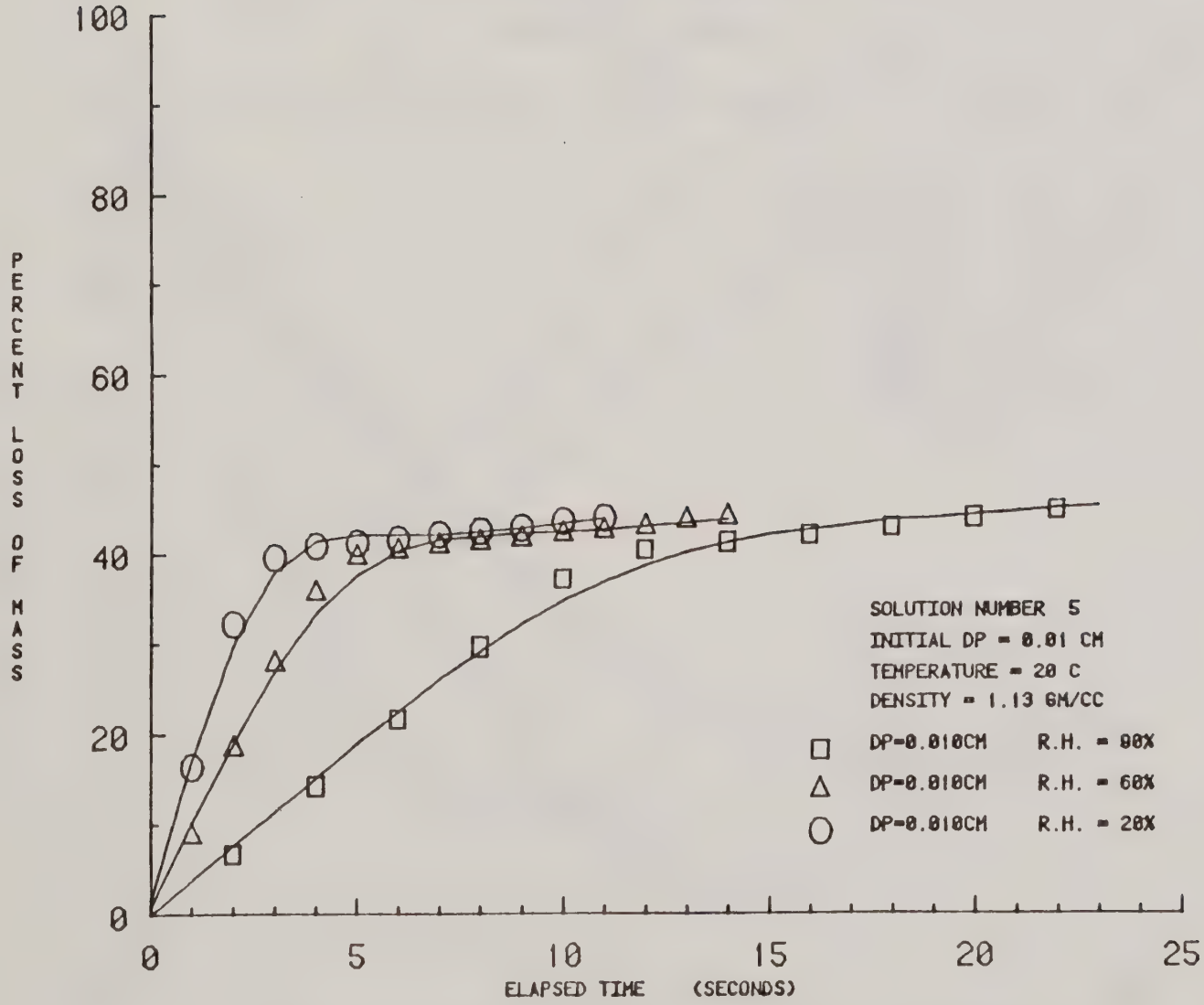

Figure 37. Relative Effects of Percent of Mass Loss by a Change in Air Humidity for Solution 5.

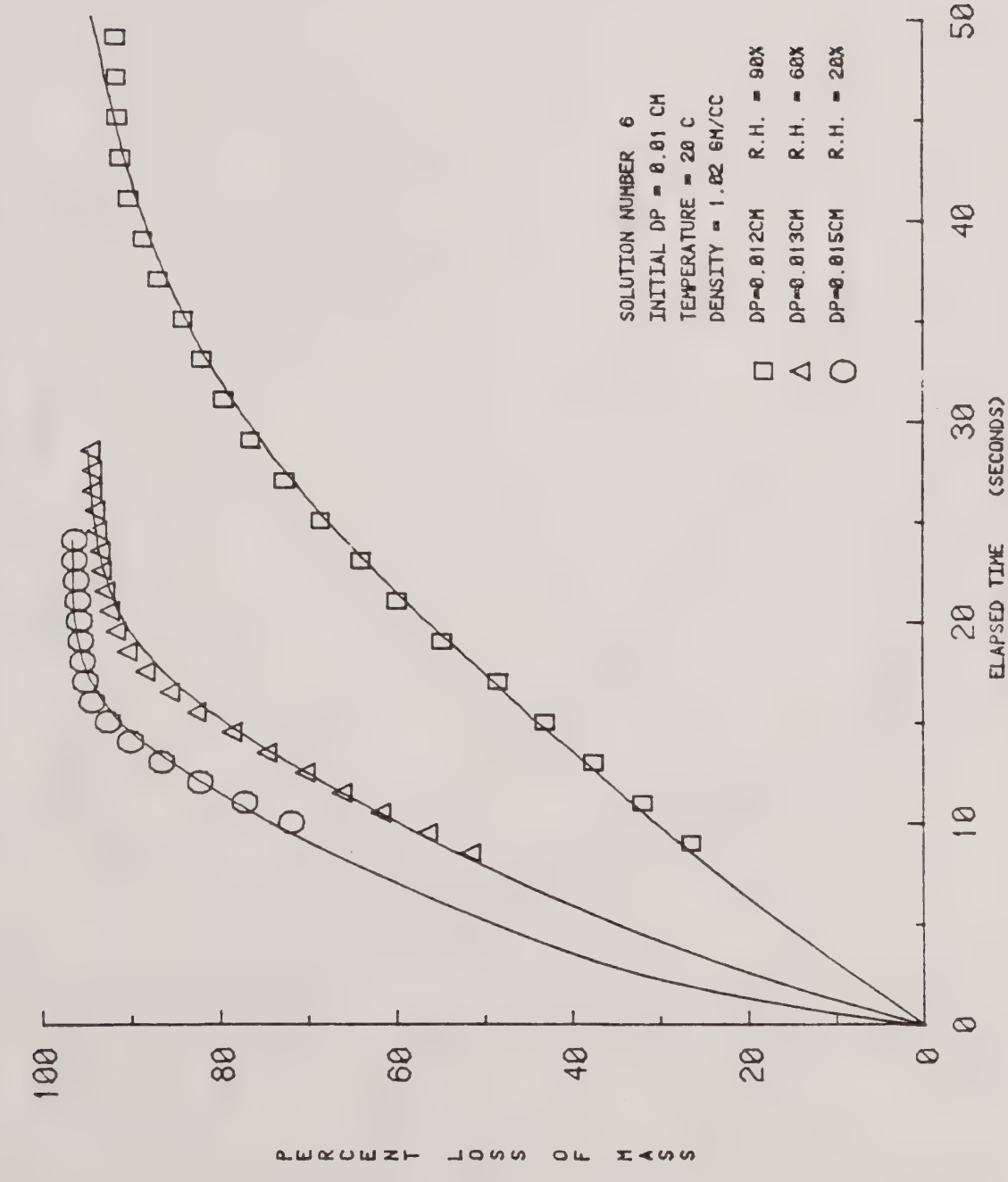

Figure 38. Relative Effects of Percent of Mass Loss by a Change in Air Humidity for Solution 6.

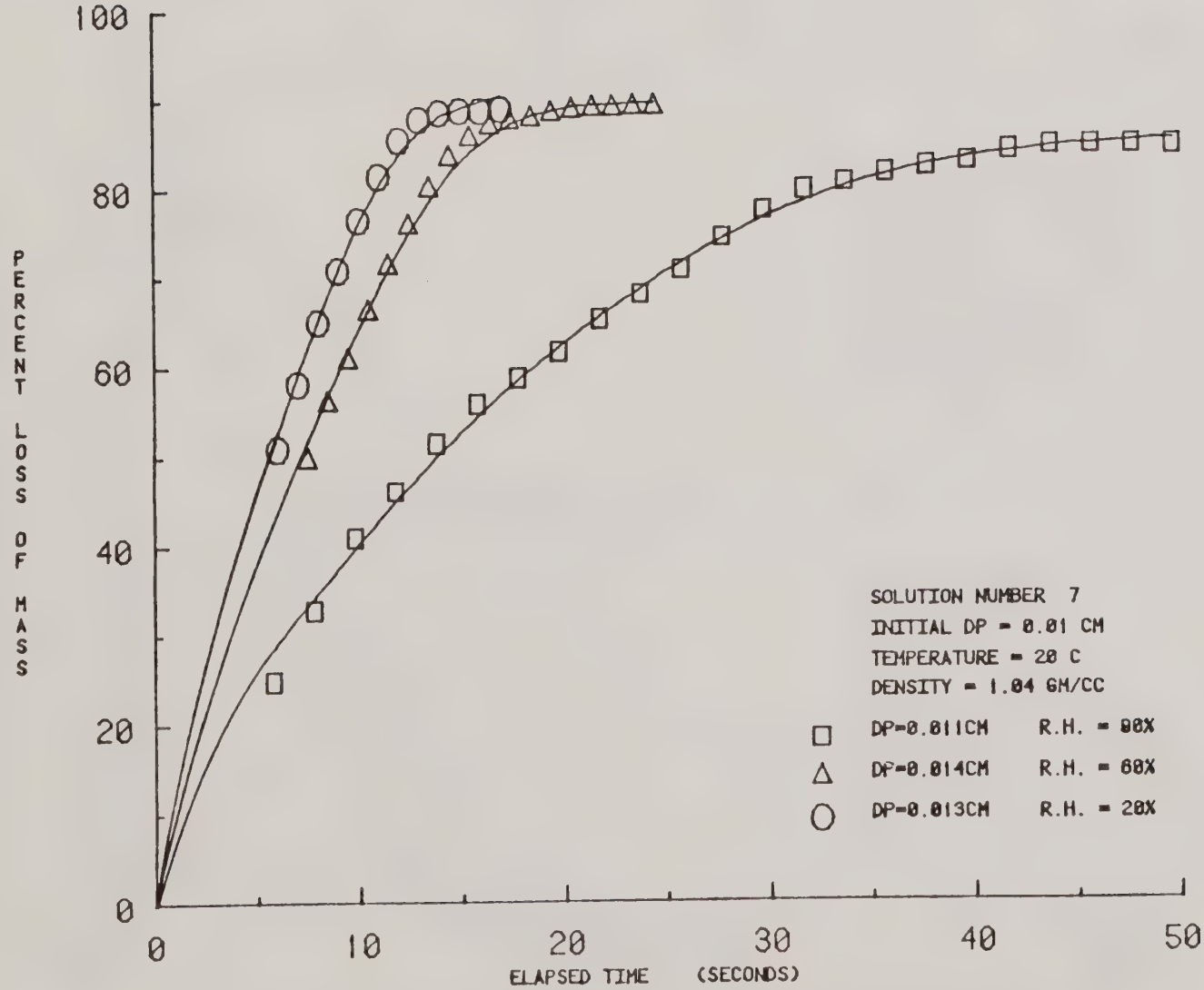

Figure 39. Relative Effects of Percent of Mass Loss by a Change in Air Humidity for Solution 7.

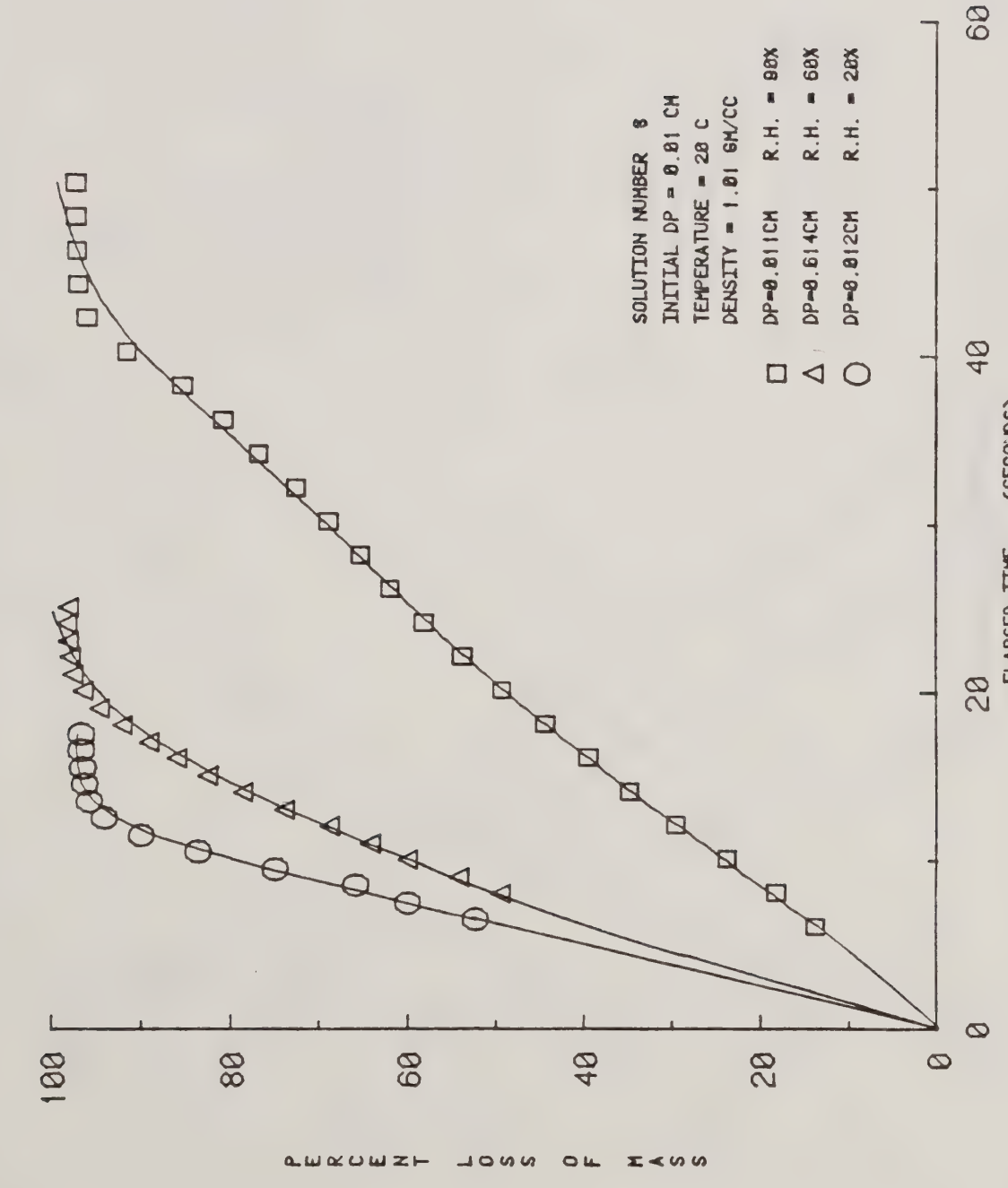

Figure 40. Relative Effects of Percent of Mass Loss by a Change in Air Humidity for Solution 8.

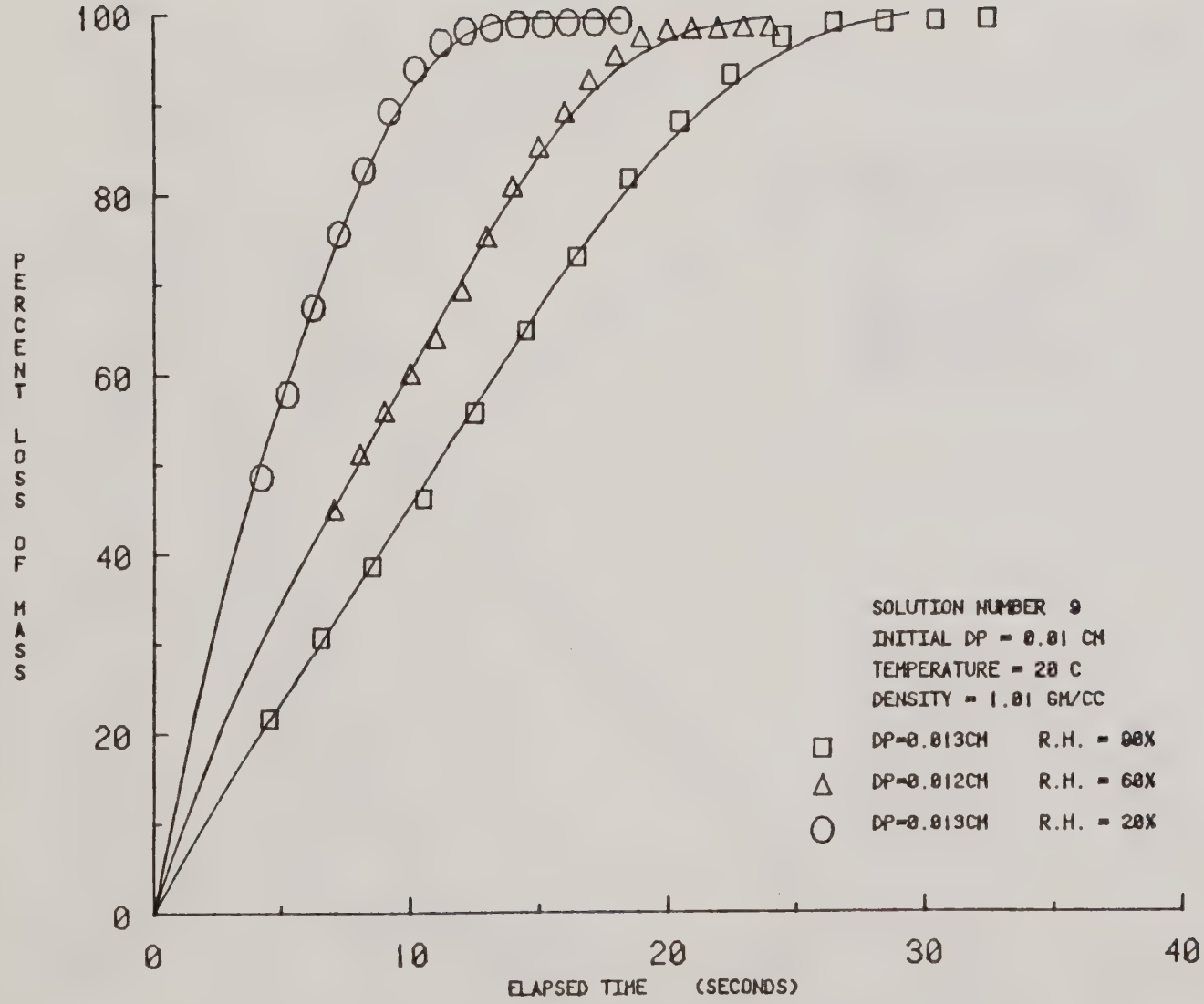

Figure 41. Relative Effects of Percent of Mass Loss by a Change in Air Humidity for Solution 9.

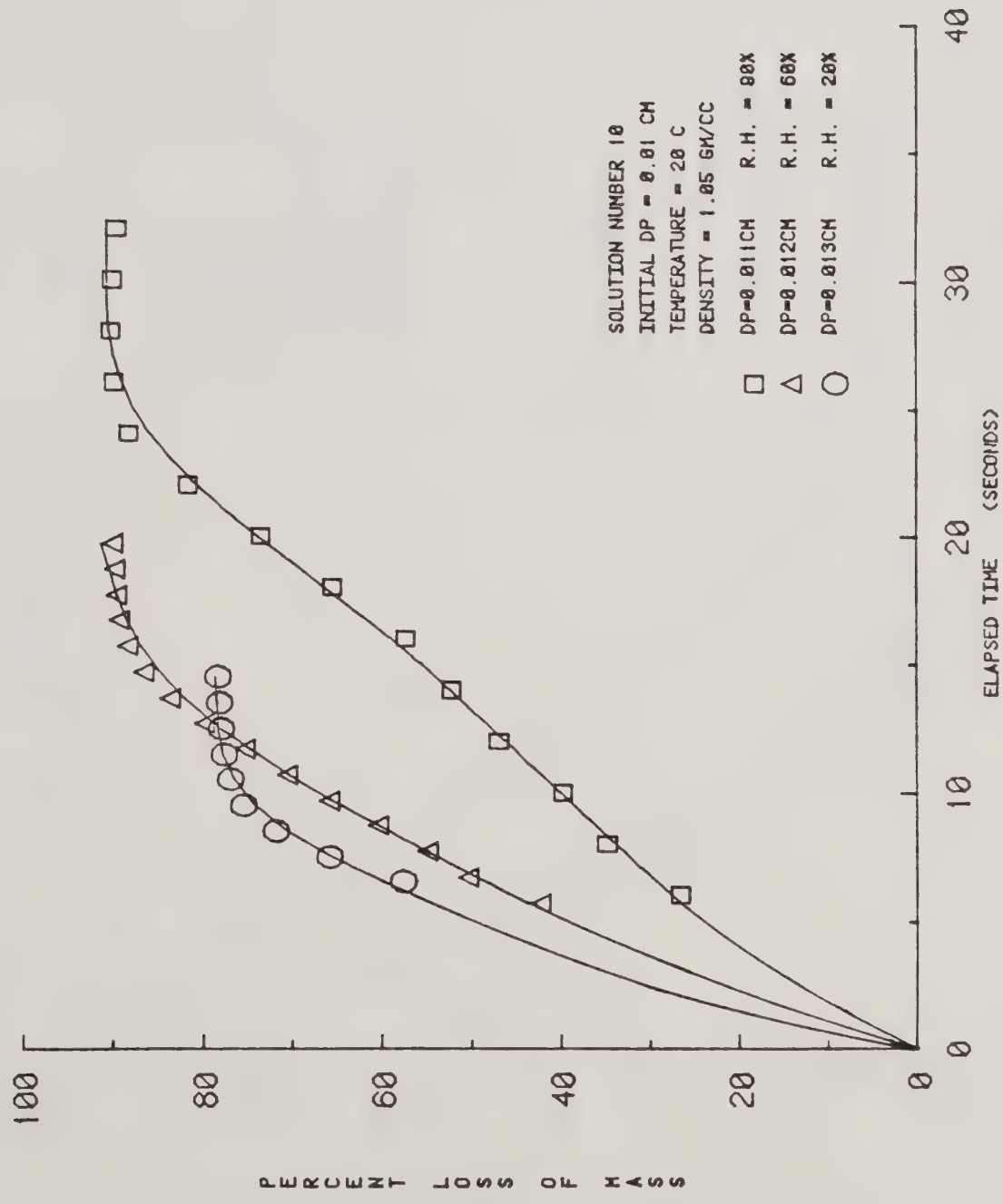

Figure 42. Relative Effects of Percent of Mass Loss by a Change in Air Humidity for Solution 10.

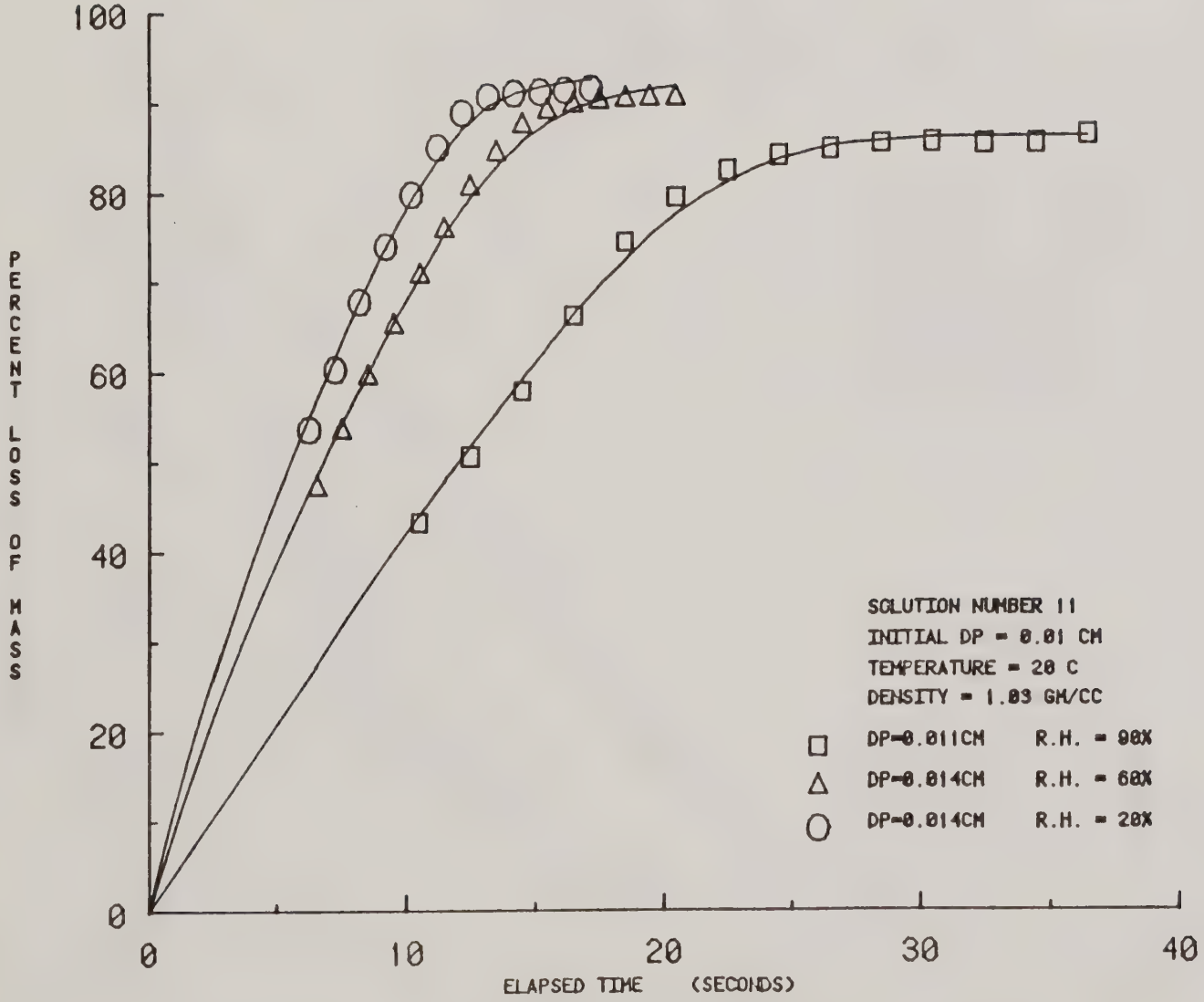

Figure 43. Relative Effects of Percent of Mass Loss by a Change in Air Humidity for Solution 11.

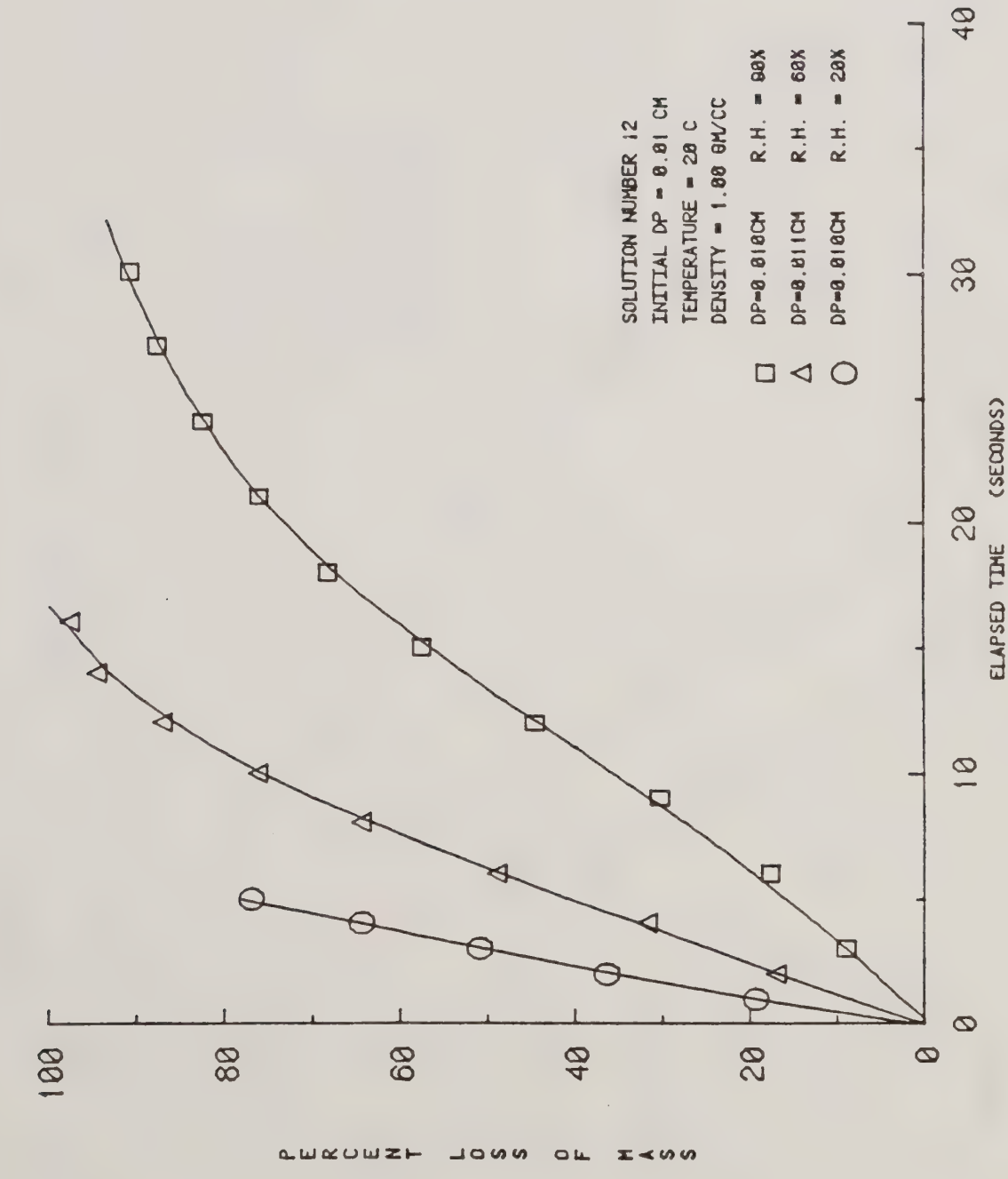

Figure 44. Relative Effects of Percent of Mass Loss by a Change in Air Humidity for Solution 12.

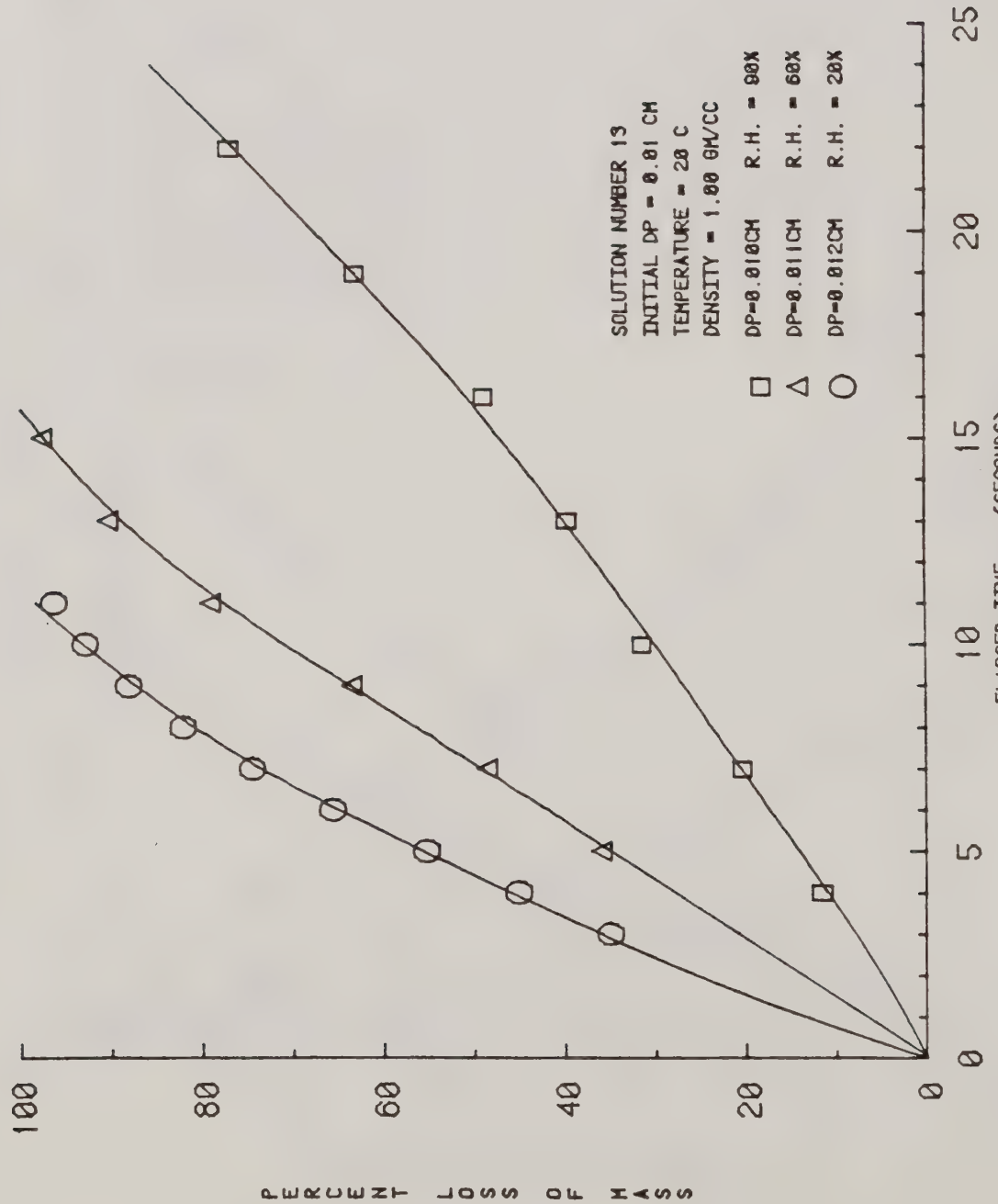

Figure 45. Relative Effects of Percent of Mass Loss by a Change in Air Humidity for Solution 13.

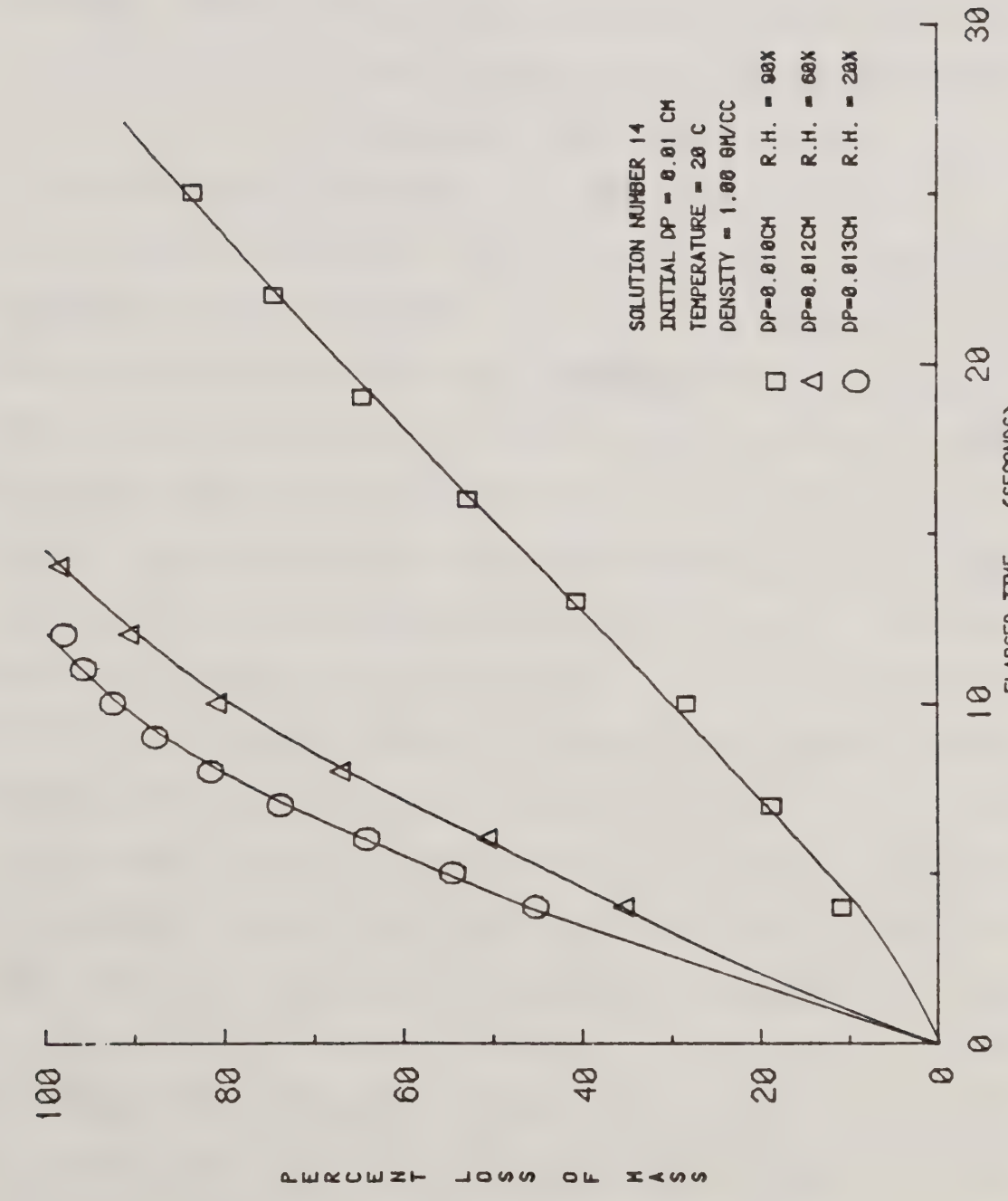

Figure 46. Relative Effects of Percent of Mass Loss by a Change in Air Humidity for Solution 14.

approximated data detailed in section 8.3.2. Plots describing solutions 13 and 14 contain only two curves. The elimination of the other tests, as mentioned in section 8.2.2, reduced the number of curves. Each figure shows the individual solution's dependence on droplet size. However, all the plots evaporate at a rate similar to water. This was a basic assumption for the approximation of data in section 8.3.2.

8.5.4.2 Change in Air Temperature

The effect on the percent loss of mass due to changing the air temperature for the volatile solutions can be seen in Figures 25 - 35. Examination of the different curves, corresponding to the different air temperatures, revealed the higher temperatures produce faster rates of evaporation. The effect of different initial droplet diameters will also alter these curves, therefore these diameters were given for each curve. An even transition from curve to curve can be seen in most of the plots. Irregularities are shown in some of the figures. These could have been caused by slight errors in the temperature and relative humidity readings for the test. For example, Figures 26, 27, 29, 31 and 33 describing solutions 5, 6, 8, 10 and 12 show a larger difference between the curves for $5^{o}C$ and $10^{o}C$ than between any of the others. This indicates that the actual humidity may have been higher than 20%. Also, Figures 28 and 30 describing solutions 7 and 9 both show near identical curves for the $5^{o}C$ and $10^{o}C$ data and the $15^{o}C$ and $20^{o}C$ data. This may be attributable to an error in the data. Interpolation between the $5^{o}C$ and the $20^{o}C$ data should give an accurate approximation. Generally, the trend caused by the change in air temperature change can be seen with these plots.

8.5.4.3 Change in Air Relative Humidity

Figures 36 - 46 show plots of the percent mass loss as a function of time for each solution over a range of air relative humidities. Each solution was described by the different figures. As the humidity increased, the rate of mass loss was seen to decrease. This effect generally seemed to get more pronounced as larger amounts of moisture were added to the air. This observation was very much different from what was seen with the low volatility solutions. The reason for this difference in the high volatility solutions can be seen by recalling the driving force of evaporation, equation 8.6. The vapor concentration at the surface of these droplets should be similar to the vapor concentration of water. This is because the basic component of these solutions was water. As more and more water is added to the environmental air, the C_∞ term should increase. The total effect would be to decrease the term given by 8.6 and therefore the entire evaporation.

8.5.5 Summary of Mass Loss Plots

A general summary of the results given in sections 8.5.3 and 8.5.4 will give an overall view of the effects of changing each initial condition. The individual effects on each solution can be determined by examining the respective figures. The physical process will be examined so as to determine the cause of the different effects on mass transfer.

Rearranging the equation for the Sherwood number, equation 2.6, allows a value for the rate of convection mass transfer:

$$\left(\frac{dm}{dt}\right)_c = \left(\frac{Sh}{2}\right)\left(\frac{-4\pi aDM\ell}{R}\right)\left(\frac{P_0}{T_0} - \frac{P_\infty}{T_\infty}\right) \qquad (8.7)$$

Assuming a functional form of Sh can be determined for all solutions such that Sh = Sh(Re,Sc), 8.7 becomes:

$$\left(\frac{dm}{dt}\right)_c = Sh(Re,Sc)\left(\frac{-2\pi\ a\ DM\ell}{R}\right)\left(\frac{P_0}{T_0} - \frac{P_\infty}{T_\infty}\right) \qquad (8.8)$$

Equation 8.8 defines the theoretical rate of transfer of mass from droplets. The relative effects on this value due to the changes of conditions can be examined with this expression.

Of all the changes of initial conditions, the change of initial droplet diameter had the greatest effect on the mass transfer. As the initial diameters decreased (an increase in the surface area to volume ratio), a larger percentage of mass was lost for identical time intervals. The cause of this effect can be seen by examining the initial values of the masses. Because the initial mass of the smaller diameter droplets was itself small, small changes in the diameter as the droplet evaporates corresponded to large percentages of its mass. The $\left(\frac{dm}{dt}\right)_c$ value from equation 8.8 can be shown to decrease for smaller values of droplet diameters. This effect was doubled when using freely falling droplets because Re decreased as the diameter decreases. This indicates a reduction in the rates of mass transfer. However, this reduction is caused by the continuing decrease in the amount of available droplet mass.

Changing the air relative humidity caused the next greatest effect on the mass transfer in the high volatility solutions. As discussed in section 8.5.3.3, the addition of moisture into the air had negligible effects on the evaporation of the oil-based solutions. The effect of increased humidity on the water-based solutions was discussed in detail in section 8.5.4.3. Since the driving force term, given by equation 8.6,

was seen to decrease as the humidity increased, the rate of mass transfer, equation 8.8, of these solutions must also decrease. Using identical initial droplets in different air humidities, the percent loss of mass can easily be seen to be larger for the droplet in the lower humidity. An example using 20% and 60% relative humidities is shown in Figure 47.

The last change of testing conditions was the varying of the air temperature. The effects of this change were relatively small compared to those caused by changing the initial droplet size. Changing the air temperature affected several terms in equation 8.8. Values of Re, Sc, D, P_0, P_∞ and T_0 were altered by the change in air temperature, T_∞. The values of Re, Sc, and D should vary slightly with the changes in air temperatures used in this study. Realizing the temperatures, T_0 and T_∞, were expressed in units of degrees Kelvin, the range from 5^oC to 20^oC becomes insignificant also. The values of the vapor pressures should vary little more than D with temperature, see Table 4 for an example. Therefore, changes in air temperatures have only slight effects on the mass transfer as compared with the other changes. The exception to this was the effect of varying humidity on the oil-based solutions. However slight, the rates of mass transfer were decreased as the temperatures were lowered. As seen in Figure 47 with different humidities, it can be shown that the percent loss of mass also decreased as the temperature decreased.

Figure 47

Calculations Relating Rate of Mass
to Percent of Mass Loss

Given that rate of mass transfer is
greater for lower humidity values

$$\left(\frac{dm}{dt}\right)_{20\%} > \left(\frac{dm}{dt}\right)_{60\%}$$

or

$$\left(\frac{m_0 - m_1}{\Delta t}\right)_{20\%} > \left(\frac{m_0 - m_2}{\Delta t}\right)_{60\%}$$

The time intervals are the same

$$(m_0 - m_1)_{20\%} > (m_0 - m_2)_{60\%}$$

Dividing by the initial mass

$$\left(\frac{m_0 - m_1}{m_0}\right)_{20\%} > \left(\frac{m_0 - m_2}{m_0}\right)_{60\%}$$

These are percent loss of mass values

$$(\text{percent loss of mass})_{20\%} > (\text{percent loss of mass})_{60\%}$$

8.6 Estimation of Error

8.6.1 Error Due to Supporting Wire

Experiments using pendant droplets have been examined with extreme caution by previous authors. The main concern with such experiments has been the error introduced by the wire used to support the droplet. The heat supplied to the droplet by the wire has been the subject of most of this criticism. This section will attempt to show that the error introduced by the supporting wire in this study was negligible.

The heat transfer of a ventilated droplet is an analogous procedure to the mass transfer of the same system. The effects of forced convection on this heat transfer are contained in the Nusselt number, Nu. Since the physical processes of heat and mass transfer are similar, the Nusselt number and Sherwood number should have similar empirical expressions. Therefore, an expression for the Nusselt number as a function of Re and the Prandtl number can be given.

$$Nu = 1.755 + 0.535\ Re^{1/2}\ Pr^{1/3} \tag{8.9}$$

Equation 8.9 can be used to determine values of Nu for any droplet size. The Nusselt number was defined as a wind factor in equation 2.7.

$$Nu = 2\frac{\left(\ell\frac{dm}{dt}\right)_c}{\left(\ell\frac{dm}{dt}\right)_0} = \frac{\left(\ell\frac{dm}{dt}\right)_c}{2\pi ak(T_\infty - T_a)} \tag{2.7}$$

This expression can be rearranged and a value of $\left(\ell\frac{dm}{dt}\right)_c$ determined for any droplet falling freely through air. The $\left(\ell\frac{dm}{dt}\right)_c$ term represents the rate of heat transfer of a ventilated droplet. Comparing the heat conducted through the supporting wire to this value will reveal the relative amount of error introduced.

The heat conducted through the supporting wire can be calculated easily using the general equation for the heat flux:

$$\frac{dQ}{dt} = KA \frac{dT}{dL} = KA \frac{(T_\infty - T_a)}{L} \qquad (8.11)$$

where L is one half of the length of the wire. As described earlier, three different types and sizes of wires were used. This analysis will include the 17.8 micron platinum and the 5 micron tungsten wires as they were used most frequently. Applying equation 8.11 with the most extreme of the environmental conditions, 20°C and 20% relative humidity, values of the heat flux can be calculated. These values are compared with the values obtained from equation 8.10 in Table 5. It should be noted that the smaller wire was used when testing the smaller sized droplets. Therefore, the heat flux values calculated for the wires were compared to the heat transfer values of the droplets with which they were commonly used. The largest percentage obtained by this analysis was 3.4%, which occurred at 50 microns using the small wire. It is believed that such a percentage is not significant. This addition of heat would cause a rise of the droplet temperature of approximately 1%. This is about the same as the error expected in measuring the air temperature. Therefore, the heat conducted by the wire is negligible as compared with the heat transfer of the pendant droplet.

8.6.2 Estimation of Experimental Error

An error analysis was performed for this study to determine an expected error of the results. The step-by-step analysis can be seen in Appendix 4. This analysis was used to determine expected errors for Sh and C for the ranges used in obtaining the plot shown in Figure 4. This, in turn, should give a good indication of the actual

Table 5

Heat Conduction Through Supporting Wire

$Nu = 1.755 + 0.535\ Re^{1/2} Pr^{1/3}$

Pr = 0.72 at 20°C from Davies

Droplet Diameter (microns)	Nu	$\ell \dot{m}_c$ (cal/sec)	$\frac{dQ}{dt}$ (cal/sec)	$\frac{dQ}{dt} / \ell \dot{m}_c$	Percentage
400	4.62	3.80×10^{-4}	3.65×10^{-6}	0.010	1.0
300	3.88	2.39×10^{-4}	3.65×10^{-6}	0.015	1.5
200	3.10	1.27×10^{-4}	3.65×10^{-6}	0.029	2.9
100	2.32	4.77×10^{-5}	7.03×10^{-7}	0.015	1.5
50	2.00	2.06×10^{-5}	7.03×10^{-7}	0.034	3.4

Values used for thermal conductivity*

platinum K = 0.17447 cal/sec cm deg

tungsten K = 0.4254 cal/sec cm deg

*Values taken from Handbook of Chemistry and Physics, 52nd edition, The Chemical Rubber Co. (1971).

expected error in α and β, the regression coefficients, and therefore the results of the entire study. An expected error of 8.5% was obtained. The average error of the Sh versus C curve was found to be 16.5%, approximately double the expected error. This indicates that the facility did not control one of the variables as well as expected.

It is believed that the control of humidity was not as good as anticipated. Large errors could easily be introduced when the measurement of the humidity depended on wet and dry bulb readings. An error in reading either one or both of the temperatures could have easily created the errors shown. Another possible error source in measuring and controlling the humidity was the distance between the source of humidity, the actual test section, and the point of measurement. The source of humidity was located approximately five feet upstream of the position of the supporting wire. The psychometer was located another foot downstream of this wire. Therefore, the air must pass six feet before its humidity can be measured. When the humidity exceeded the desired value and the controlling circuitry turned the water atomizer off, an additional five feet of the humid air passed through the test section. Additionally, the air may not have been adequately mixed and thus a non-homogeneous air stream may have resulted.

Chapter 9

CONCLUSIONS AND REMARKS

1) The experimental facility that was developed accurately and reproducibly measured the droplet sizes and adjusted the wind tunnel velocity to the corresponding terminal velocity. The heat gain from the supporting wire was negligible when compared to the heat transfer of the droplet. Therefore, the facility simulated free fall conditions and represents a viable and flexible resource which can be applied to future tests of this nature.

2) The procedure used to approximate the 50 micron tests was supported by observations of experimental results. Subsequent analysis of the data showed that the assumptions used in the procedure remained consistent throughout the study.

3) A correlation between the Sherwood number and $Re^{1/2}Sc^{1/3}$ was determined for water as:

$$Sh = 1.755 + 0.535\ Re^{1/2}Sc^{1/3}$$

A correlation coefficient of 0.799 was obtained with this equation and indicated a good fit of the data. This equation agreed well with previous works with the exception of the intercept term. This value was determined to be less than the theoretical limit and indicated a discrepancy between the theory and experimental data.

4) Percent loss of mass versus time data were obtained for each solution. A standard condition of $20^{o}C$, 20% relative humidity, and a 100 micron initial diameter was used. Each of the three test variables, initial droplet diameter, temperature and relative humidity, were changed

and the resulting curves plotted to show the relative effects on mass transfer. The results were representative of the actual process and an error of 8.5% can be expected. In general, the largest effect on the transfer of mass resulted from a change in the initial droplet diameter.

5) The psychrometer measurement and the control of the air humidity was the source of greatest error in this study. A more accurate mode of measurement should be employed, such as a set of wet and dry bulb thermistors. The source and measurement of humidity should be set closer to the position of the supporting wire with perhaps a need for better mixing. This will allow for the reduction of varying humidities along the wind tunnel.

BIBLIOGRAPHY

1. Beard, K.V. and Pruppacher, H.R., "The Rate of Evaporation of Small Water Drops Falling at Terminal Velocity in Air". Conference on Cloud Physics. Fort Collins, Colorado, 1970.

2. Bowker, A.H. and Lieberman, G.J. Engineering Statistics. 2nd ed. Prentice Hall. Englewood Cliffs, 1972.

3. Davies, C.N. "Evaporation of Airborne Droplets". In Fundamentals of Aerosol Science, pp. 135-164. Edited by D.T. Shaw. John Wiley & Sons, New York, 1978.

4. Froessling, N. Gerlands Beitrage Geophys., Vol. 52, p. 170, 1938.

5. Fuchs, N.A. Evaporation and Droplet Growth in Gaseous Media. Pergamon Press, Oxford, 1959.

6. Kinzer, G.D. and Gunn, R. "The Evaporation, Temperature and Thermal Relaxation-Time of Freely Falling Waterdrops". Journal of Meteorology. Vol. 8, p. 71, 1951.

7. Langmuir, I. Phy. Rev. Vol. 12, p. 368, 1918.

8. Maxwell, J.C. Collected Scientific Papers. Cambridge, Vol. 11, p. 625, 1890.

9. Picot, J.J.C., Chitrangad, B. and Henderson, G. "Evaporation Rate Correlation for Atomized Droplets". Transactions of the ASAE. Vol. 24, No. 3, p. 552, 1981.

10. Ranz, W.E. and Marshall, W.R., Jr. "Evaporation from Drops, Part I". Chemical Engineering Progress. Vol. 48, p. 141, 1952.

11. Van Wylen, G.J. and Sonntag, R.E. Fundamentals of Classical Thermodynamics. 2nd ed. John Wiley & Sons, New York, 1976.

12. White, F.M. Viscous Fluid Flow. McGraw-Hill, New York, 1974.

13. Williamson, R.E. and Threadgrill, E.D. "A Simulation for the Dynamics of Evaporating Spray Droplets in Agricultural Spraying". Transactions of the ASAE. Vol. 17, No. 2, p. 254, 1974.

14. Wolf, W.R. "Study of the Vibrating Reed in the Production of Small Droplets and Solid Particles of Uniform Size". The Review of Scientific Instruments. Vol. 32, p. 1124, 1961.

Appendix 1

ELIMINATION OF LOW VOLATILITY SOLUTIONS

Table 6

Rationale for the Elimination of Selected Tests

Solution #1

Test Number	Temperature (°C)	Relative Humidity (%)	Initial Particle Diameter (microns)	Final Particle Diameter (microns)	Time Length of Test (sec)	Change in Diameter (%)	Change in Mass (%)
301144	20	20	399.0	380.4	65	4.66	13.34
101143	20	20	242.7	233.5	113	3.79	10.95
201243	20	60	263.1	255.0	101	3.08	8.95
101134	15	20	445.1	436.2	56	2.07	6.07
201133	15	20	273.4	264.2	98	3.37	9.76
101233	15	60	264.4	252.7	101	4.43	12.70
101124	10	20	386.2	368.6	68	4.56	13.06
201123	10	20	262.4	257.8	101	1.75	5.17
101224	10	60	[illegible]	377.5	65	3.90	11.24
101223	10	60	258.0	250.7	101	.83	8.25

Table 7

Rationale for the Elimination of Selected Tests

Solution 53

Test Number	Temperature (°C)	Relative Humidity (%)	Initial Particle Diameter (microns)	Final Particle Diameter (microns)	Time Length of Test (sec)	Change in Diameter (%)	Change in Mass (%)
103144	20	20	420.4	409.5	56	2.59	7.58
103143	20	20	240.8	229.8	104	4.57	13.09
103244	20	60	421.8	410.7	56	2.63	7.69
103243	20	60	251.3	240.4	98	4.34	12.46
103134	15	20	402.7	391.3	59	2.83	8.25
103133	15	20	247.8	236.5	101	4.56	13.07
103234	15	60	400.5	393.8	59	1.67	4.94
103233	15	60	252.8	244.8	98	3.16	9.20
103223	10	60	241.9	238.1	101	1.57	4.64

Table 8

Rationale for the Elimination of Selcted Tests

Solution #4

Test Number	Temperature (^{O}C)	Relative Humidity (%)	Initial Particle Diameter (microns)	Final Particle Diameter (microns)	Time Length of Test (sec)	Change in Diameter (%)	Change in Mass (%)
104144	20	20	328.8	319.8	77	2.74	7.99
104143	20	20	282.5	271.9	95	3.75	10.84
101244	20	60	340.5	331.9	74	2.53	7.39
104245	20	60	234.9	227.7	119	3.07	8.92
104134	15	20	372.6	367.7	68	1.32	3.89
104133	15	20	241.7	235.8	113	2.44	7.15

Table 9

Rationale for the Elimination of Selected Tests

Solution #1

Test Number	Temperature (°C)	Relative Humidity (%)	Initial Diameter (microns)	Final Diameter (microns)	Total * Time (secs)	Change in Diameter (%)	Change in Mass (%)
101112	5	20	96.3	89.7	452 (10.3)	6.85	19.18
201112	5	20	94.0	87.5	460 (10.0)	6.91	19.34
101212	5	60	110.1	101.0	400 (7.7)	8.27	22.80
101122	10	20	110.0	101.9	411 (10.5)	7.36	20.50
201122	10	20	100.5	92.4	451 (6.0)	8.06	22.28
101222	10	60	95.0	84.3	451 (5.8)	11.26	30.13
201222	10	60	114.3	103.0	402 (6.5)	9.89	26.82
101132	15	20	94.7	84.1	500 (7.5)	11.19	29.96
201132	15	20	103.0	89.5	550 (10.0)	13.11	34.39
101232	15	60	107.4	93.1	505 (5.0)	13.31	34.86
101142	20	20	102.7	91.5	361 (7.0)	10.91	29.28
201142	20	20	107.4	94.1	361 (6.5)	12.38	32.74
101242	20	60	96.0	81.3	550 (9.2)	15.31	39.26

Table 10 Rationale for the Elimination of Selected Tests

Solution #3

Test Number	Temperature (°C)	Relative Humidity (%)	Initial Diameter (microns)	Final Diameter (microns)	Total * Time (secs)	Change in Diameter (%)	Change in Mass (%)
103112	5	20	94.6	87.7	453 (8.5)	7.29	20.32
203112	5	20	107.6	100.0	401 (6.0)	7.06	19.73
103212	5	60	114.6	106.3	351 (9.8)	7.24	20.19
203212	5	60	95.7	87.4	452 (8.5)	8.67	23.83
103122	10	20	104.3	97.0	400 (7.5)	7.00	19.56
103222	10	60	97.3	86.7	451 (5.5)	10.89	29.25
203222	10	60	100.6	92.2	400 (9.0)	8.35	23.02
103132	15	20	110.1	100.7	400 (6.5)	8.54	23.49
103232	15	60	98.9	90.8	412 (9.0)	8.19	22.61
203232	15	60	117.1	112.2	302 (7.5)	4.18	12.04
303232	15	60	110.3	100.8	401 (5.5)	8.61	23.68
103142	20	20	105.4	94.7	400 (5.3)	10.15	27.47
103242	20	60	102.4	90.3	412 (5.0)	11.82	31.43
203242	20	60	99.7	88.2	451 (6.1)	11.53	30.77

Table 11

Rationale for the Elimination of Selected Tests

Solution #4

Test Number	Temperature (°C)	Relative Humidity (%)	Initial Diameter (microns)	Final Diameter (microns)	Total * Time (secs)	Change in Diameter (%)	Change in Mass (%)
104112	5	20	96.0	90.2	501 (7.9)	6.04	17.05
104212	5	60	107.0	99.5	400 (4.7)	7.01	19.59
104122	10	20	97.2	90.2	449 (5.4)	7.20	20.09
104222	10	60	104.0	94.1	452 (11.0)	9.52	25.93
104132	15	20	94.8	87.3	501 (9.0)	7.91	21.91
204132	15	20	116.2	107.6	400 (11.0)	7.40	20.60
104232	15	60	103.3	91.9	452 (9.5)	11.04	29.59
104142	20	20	113.8	102.0	403 (10.0)	10.37	27.99
104242	20	60	97.2	81.8	550 (8.5)	15.84	40.40

Table 12 Rationale for the Elimination of Selected Tests

Test Number	Temperature (°C)	Relative Humidity (%)	Initial Diameter (microns)	Final Diameter (microns)	Total * Time (secs)	Change in Diameter (%)	Change in Mass (%)
Solution 1							
101141	20	20	54.4	43.0	1660 (11.0)	21.0	50.6
101241	20	60	56.1	45.0	1584 (8.0)	19.8	48.4
Solution 3							
203141	20	20	56.6	48.6	1279 (7.7)	14.1	36.7
103241	20	60	48.1	42.5	1660 (8.6)	12.0	31.5
Solution 4							
104141	20	20	50.8	32.0	1799 (10.0)	37.0	75.0
104241	20	60	56.9	37.2	1799 (10.0)	34.6	72.5

Appendix 2

COMPARISON OF SOLUTIONS 13 AND 14 TO WATER

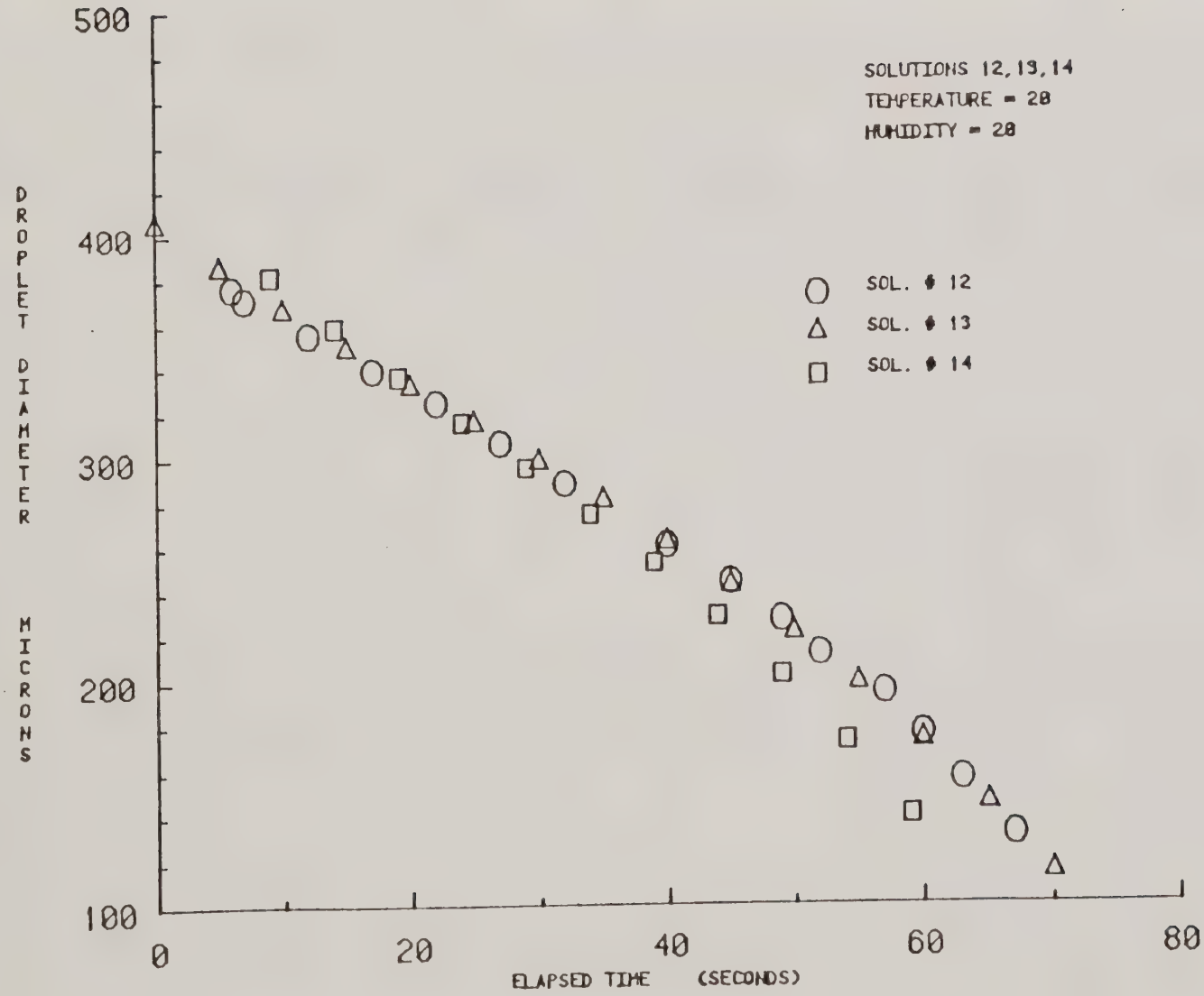

Figure 48. Plot Comparing the Evaporation of Solutions Containing Nalco-Trol With Water.

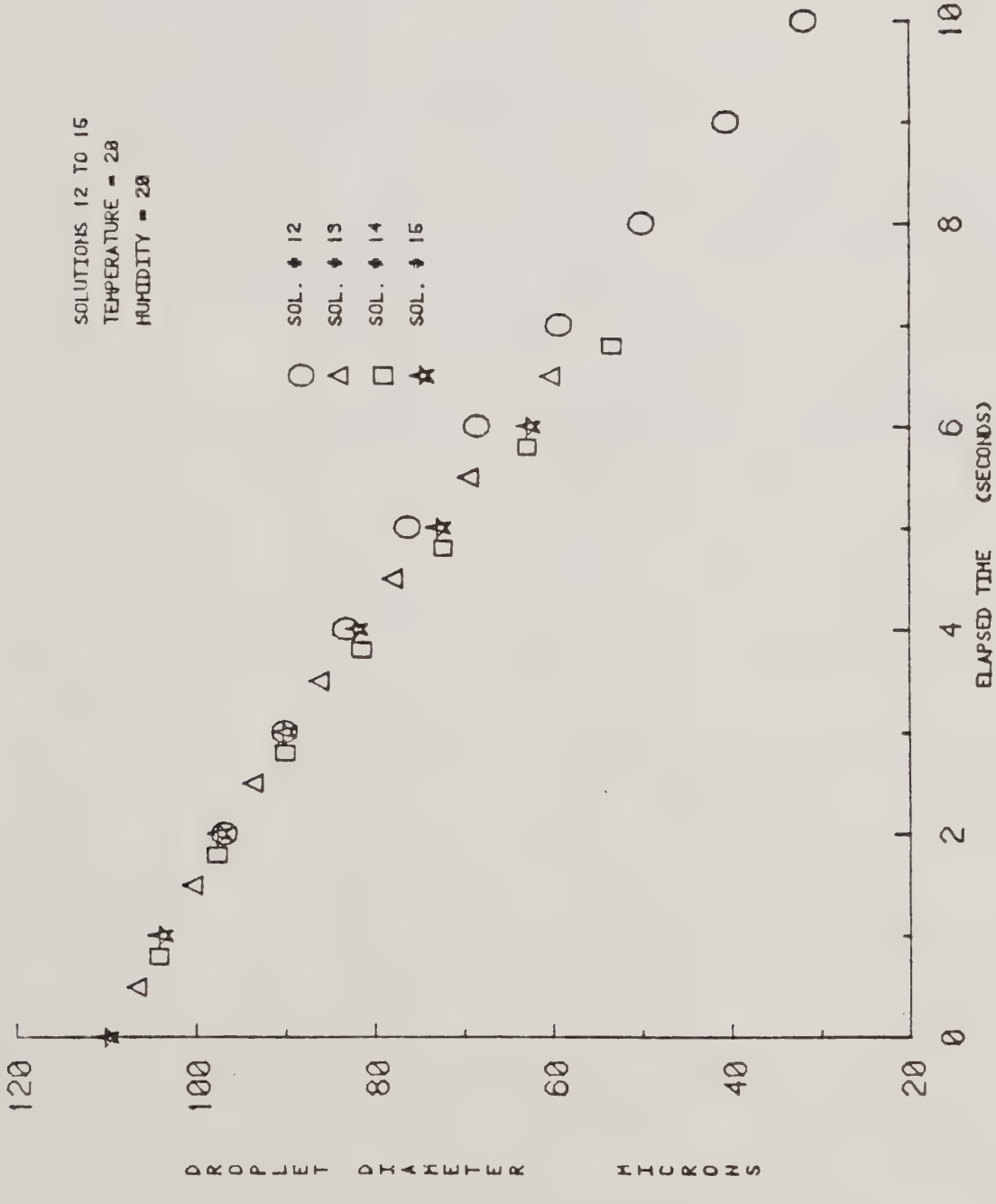

Figure 49. Plot Comparing the Evaporation of Solutions Containing Nalco-Trol With Water.

Table 13

Free Evaporation from Beakers

Approximately 10 cm^3 of each solution was measured and placed into 100 ml beakers

Time and Day of Measurement	Elapsed Time (hours)	Weight of Beaker and Solution, Weight Loss		
		Sol. 12 Distilled Water	Sol. 13 5 oz. N.T./ 100 gal. water	Sol. 14 10 oz. N.T./ 100 gal. water
4:30 p.m. 1/25/82	0.0	Beaker + Sol.=59.598g Mass Loss = 0.0g	Beaker + Sol.=57.9560g Mass Loss = 0.0g	Beaker + Sol.=59.3768g Mass Loss = 0.0g
8:20 a.m. 1/26/82	15.83	Beaker + Sol.=57.532g Mass Loss = 2.0251g	Beaker + Sol.=55.948g Mass Loss = 2.0071g	Beaker + Sol.=57.5141g Mass Loss = 1.8627g
4:30 p.m. 1/26/82	24.0	Beaker + Sol.=56.1218g Mass Loss = 3.4765g	Beaker + Sol.=54.541g Mass Loss = 3.415g	Beaker + Sol.=55.921g Mass Loss = 3.4557g
9:00 a.m. 1/27/82	40.5	Beaker + Sol.=53.7291g Mass Loss = 5.8692g	Beaker + Sol.=52.353g Mass Loss = 5.6028g	Beaker + Sol.=53.582g Mass Loss = 5.7948g
4:30 p.m. 1/27/82	48.0	Beaker + Sol.=52.5134g Mass Loss = 7.0849g	Beaker + Sol.=51.182g Mass Loss = 6.7732g	Beaker + Sol.=52.5359g Mass Loss = 6.8409g
8:20 a.m. 1/28/82	63.83	Beaker + Sol.=50.2656g Mass Loss = 9.3327g	Beaker + Sol.=48.907g Mass Loss = 9.049g	Beaker + Sol.=50.2748g Mass Loss = 9.102g
4:30 p.m. 1/28/82	72.0	Beaker + Sol.=49.6973g Mass Loss = 9.901g	Beaker + Sol.=48.1028g Mass Loss = 9.8532g	Beaker + Sol.=49.4117g Mass Loss = 9.9651g

Table 14

Percentage Mass Loss for

Free Evaporation from 100 ml Beakers

Total mass lost

Solution 12 - 9.9010 g

Solution 13 - 9.8532 g

Solution 14 - 9.9651 g

Elapsed Time (hours)	Percent Mass Loss		
	Solution 12 Distilled Water	Solution 13 5 oz NT/100 gal H_2O	Solution 14 10 oz NT/100 gal H_2O
0.0	0%	0%	0%
15.83	20.45%	20.37%	18.69%
24.0	35.11%	34.66%	34.68%
40.5	59.28%	56.86%	58.15%
48.0	71.54%	68.74%	68.65%
63.83	94.26%	91.84%	91.34%
72.0	100.0%	100.0%	100.0%

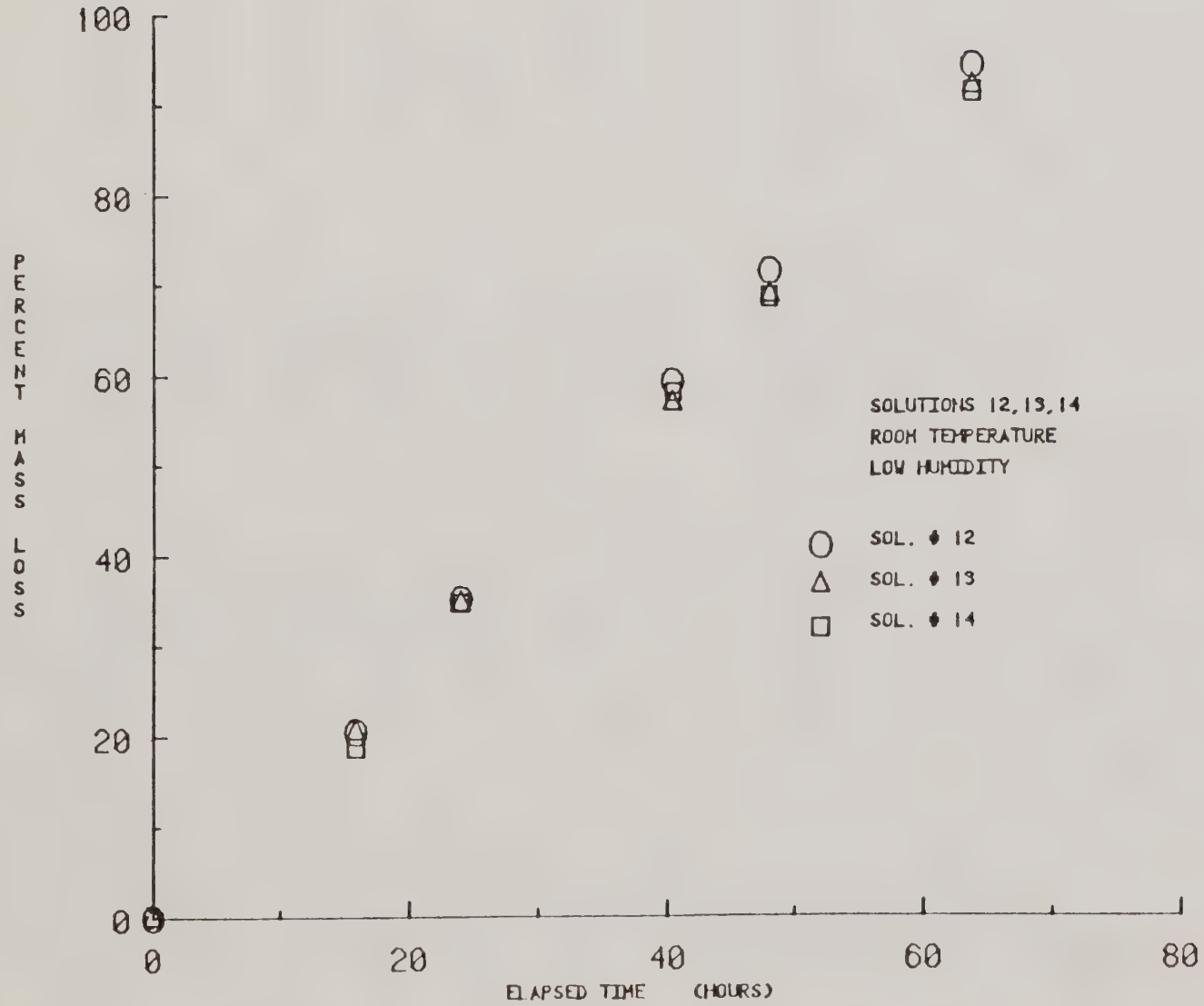

Figure 50. Plot Comparing the Free Evaporation of Solutions of Nalco-Trol With Water

Appendix 3

PROCEDURE FOR APPROXIMATION OF DATA

I. Parameters Used in the Approximation Scheme

D_0 - Original droplet diameter. Diameter of the droplet at the start of the evaporation rate history or at time = 0. This value is expressed in microns.

D_c - Critical droplet diameter. Diameter at which the rate of evaporation of the droplet changes drastically. At this diameter crystallization of the solid matter of the droplet solution begins causing the evaporation rate to decrease significantly.

t_c - Critical time. Time needed for the droplet to evaporate from D_0 to D_c. Expressed in the units of seconds.

t_∞ - Final time. Time at which the evaporation can be considered over. Expressed in seconds.

V_c - Initial volume concentration of non-volatile material of the solution, a dimensionless value.

II. Assumptions Used in the Approximation Scheme

1. A water-based solution evaporates at the same rate as water until the solid material begins to crystallize or solidify.

2. The droplet diameter at which crystallization starts is unique for any initial droplet diameter. This value will not change for a variety of temperatures and relative humidities.

3. The ratio of the volumes of the droplet at crystallization to the initial droplet is the same for any diameter droplet

4. After the point of crystallization, the rate of evaporation is not dependent upon droplet size and can be approximated by a constant slope line.

III. Calculations for Assumptions

V_C - Volume concentration of non-volatile material

$$V_C = \frac{\text{Volume of non-volatile material of initial mixture}}{\text{Total volume of initial mixture}}$$

Assuming each solution is completely mixed, V_C would be constant for all sizes of droplets

D_∞ - final droplet diameter, all volatile material has evaporated

then

$$\frac{4/3\pi\left(\frac{D_\infty}{2}\right)^3}{4/3\pi\left(\frac{D_\infty}{2}\right)^3} = V_C \qquad \text{A3.1}$$

or

$$\left(\frac{D_\infty}{D_0}\right)^3 = V_C \qquad \text{A3.2}$$

so that

$$\frac{D_\infty}{D_0} = V_C^{1/3} = \text{const.} = K_1 \qquad \text{A3.3}$$

where K_1 is unitless.

Using assumption 4, dD/dt - const. for $t \geq t_c$ for a given environmental condition, so that

$$\frac{D_C - D_\infty}{dt} = \text{const.} = K_2 \qquad \text{where } dt = t_c - t_\infty \qquad \text{A3.4}$$

or

$$D_\infty = D_C - K_2(dt) \qquad \text{A3.5}$$

where K_2 has the units of microns per second.

Combining equations A3.3 and A3.5:

$$\frac{[D_C - K_2(dt)]}{D_0} = K_1 \qquad \text{A3.6}$$

or

$$\frac{D_C}{D_0} = K_1 + \frac{K_2(dt)}{D_0} \qquad \text{A3.7}$$

Assumption 4 states that the second stage crystallization is not dependent upon size, therefore dt is not dependent on size. Examination of equation 3 reveals everything on the right hand side of equation 3 is constant for a given environmental condition. Therefore,

$$\frac{D_C}{D_0} = \text{const.} \qquad \text{A3.8}$$

for a given environmental condition and all sizes. This is what was stated in assumption 3.

Examination of tests with different temperatures and relative humidities indicates that the value of dt varies little between tests. Therefore,

$$\frac{D_C}{D_0} = \text{const.} \qquad \text{A3.9}$$

for all environmental conditions. This is what was stated in assumption 2.

Table 15

Summary of Errors Obtained
with Approximation of Tests

Statistical Formulas

standard deviation = σ

mean absolute error = $\sigma\sqrt{2\pi}$

probable error = $0.6745\ \sigma$

Solution Number	Average D_c/D_0	Standard Deviation	Mean Absolute Error	Percent Mean Absolute Error	Probable Error	Percent Probable Error
2	0.564	0.054	0.0431	7.64%	0.0364	6.45%
5	0.841	0.040	0.0319	3.79%	0.0269	3.21%
6	0.400	0.018	0.0144	3.60%	0.0121	3.03%
7	0.526	0.0256	0.0204	3.88%	0.0173	3.29%
8	0.295	0.0232	0.0185	6.22%	0.0156	5.27%
9	0.265	0.01488	0.01187	4.48%	0.01004	3.79%
10	0.524	0.0519	0.0414	7.90%	0.03501	6.68%
11	0.465	0.0513	0.0409	8.80%	0.0346	7.44%

Table 16

Parameters Required for Second Stage of Evaporation

Solution Number	Average D/D_0	Average second stage slope microns/sec
2	0.548	0.076
5	0.793	0.208
6	0.394	0.200
7	0.490	0.393
8	0.260	0.067
9	0.236	0.100
10	0.488	0.100
11	0.440	0.088

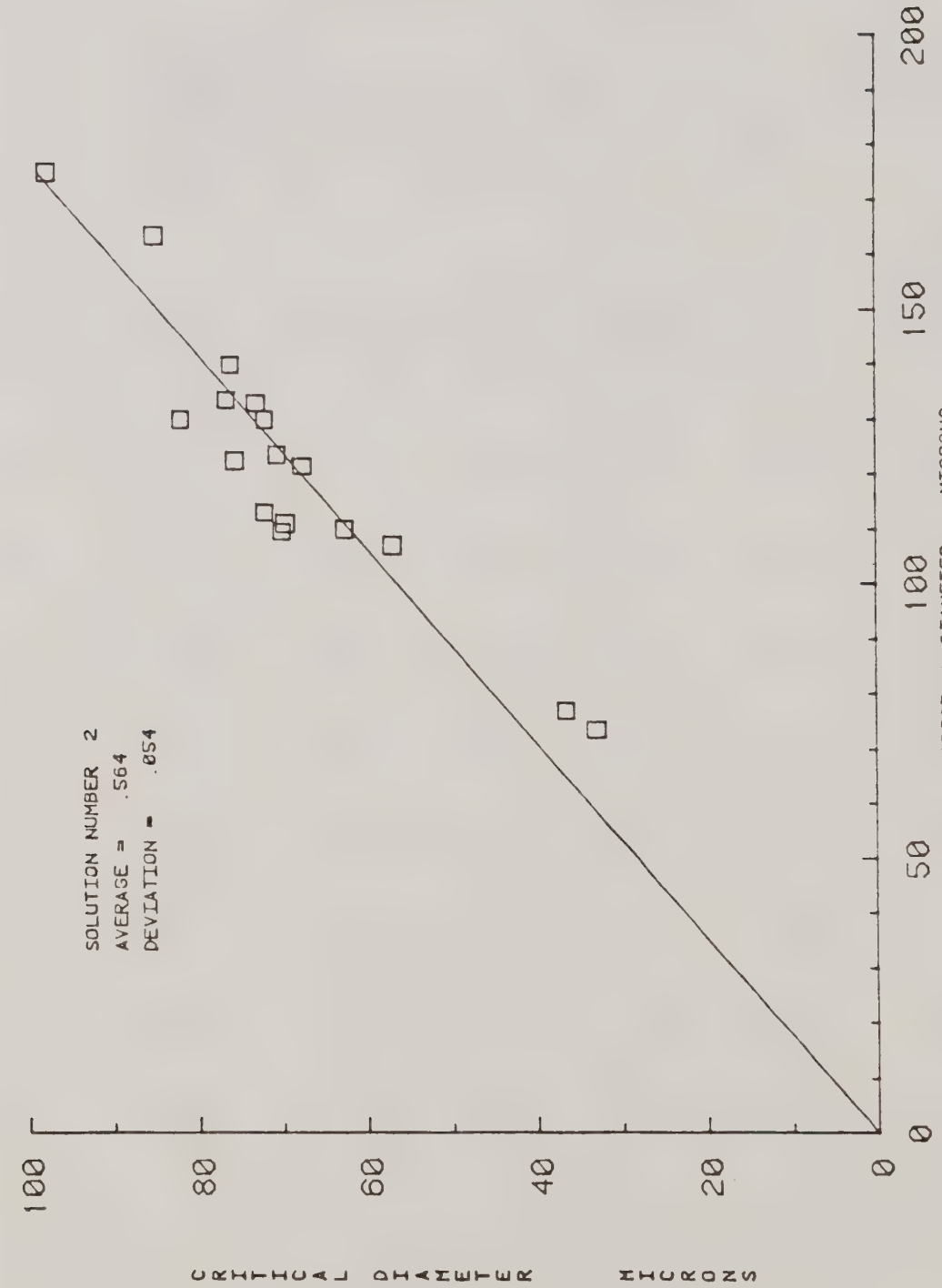

Figure 51. Critical Diameter vs Original Diameter Solution 2

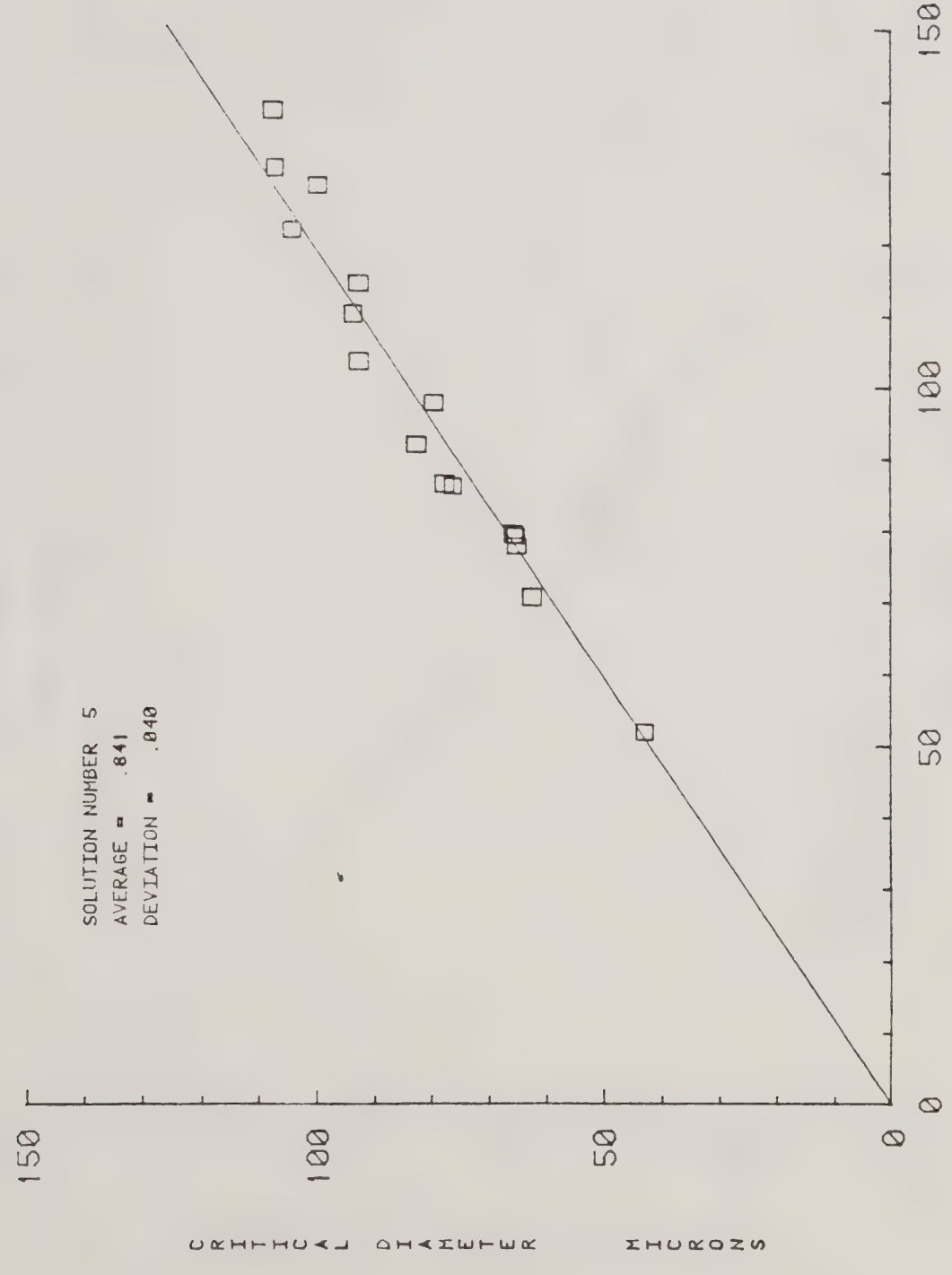

Figure 52. Critical Diameter vs Original Diameter
Solution 5

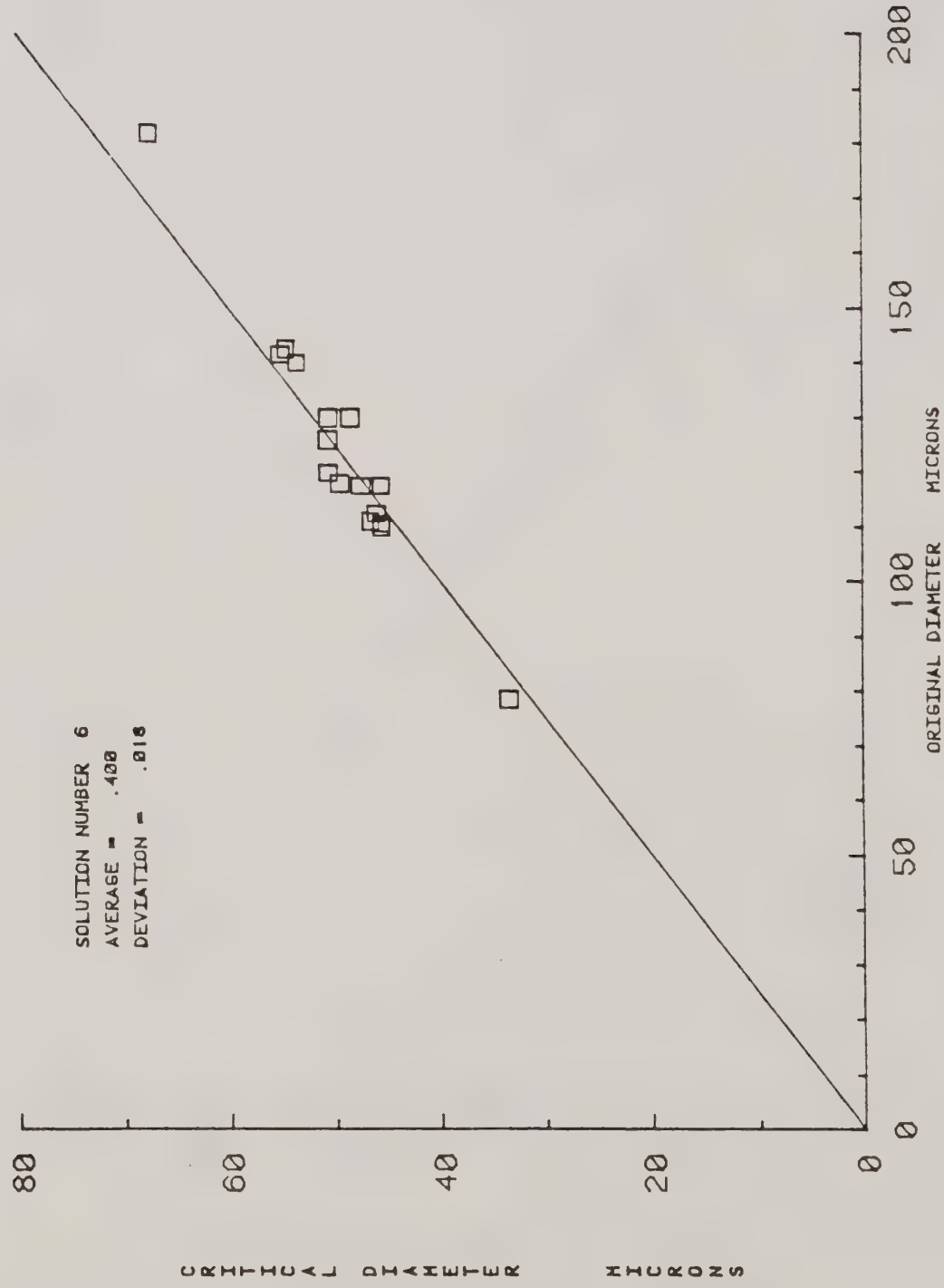

Figure 53. Critical Diameter vs Original Diameter Solution 6

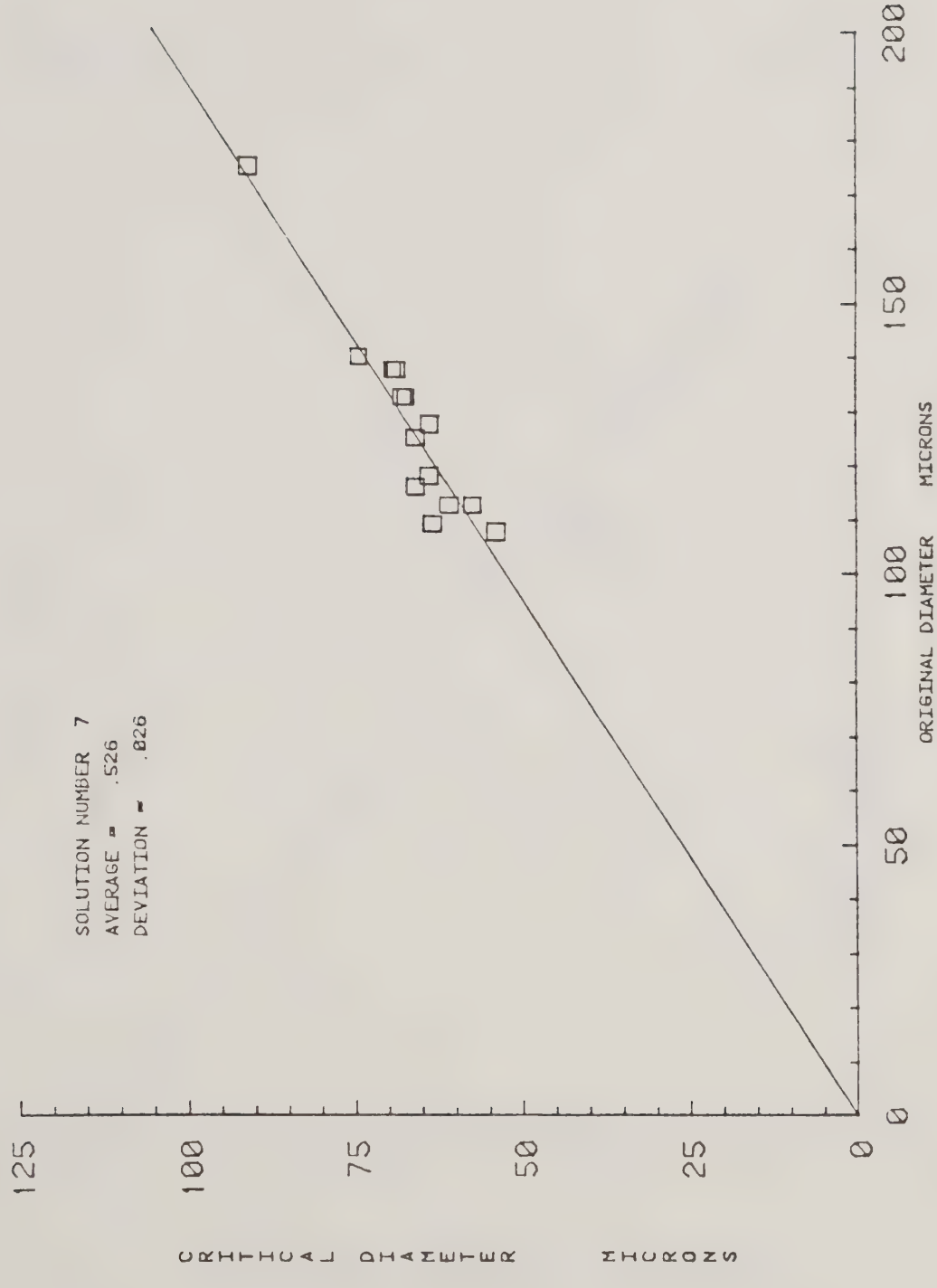

Figure 54. Critical Diameter vs Original Diameter Solution 7

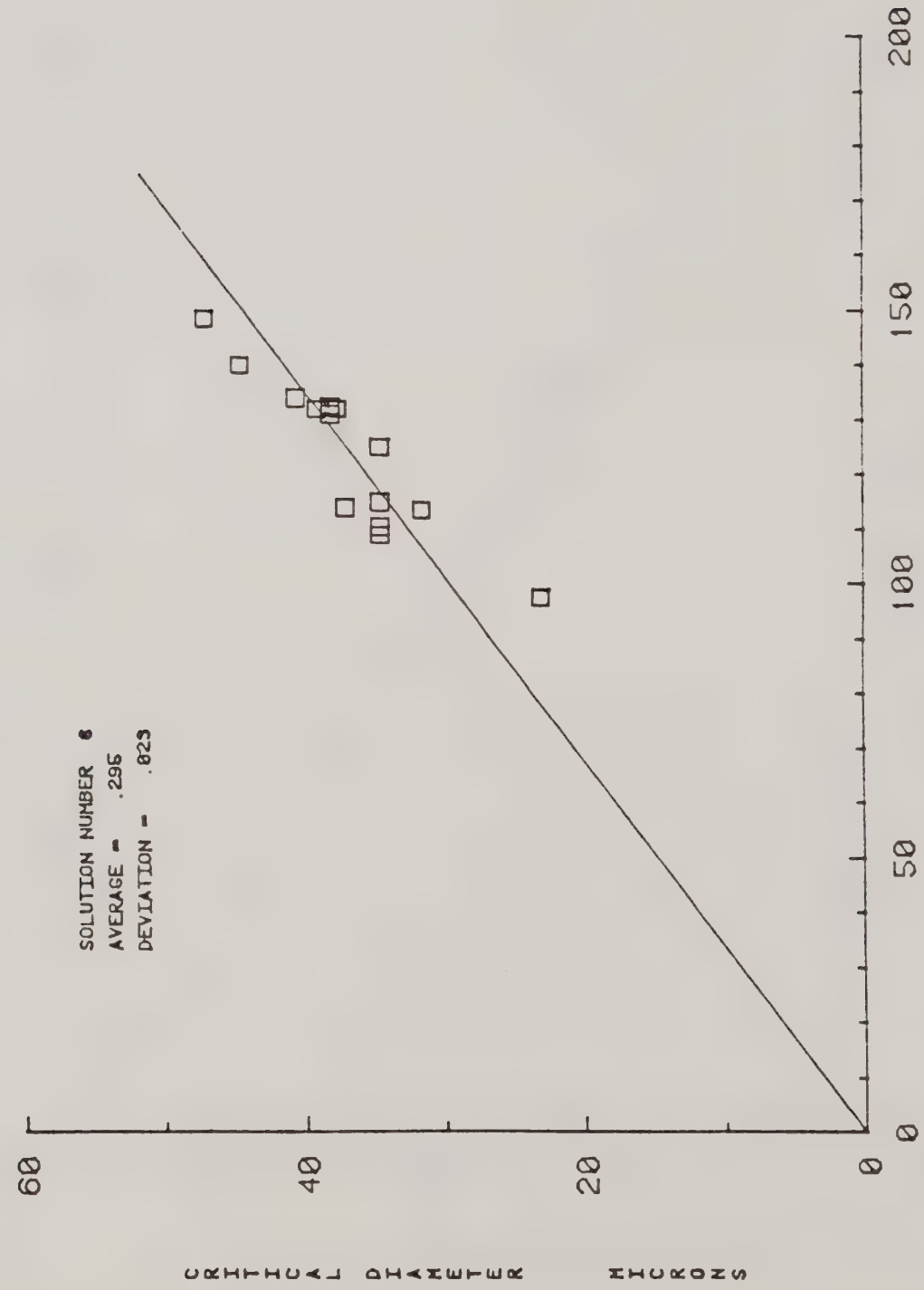

Figure 55. Critical Diameter vs Original Diameter Solution 8

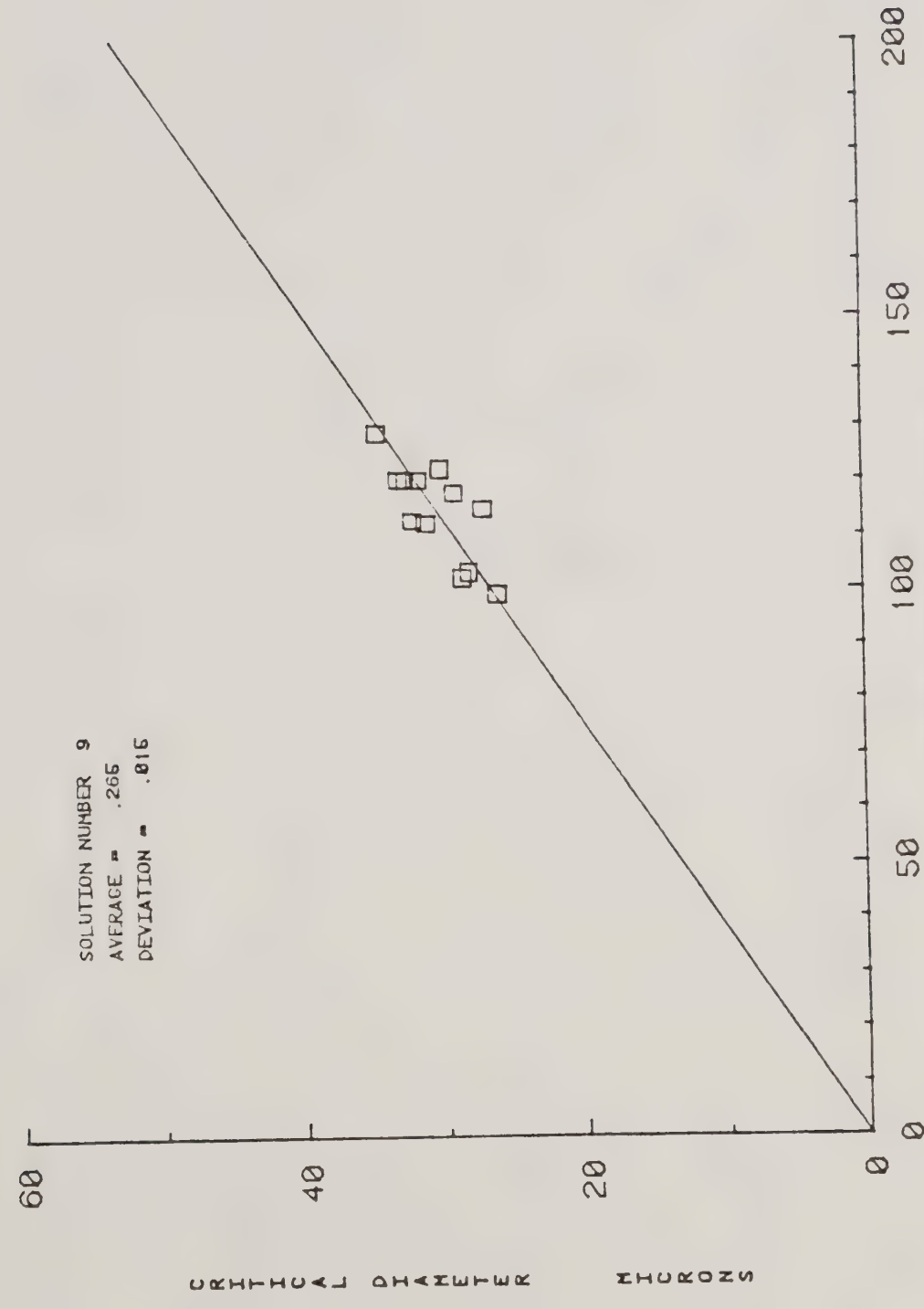

Figure 56. Critical Diameter vs Original Diameter Solution 9

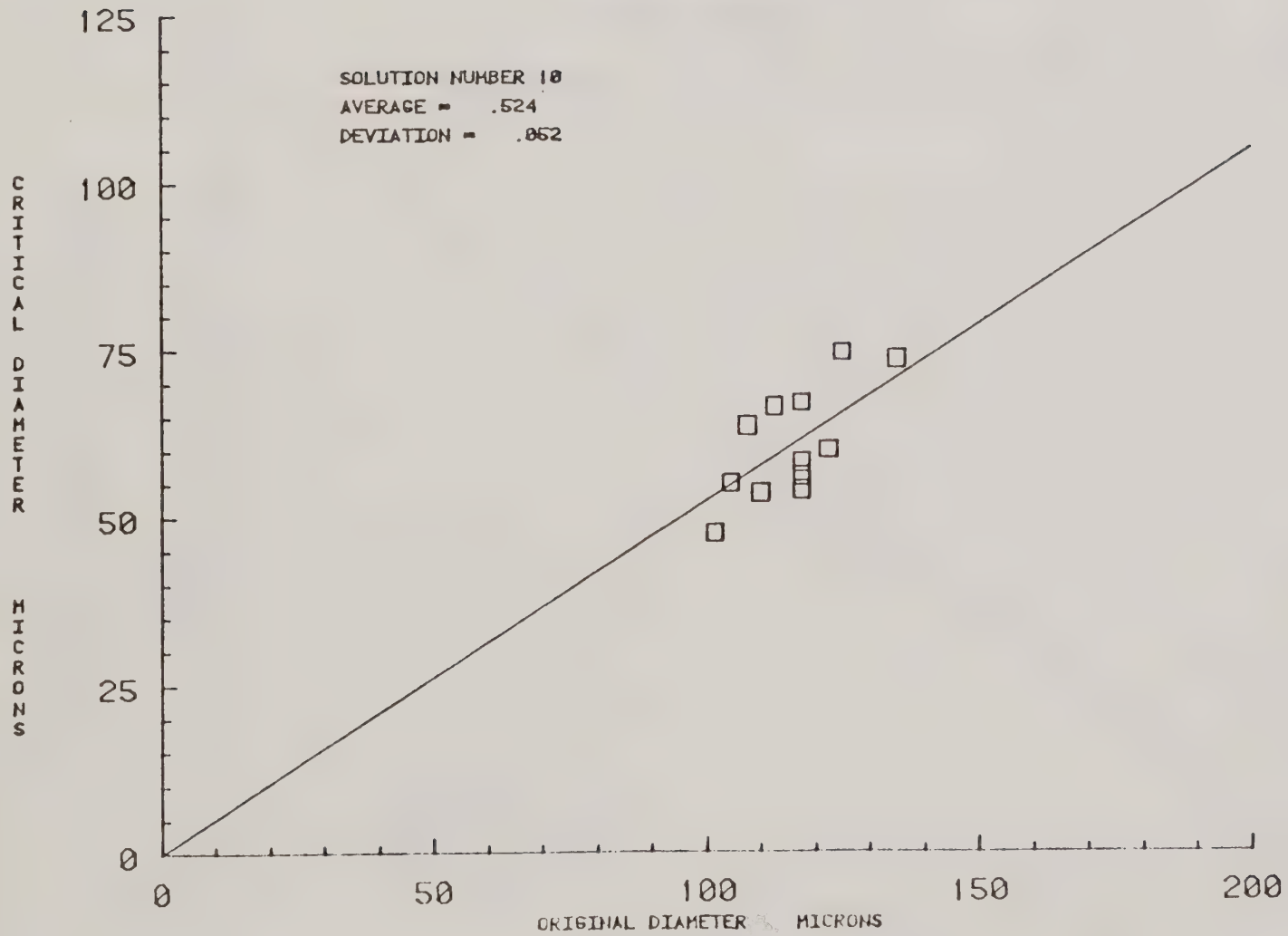

Figure 57. Critical Diameter vs Original Diameter
Solution 10

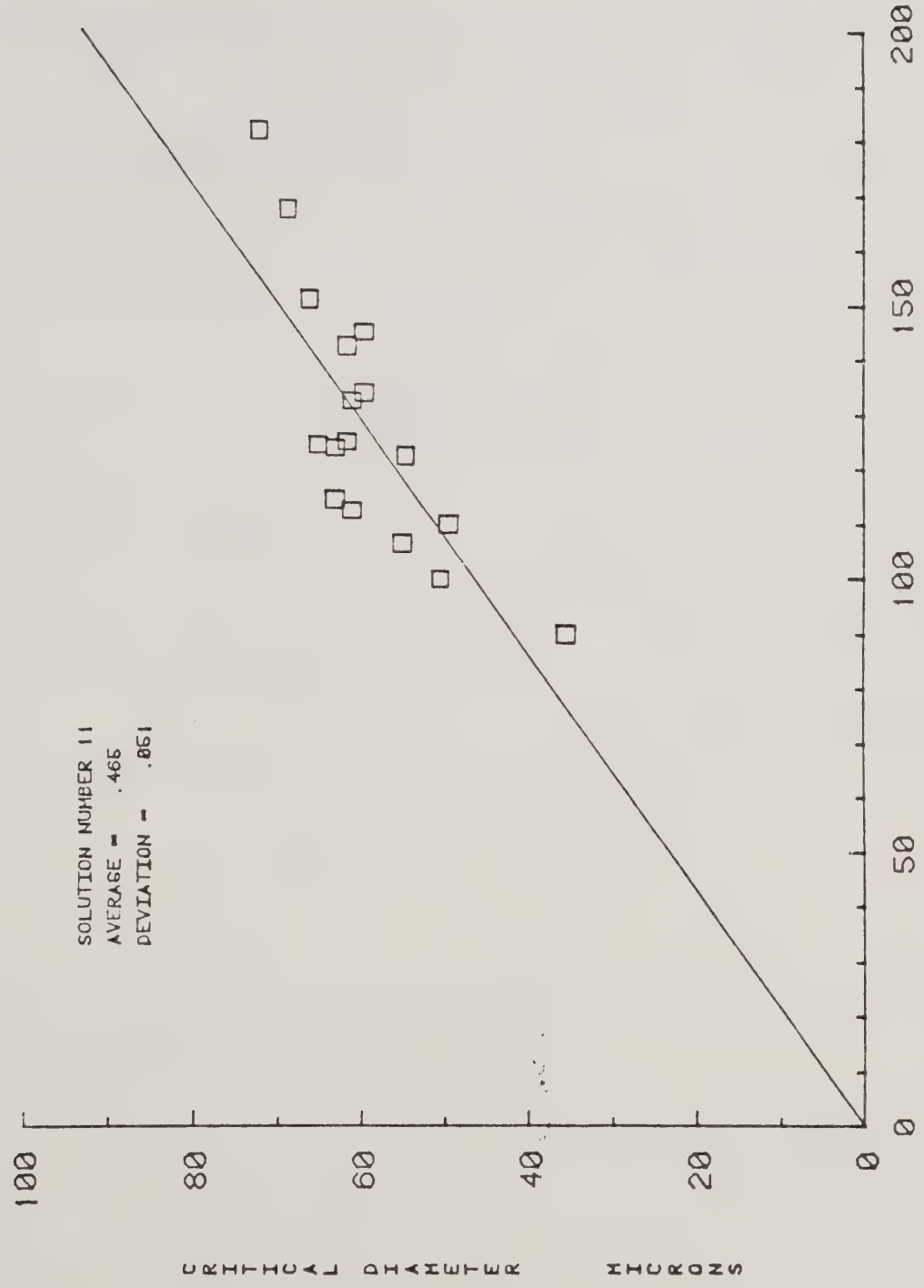

Figure 58. Critical Diameter vs Original Diameter Solution 11

Appendix 4

ERROR ANALYSIS

Experimental Error Analysis

Four variables that contribute to error:

Temperature, Humidity, Diameter, Velocity

Errors in Measurement of the Variables

i) Temperature - for a given environmental condition $\pm .2^{o}C$ at $20^{o}C$

so that $\frac{W_{TEMP}}{TEMP} = 0.01$

Absolute Temperature $\frac{W_{ABT}}{ABT} = \frac{0.2}{293.1} = 0.00068$

i) Humidity $\frac{W_{HUMID}}{HUMID} = 0.05$

i) Diameter measurement from microscope - camera set up approximately

1 micron @ 100 micron diameter $\frac{W_D}{D} = \frac{1}{100} = 0.01$

i) Velocity - average percent error approximately 10%

$$\frac{W_V}{V} = 0.10$$

- The viscosity, diffusion coefficient, and saturation vapor coefficient vary linerally with the air temperature

Visc with $(ABTEMP)^{1/2}$ so that $\frac{W_\mu}{\mu} = \frac{0.00068}{2} = 0.00034$

Del with TEMP so that $\frac{W_\nabla}{\nabla} = 0.01$

Satvap with TEMP so that $\frac{W_s}{s} = 0.01$

Density

$$\rho = \left(\frac{P_{ATM} \cdot M_a}{R \cdot ABTEMP} \right) \cdot W \qquad W = 1 + 0.622 \left(\frac{HUMID \cdot Satvap}{P_{ATM} - HUMID \cdot Satvap} \right)$$

$$\frac{w_W}{W} = \left[\left(\frac{w_{HUMID}}{HUMID} \right)^2 + \left(\frac{w_s}{s} \right)^2 \right]^{1/2} = \left[0.05^2 + 0.01^2 \right]^{1/2} = 0.05099 \qquad \text{A4.1}$$

$$\frac{w_\rho}{\rho} = \left[\left(\frac{w_{ABT}}{ABT} \right)^2 + \left(\frac{w_W}{W} \right)^2 \right]^{1/2} = \left[0.0068^2 + 0.05099^2 \right]^{1/2} = 0.050995$$

Error in P_{coeff}

$$P_{coeff} = \left(\frac{Satvao(T_a)}{ABT_a} - \frac{HUMID \cdot Satvap(T_0)}{ABT_0} \right)$$

$$\frac{w_{P_{coeff}}}{P_{coeff}} \cong \left[2\left(\frac{w_s}{s} \right)^2 + 2\left(\frac{w_{ABT}}{ABT} \right)^2 + \left(\frac{w_{HUMID}}{HUMID} \right)^2 \right]^{\frac{1}{2}} \qquad \text{A4.2}$$

$$\frac{w_{P_{coeff}}}{P_{coeff}} \cong \left[2(0.01)^2 + 2(0.00068)^2 + (0.05)^2 \right]^{\frac{1}{2}}$$

$$\frac{w_{P_{coeff}}}{P_{coeff}} = 0.052$$

Error in Determination of Sc = $\frac{\mu}{\rho\nabla}$

$$\frac{w_{Sc}}{Sc} = \left[\left(\frac{w_\mu}{\mu}\right)^2 + \left(\frac{w_\rho}{\rho}\right)^2 + \left(\frac{w_\nabla}{\nabla}\right)^2\right]^{\frac{1}{2}} \qquad \text{A4.3}$$

$$\frac{w_{Sc}}{Sc} = 0.05197$$

Error in Determination of Re = $\frac{Vd\,\rho}{\mu}$

$$\frac{w_{Re}}{Re} = \left[\left(\frac{w_V}{V}\right)^2 + \left(\frac{w_d}{d}\right)^2 + \left(\frac{w_\rho}{\rho}\right)^2 + \left(\frac{w_\mu}{\mu}\right)^2\right]^{\frac{1}{2}} \qquad \text{A4.4}$$

$$\frac{w_{Re}}{Re} = 0.1127$$

Error in Determination of $C = Re^{1/2}Sc^{1/3}$

$$\frac{w_C}{C} = \left[\left(\frac{1}{2}\frac{w_{Re}}{Re}\right)^2 + \left(\frac{1}{3}\frac{w_{Sc}}{Sc}\right)^2\right]^{\frac{1}{2}} \qquad \text{A4.5}$$

$$\frac{w_C}{C} = 0.06205$$

Error in Determination of Rate = $\left(\frac{dm}{dt}\right)_0 = \frac{-4\pi\nabla aM}{R}\left(\left(\frac{Satvap}{ABT}\right)_a - \left(\frac{Satvap}{ABT}\right)_\infty\right)$

$$\frac{w_{RATE}}{RATE} = \left[\left(\frac{w_d}{d}\right)^2 + \left(\frac{w_\nabla}{\nabla}\right)^2 + \left(\frac{w_{Pcoeff}}{P_{coeff}}\right)^2\right]^{\frac{1}{2}} \qquad \text{A4.6}$$

$$\frac{w_{RATE}}{RATE} = 0.0539$$

Error in Determination of $\left(\frac{dm}{dt}\right)_c$ = CONV.

$$CONV. = \frac{\rho\pi D^2}{2} \quad \frac{d(D)}{dt}$$

$$\frac{w_{CONV.}}{CONV.} = \left[\left(2\,\frac{w_D}{D}\right)^2 + \left(\frac{w_{dD}}{dD}\right)^2\right]^{1/2} = \left[(0.02)^2 + (0.01)^2\right]^{1/2} \qquad A4.7$$

$$\frac{w_{CONV.}}{CONV.} = 0.0224$$

Error in Sh = 2 $\frac{CONV.}{RATE}$

$$\frac{w_{sh}}{sh} = \left[\left(\frac{w_{CONV.}}{CONV.}\right)^2 + \left(\frac{w_{RATE}}{RATE}\right)^2\right]^{1/2} = \left[(0.0539)^2 + (0.0244)^2\right]^{1/2} \qquad A4.8$$

$$\frac{w_{sh}}{sh} = 0.0584$$

Error in β and α, the regression coefficients

$$\frac{w_{\beta,\alpha}}{\beta,\alpha} = \left[\left(\frac{w_{sh}}{sh}\right)^2 + \left(\frac{w_c}{c}\right)^2\right]^{1/2} = 0.0852 \qquad A4.9$$

The error in plots of percent loss of mass versus time should be the same as the error involved with the determination of the regression coefficients.

Therefore $$\frac{W_{M.L.}}{M.L.} = 0.0852 \qquad A4.10$$

Errors Caused by the Deformation of Droplets

Deformation of the droplets defined by the aspect ratio $\eta = \frac{b}{a}$

the volume of sphere with unit radius $V = 4/3\ \pi$ A4.11

the volume of spheriod $V^* = 4/3\ \pi\ a\ b^2 = 4/3\ \pi\ \eta^2\ a^3$ A4.12

equate A4.11 and A4.12:

$$V = V^* \ ; \quad 4/3\ \pi = 4/3\ \pi\ \eta^2\ a^3 \qquad \text{A4.13}$$

$$a^3\ \eta^2 = 1 \quad \text{or} \quad a = \eta^{-2/3} \qquad \text{A4.14}$$

replace a into the definition of the aspect ratio

$$b = a\ \eta = \eta^{1/3} \qquad \text{A4.15}$$

find the cross sectional area

$$A^* = \pi ab = \pi\ \eta^{-1/3} \qquad \text{A4.16}$$

equate with equivalent area of a circle

$$\pi\ \eta^{-1/3} = \pi\ r_{eq}^2 \qquad \text{A4.17}$$

$$r_{eq} = \eta^{-1/6} \qquad \text{A4.18}$$

a unit radius was assumed in A4.11

$$r_{eq} / r_{act} = \eta^{-1/6} \qquad \text{A4.19}$$

Therefore, the ratio of the equivalent radius as determined by the cross sectional area measurement to the actual radius of the sphere is equal to the negative one sixth power of the aspect ratio. An aspect ratio of up to 0.55 can be used and still cause only a 10% error in the measurement of the radius.

Effect of the Aspect Ratio on the Drag Coefficient

The drag coefficient is defined as:

$$C_D = 2(DRAG)/(\pi\ r^2 \rho_a\ V_t^2) \qquad \text{A4.20}$$

using A4.19 $C_{D\ eq}$ can be calculated

$$C_{D\ eq} = 2(DRAG)/(\pi\ \eta^{-1/3} r_{act}^2\ \rho_a V_t^2) \qquad \text{A4.21}$$

using A4.20 and A4.21 the effect on the drag coefficient can be determined as:

$$\frac{C_{D\ eq}}{C_{D\ act}} = \eta^{-1/3} \qquad \text{A4.22}$$

Effect of the Aspect Ratio on the Terminal Velocity

The terminal velocity is a function of the drag coefficient

$$V_t = f(C_D^{-1/2}) \qquad \text{A4.23}$$

substituting A4.22 into A4.23 allows the effect on the terminal velocity as:

$$\frac{V_{t\ eq}}{V_{t\ act}} = \eta^{1/6} \qquad \text{A4.24}$$

The effect of the aspect ratio on the terminal velocity varies with the one sixth power of the aspect ratio. This effect will be only 10% for an aspect ratio of $\eta = 0.55$.

Appendix 5

Magnetic Tape Procedures

The test numbers of all 496 files stored on magnetic tape can be seen in Table 17 along with their corresponding test variables. This table also lists the order in which these tests were stored. The first line of each file contains six numbers that describe the test. The first of these numbers is the test number or name given to that file. The second number indicated the solution index number. The third and forth numbers give the environmental temperature, in ^{o}C, and relative humidity, in %, used for that specific test. The delay time, in seconds, for the test is displayed in the fifth number. Finally, the remaining number lines or records of the test is given by the sixth number. Each of these remaining lines contains three seconds of data. For each second of data, three values are given; the elapsed time in seconds, the droplet diameter in microns, and the actual wind tunnel velocity in centimeters per second. Therefore each line of data contains nine values, three times, three droplet diameters, and three velocities.

The file numbers are determined by the testing variables of solution number, temperature, humidity, and initial droplet diameter. A test iteration number was also used to keep track of the tests when several runs were performed. The test iteration was the first digit of the test number. The next two digits correspond to the solution index number. The third digit represents the humidity used in the study. The fifth digit represents a temperature value. The sixth and final digit designates an initial droplet diameter. The index numbers and values for humidity, temperature, and initial diameter are shown in Table 18. This system allows a unique number to be given for any specific test.

In order to access the files stored on the magnetic tape, a set of procedures must be performed. These procedures along with a sample file can be

seen in Figure 59. After logging onto the system, the main program must be called up. This is done by the following command;

```
asg, a  evap*progs.
```

A request to mount the tape is then summitted by;

```
asg, t  evap*tape., u 9v//////q, f32032
```

where f32032 is the tape number. At this point the system must be readied to read from tape 8 and write on tape 9. The following procedures prepare the system for this operation.

```
use 8., evap*tape.
asg,t evap*disk.
use 9., evap*disk.
```

In order to access a given file, the system must move on the tape to the start of that file. The operator may move to the desired file by using the command;

```
move 8., N
```

where N is the number of files to be moved. In the example given in Figure 59 N=20. Note that the file 101134 is stored in the twenty first position. Therefore, to move to a desired file, the file number, given in Table 17, must be known. Subtracting one from this file number would give the number of files to be moved. Once the start of a necessary file has been found, a program to read and write these is initiated;

```
xqt  evap*progs.read
```

A listing of this program can be seen in Figure 60. The number of records contained in the file will be displayed once the program has ended. At this point, a temporary file has been created that will last until the operator logs off. In order to create a permanent file, a file name must be assigned after the tape has been mounted;

asg,up filename.

Once the desired file has been read in, the system is located at the start of the next file. If it is desired to examine an additional file, the operator can move from this position. In the example given, the twenty-first file was read in. Once this was performed, the system was located at the start of the twenty-second file. If, for example, the operator wished to examine the twenty-forth file, the move command must be used with N=2. If the operator wanted to examine the sixteenth file, the system may be moved backward with the following command;

move,b 8.,N

where N would be six. Moving backward tends to stretch the tape so that the operator may wish to rewind the tape and then move forward the desired amount of files.

The example shown in Figure 59 shows the format in which the data are stored in the files. The first line contains the test number, solution number, temperature, relative humidity, delay time, and remaining lines of data respectively. The lines of data consist of three sets of elapsed time, droplet diameter, and wind tunnel velocity in that order.

Table 17

Evaporation Rate Tests Stored on Magnetic Tape

FILE	TEST DATE	SOLUTION	TEMP	HUMID	INIT DIAM
1	101111	1	5	20	50
2	101121	1	10	20	50
3	101131	1	15	20	50
4	101141	1	20	20	50
5	101241	1	20	60	50
6	101113	1	5	20	100
7	101123	1	10	20	100
8	101133	1	15	20	100
9	101143	1	20	20	100
10	101213	1	5	60	100
11	101223	1	10	60	100
12	101233	1	15	60	100
13	101243	1	20	60	100
14	101123	1	10	20	250
15	101133	1	15	20	250
16	101143	1	20	20	250
17	101223	1	10	60	250
18	101233	1	15	60	250
19	101243	1	20	60	250
20	101124	1	10	20	400
21	101134	1	15	20	400
22	101144	1	20	20	400
23	101224	1	10	60	400
24	102111	2	5	20	50
25	102121	2	10	20	50
26	102131	2	15	20	50
27	102141	2	20	20	50
28	102211	2	5	60	50

FILE	TEST NAME	SOLUTION	TEMP	HUMID	INIT DIAM
29	102221	2	10	60	50
30	102231	2	15	60	50
31	102241	2	20	60	50
32	102311	2	5	90	50
33	102321	2	10	90	50
34	102331	2	15	90	50
35	102341	2	20	90	50
36	102112	2	5	20	100
37	102122	2	10	20	100
38	202132	2	15	20	100
39	102142	2	20	20	100
40	102212	2	5	60	100
41	102222	2	10	60	100
42	202232	2	15	60	100
43	102242	2	20	60	100
44	102312	2	5	90	100
45	102322	2	10	90	100
46	102332	2	15	90	100
47	202342	2	20	90	100
48	102117	2	5	20	250
49	102127	2	10	20	250
50	102137	2	15	20	250
51	102147	2	20	20	250
52	102217	2	5	60	250
53	102227	2	10	60	250
54	102237	2	15	60	250
55	102247	2	20	60	250
56	202317	2	5	90	250

FILE	TEST NAME	SOLUTION	TEMP	HUMID	INIT DIAM
57	202333	2	10	90	250
58	102333	2	15	90	250
59	202343	2	20	90	250
60	102114	2	5	20	400
61	102124	2	10	20	400
62	102134	2	15	20	400
63	102144	2	20	20	400
64	102214	2	5	60	400
65	102224	2	10	60	400
66	102234	2	15	60	400
67	202244	2	20	60	400
68	102314	2	5	90	400
69	102324	2	10	90	400
70	102334	2	15	90	400
71	102344	2	20	90	400
72	103111	3	5	20	50
73	103121	3	10	20	50
74	103131	3	15	20	50
75	203141	3	20	20	50
76	103241	3	20	60	50
77	203113	3	5	20	100
78	103123	3	10	20	100
79	103133	3	15	20	100
80	103143	3	20	20	100
81	203213	3	5	60	100
82	103223	3	10	60	100
83	203233	3	15	60	100
84	103243	3	20	60	100

FILE	TEST NAME	SOLUTION	TEMP	HUMID	INIT DIAM
85	103153	3	15	20	250
86	103143	3	20	20	250
87	103223	3	10	60	250
88	103233	3	15	60	250
89	103243	3	20	60	250
90	103134	3	15	20	400
91	103144	3	20	20	400
92	103234	3	15	60	400
93	103244	3	20	60	400
94	104111	4	5	20	50
95	104121	4	10	20	50
96	104131	4	15	20	50
97	104141	4	20	20	50
98	104241	4	20	60	50
99	104112	4	5	20	100
100	104122	4	10	20	100
101	104132	4	15	20	100
102	104142	4	20	20	100
103	104212	4	5	60	100
104	104222	4	10	60	100
105	104232	4	15	60	100
106	104242	4	20	60	100
107	104133	4	15	20	250
108	104143	4	20	20	250
109	104243	4	20	60	250
110	104134	4	15	20	400
111	104144	4	20	20	400
112	104244	4	20	60	400

FILE	TEST NAME	SOLUTION	TEMP	HUMID	INIT DIAM
113	105111	5	5	20	50
114	105121	5	10	20	50
115	105131	5	15	20	50
116	105141	5	20	20	50
117	105211	5	5	60	50
118	105221	5	10	60	50
119	105231	5	15	60	50
120	105241	5	20	60	50
121	105311	5	5	90	50
122	105321	5	10	90	50
123	105331	5	15	90	50
124	105341	5	20	90	50
125	105112	5	5	20	100
126	105122	5	10	20	100
127	105132	5	15	20	100
128	105142	5	20	20	100
129	105212	5	5	60	100
130	105222	5	10	60	100
131	105232	5	15	60	100
132	105242	5	20	60	100
133	105312	5	5	90	100
134	105322	5	10	90	100
135	105332	5	15	90	100
136	105342	5	20	90	100
137	205113	5	5	20	250
138	205123	5	10	20	250
139	205133	5	15	20	250
140	205143	5	20	20	250

FILE	TEST NAME	SOLUTION	TEMP	HUMID	INIT DIAM
141	205213	5	5	60	250
142	305223	5	10	60	250
143	205233	5	15	60	250
144	105243	5	20	60	250
145	305313	5	5	90	250
146	405323	5	10	90	250
147	105333	5	15	90	250
148	105343	5	20	90	250
149	306114	6	5	20	400
150	205124	6	10	20	400
151	405134	6	15	20	400
152	106144	6	20	20	400
153	105214	6	5	60	400
154	205224	6	10	60	400
155	205234	6	15	60	400
156	105244	6	20	60	400
157	205314	6	5	90	400
158	205324	6	10	90	400
159	205334	6	15	90	400
160	205344	6	20	90	400
161	106111	6	5	20	50
162	106121	6	10	20	50
163	106131	6	15	20	50
164	106141	6	20	20	50
165	106211	6	5	60	50
166	106221	6	10	60	50
167	106231	6	15	60	50
168	106241	6	20	60	50

FILE	TEST NAME	SOLUTION	TEMP	HUMID	INIT DIAM
169	106311	6	5	90	50
170	106321	6	10	90	50
171	106331	6	15	90	50
172	106341	6	20	90	50
173	106112	6	5	20	100
174	106122	6	10	20	100
175	206132	6	15	20	100
176	206142	6	20	20	100
177	106212	6	5	60	100
178	206222	6	10	60	100
179	106232	6	15	60	100
180	206242	6	20	60	100
181	206312	6	5	90	100
182	306322	6	10	90	100
183	106332	6	15	90	100
184	106342	6	20	90	100
185	106113	6	5	20	250
186	106123	6	10	20	250
187	106133	6	15	20	250
188	206143	6	20	20	250
189	406213	6	5	60	250
190	206223	6	10	60	250
191	106233	6	15	60	250
192	106243	6	20	60	250
193	206313	6	5	90	250
194	106323	6	10	90	250
195	106333	6	15	90	250
196	106343	6	20	90	250

FILE	TEST NAME	SOLUTION	TEMP	HUMID	INIT DIAM
197	106114	6	5	20	400
198	106124	6	10	20	400
199	106134	6	15	20	400
200	106144	6	20	20	400
201	306214	6	5	60	400
202	106224	6	10	60	400
203	106234	6	15	60	400
204	106244	6	20	60	400
205	106314	6	5	90	400
206	106324	6	10	90	400
207	106334	6	15	90	400
208	106344	6	20	90	400
209	107111	7	5	20	50
210	107121	7	10	20	50
211	107131	7	15	20	50
212	107141	7	20	20	50
213	107211	7	5	60	50
214	107221	7	10	60	50
215	107231	7	15	60	50
216	107241	7	20	60	50
217	107311	7	5	90	50
218	107321	7	10	90	50
219	107331	7	15	90	50
220	107341	7	20	90	50
221	207112	7	5	20	100
222	107122	7	10	20	100
223	307132	7	15	20	100
224	207142	7	20	20	100

FILE	TEST NAME	SOLUTION	TEMP	HUMID	INIT DIAM
225	207212	7	5	60	100
226	207222	7	10	60	100
227	107232	7	15	60	100
228	207242	7	20	60	100
229	107312	7	5	90	100
230	207322	7	10	90	100
231	207332	7	15	90	100
232	207342	7	20	90	100
233	207113	7	5	20	250
234	107123	7	10	20	250
235	107133	7	15	20	250
236	107143	7	20	20	250
237	107213	7	5	60	250
238	107223	7	10	60	250
239	107233	7	15	60	250
240	107243	7	20	60	250
241	207313	7	5	90	250
242	107323	7	10	90	250
243	107333	7	15	90	250
244	107343	7	20	90	250
245	107114	7	5	20	400
246	207124	7	10	20	400
247	107134	7	15	20	400
248	307144	7	20	20	400
249	207214	7	5	60	400
250	107224	7	10	60	400
251	107234	7	15	60	400
252	107244	7	20	60	400

FILE	TEST NAME	SOLUTION	TEMP	HUMID	INIT DIAM
253	107314	7	5	90	400
254	207324	7	10	90	400
255	107334	7	15	90	400
256	107344	7	20	90	400
257	108111	8	5	20	50
258	108121	8	10	20	50
259	108131	8	15	20	50
260	108141	8	20	20	50
261	108211	8	5	60	50
262	108221	8	10	60	50
263	108231	8	15	60	50
264	108241	8	20	60	50
265	108311	8	5	90	50
266	108321	8	10	90	50
267	108331	8	15	90	50
268	108341	8	20	90	50
269	208112	8	5	20	100
270	108122	8	10	20	100
271	208132	8	15	20	100
272	208142	8	20	20	100
273	208212	8	5	60	100
274	208222	8	10	60	100
275	208232	8	15	60	100
276	208242	8	20	60	100
277	208312	8	5	90	100
278	308322	8	10	90	100
279	208332	8	15	90	100
280	108342	8	20	90	100

FILE	TEST NAME	SOLUTION	TEMP	HUMID	INIT DIAM
281	108113	8	5	20	250
282	208123	8	10	20	250
283	108133	8	15	20	250
284	108143	8	20	20	250
285	108213	8	5	60	250
286	208223	8	10	60	250
287	108233	8	15	60	250
288	208243	8	20	60	250
289	108313	8	5	90	250
290	208323	8	10	90	250
291	208333	8	15	90	250
292	208343	8	20	90	250
293	209114	9	5	20	400
294	109124	9	10	20	400
295	109134	9	15	20	400
296	209144	9	20	20	400
297	209214	9	5	60	400
298	209224	9	10	60	400
299	209234	9	15	60	400
300	109244	9	20	60	400
301	109314	9	5	90	400
302	109324	9	10	90	400
303	109334	9	15	90	400
304	109344	9	20	90	400
305	109111	9	5	20	50
306	109121	9	10	20	50
307	109131	9	15	20	50
308	109141	9	20	20	50

FILE	TEST NAME	SOLUTION	TEMP	HUMID	INIT DIAM
309	109211	9	5	60	50
310	109221	9	10	60	50
311	109231	9	15	60	50
312	109241	9	20	60	50
313	109311	9	5	90	50
314	109321	9	10	90	50
315	109331	9	15	90	50
316	109341	9	20	90	50
317	209112	9	5	20	100
318	209122	9	10	20	100
319	109132	9	15	20	100
320	109142	9	20	20	100
321	209212	9	5	60	100
322	109222	9	10	60	100
323	109232	9	15	60	100
324	109242	9	20	60	100
325	209312	9	5	90	100
326	209322	9	10	90	100
327	209332	9	15	90	100
328	109342	9	20	90	100
329	109113	9	5	20	250
330	309123	9	10	20	250
331	109133	9	15	20	250
332	209143	9	20	20	250
333	109213	9	5	60	250
334	109223	9	10	60	250
335	109233	9	15	60	250
336	209243	9	20	60	250

FILE	TEST NAME	SOLUTION	TEMP	HUMID	INIT DIAM
337	109313	9	5	80	250
338	109323	9	10	90	250
339	209333	9	15	90	250
340	209343	9	20	90	250
341	109114	9	5	20	400
342	109124	9	10	20	400
343	109134	9	15	20	400
344	109144	9	20	20	400
345	109214	9	5	60	400
346	109224	9	10	60	400
347	109234	9	15	60	400
348	109244	9	20	60	400
349	109314	9	5	90	400
350	109324	9	10	90	400
351	109334	9	15	90	400
352	109344	9	20	90	400
353	110111	10	5	20	50
354	110121	10	10	20	50
355	110131	10	15	20	50
356	110141	10	20	20	50
357	110211	10	5	60	50
358	110221	10	10	60	50
359	110231	10	15	60	50
360	110241	10	20	60	50
361	110311	10	5	90	50
362	110321	10	10	90	50
363	110331	10	15	90	50
364	110341	10	20	90	50

FILE	TEST NAME	SOLUTION	TEMP	HUMID	INIT DIAM
365	210112	10	5	20	100
366	110122	10	10	20	100
367	110132	10	15	20	100
368	310142	10	20	20	100
369	110212	10	5	60	100
370	210222	10	10	60	100
371	110232	10	15	60	100
372	110242	10	20	60	100
373	110312	10	5	90	100
374	110322	10	10	90	100
375	210332	10	15	90	100
376	110342	10	20	90	100
377	110113	10	5	20	250
378	110123	10	10	20	250
379	110133	10	15	20	250
380	110143	10	20	20	250
381	210213	10	5	60	250
382	110223	10	10	60	250
383	310233	10	15	60	250
384	210243	10	20	60	250
385	210313	10	5	90	250
386	110323	10	10	90	250
387	110333	10	15	90	250
388	210343	10	20	90	250
389	110114	10	5	20	400
390	110124	10	10	20	400
391	110134	10	15	20	400
392	210144	10	20	20	400

FILE	TEST NAME	SOLUTION	TEMP	HUMID	INIT DIAM
393	110214	10	5	60	400
394	110224	10	10	60	400
395	110234	10	15	60	400
396	210244	10	20	60	400
397	110324	10	10	90	400
398	110314	10	5	90	400
399	110334	10	15	90	400
400	210344	10	20	90	400
401	111111	11	5	20	50
402	111121	11	10	20	50
403	111131	11	15	20	50
404	111141	11	20	20	50
405	111211	11	5	60	50
406	111221	11	10	60	50
407	111231	11	15	60	50
408	111241	11	20	60	50
409	111311	11	5	90	50
410	111321	11	10	90	50
411	111331	11	15	90	50
412	111341	11	20	90	50
413	211112	11	5	20	100
414	211122	11	10	20	100
415	211132	11	15	20	100
416	211142	11	20	20	100
417	111212	11	5	60	100
418	111222	11	10	60	100
419	211232	11	15	60	100
420	111242	11	20	60	100

FILE	TEST NAME	SOLUTION	TEMP	HUMID	INIT DIAM
421	211312	11	5	90	100
422	111322	11	10	90	100
423	211332	11	15	90	100
424	211342	11	20	90	100
425	111113	11	5	20	250
426	111123	11	10	20	250
427	111133	11	15	20	250
428	111143	11	20	20	250
429	111213	11	5	60	250
430	111223	11	10	60	250
431	111233	11	15	60	250
432	111243	11	20	60	250
433	111313	11	5	90	250
434	111323	11	10	90	250
435	111333	11	15	90	250
436	111343	11	20	90	250
437	211114	11	5	20	400
438	111124	11	10	20	400
439	111134	11	15	20	400
440	111144	11	20	20	400
441	111214	11	5	60	400
442	111224	11	10	60	400
443	111234	11	15	60	400
444	111244	11	20	60	400
445	111314	11	5	90	400
446	111324	11	10	90	400
447	211334	11	15	90	400
448	111344	11	20	90	400

FILE	TEST NAME	SOLUTION	TEMP	HUMID	INIT DIAM
449	312112	12	5	20	100
450	112122	12	10	20	100
451	112132	12	15	20	100
452	112142	12	20	20	100
453	212212	12	5	60	100
454	112222	12	10	60	100
455	112232	12	15	60	100
456	212242	12	20	60	100
457	112312	12	5	90	100
458	112322	12	10	90	100
459	112332	12	15	90	100
460	212342	12	20	90	100
461	112113	12	5	20	250
462	212123	12	10	20	250
463	112133	12	15	20	250
464	112143	12	20	20	250
465	112213	12	5	60	250
466	212223	12	10	60	250
467	112233	12	15	60	250
468	112243	12	20	60	250
469	112313	12	5	90	250
470	112323	12	10	90	250
471	212333	12	15	90	250
472	112343	12	20	90	250
473	112114	12	5	20	400
474	112124	12	10	20	400
475	212134	12	15	20	400
476	112144	12	20	20	400

FILE	TEST NAME	SOLUTION	TEMP	HUMID	INIT DIAM
477	112214	12	5	60	400
478	212224	12	10	60	400
479	112234	12	15	60	400
480	112244	12	20	60	400
481	112314	12	5	90	400
482	112324	12	10	90	400
483	212334	12	15	90	400
484	112344	12	20	90	400
485	313129	13	10	20	100
486	513142	13	20	20	100
487	313220	13	10	60	100
488	113242	13	20	60	100
489	313322	13	10	90	100
490	213342	13	20	90	100
491	113144	13	20	20	400
492	214122	14	10	20	100
493	514142	14	20	20	100
494	314242	14	20	60	100
495	214342	14	20	90	100
496	214144	14	20	20	400

Figure 59

Accessing Procedures and an Example File

```
Good [illegible]                    .evap
DATE: 071582   TIME: 134723
Weekend Hours  .HOURS,82-28 [@INFO]THURSDAY 13:49
@asg,a evap*procs.
READY
@asg,t evap*tape.,u9v//////a,132032
READY
@use 8.,evap*tape.
READY
@asg,t evap*disk.
READY
@use 9.,evap*disk.
READY
@more 8.,20
FURPUR 28R2 01 S74T11 07/16/82 13:55:14
20 FOR(S) DETECTED
END MORE
@xqt evap*procs.read
          19
 FILE CONTAINS              19 RECORDS
@ed,r 9.
READ-ONLY MODE
ED 1/R16 FRI 07/16/82-13:56:08-(0,)
EDIT
0:
p!
101134      1         15         20          6.0         19
          0       445.4      112.4          1       445.1      112.4          2       445.0      112.6
          3       444.9      112.2          4       444.7      112.4          5       444.6      112.4
          6       443.7      112.4          7       443.3      112.4          8       442.8      112.0
          9       442.9      112.6         10       442.2      112.0         11       441.9      111.8
         12       442.4      112.4         13       442.1      112.2         14       443.8      117.1
         15       443.1      136.5         16       443.5      140.9         17       443.1      149.7
         18       443.9      150.3         19       443.1      150.3         20       443.5      150.3
         21       443.9      150.1         22       443.4      150.3         23       443.5      150.3
         24       443.1      150.3         25       441.9      150.3         26       442.9      150.3
         27       442.1      150.3         28       442.4      150.3         29       442.0      150.3
         30       441.6      150.3         31       441.9      150.3         32       441.0      150.3
         33       441.6      150.3         34       440.9      150.3         35       442.7      150.3
         36       441.5      150.3         37       439.3      150.3         38       438.3      150.3
         39       439.8      150.3         40       439.9      150.3         41       439.8      150.3
         42       439.6      150.3         43       439.5      150.3         44       438.9      150.3
         45       438.1      150.3         46       437.6      150.3         47       437.3      150.3
         48       437.2      150.3         49       437.5      150.3         50       437.9      150.3
         51       437.4      150.3         52       436.9      150.3         53       436.6      150.3
         54       436.3      150.3         55       436.2      150.3         56       436.2      150.3
EOF:20
0:
exi
END ED. NO CORRECTIONS APPLIED
```

Table 18

Index Number for Test Variables

Index Number	Relative Humidity
1	20%
2	60%
3	90%

Index Number	Temperature
1	5°C
2	10°C
3	15°C
4	20°C

Index Number	Initial Droplet Diameter, Microns
1	50
2	100
3	250
4	400

Figure 60

Listing of Program Used to Read and Write the Stored Files

```
EVAP*PROGS(1).READ(7)
      1              CHARACTER*120 LINE(600)
      2              CHARACTER*60 HDR
      3           10 CALL NTRAN$ (8,2,15,HDR,L1,22)
      4              IF (L1 .EQ. -2) GO TO 900
      5              DECODE (1000,HDR) IREC
      6              PRINT *,IREC
      7              WRITE (9,1200) HDR
      8         1000 FORMAT (50X,I4,6X)
      9              MAX = IREC * 30
     10              CALL NTRAN$ (8,2,MAX,LINE,L2,22)
     11              DO 20 I = 1,IREC
     12              WRITE (9,1100) LINE(I)
     13         1100 FORMAT (A120)
     14         1200 FORMAT (A60)
     15           20 CONTINUE
     16              PRINT*,' FILE CONTAINS ',IREC,' RECORDS'
     17          900 ENDFILE 9
     18              STOP
     19              END
```

*G PO 793 - 016 (1984)